

NOTICE

**CERTAIN DATA
CONTAINED IN THIS
DOCUMENT MAY BE
DIFFICULT TO READ
IN MICROFICHE
PRODUCTS.**

NRTSC

NUCLEAR REACTOR TECHNOLOGY
AND SCIENTIFIC COMPUTATIONS

WSRC-TR--91-11

DE92 018105

Keywords:
Process Water System
Stainless Steel
Reactor
Irradiation
PTERM
CAMEL

Retention - Permanent

**REACTOR MATERIALS PROGRAM -
Mechanical Properties of Irradiated Types 304 and 304L Stainless
Steel Weldment Components (U)
Task Number: 89-023-C-1**

By

R.L. Sindelar *R.L. Sindelar*
G.R. Caskey Jr. *G.R. Caskey Jr.*

ISSUED: December 1991

G.C. Kao 1-30-92

Derivative Classifier

SRL

SAVANNAH RIVER LABORATORY, AIKEN, SC 29808
Westinghouse Savannah River Company
Prepared for the U. S. Department of Energy under Contract DE-AC09-89SR18035

MASTER

DISTRIBUTION OF THIS DOCUMENT IS UNLIMITED

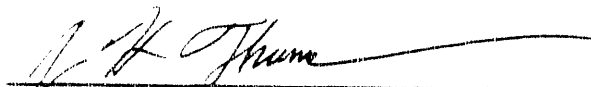
PROJECT: REACTOR MATERIALS PROGRAM

DOCUMENT: WSRC-TR-91-11

TITLE: REACTOR MATERIALS PROGRAM -
Mechanical Properties of Irradiated Types 304 and
304L Stainless Steel Weldment Components (U)

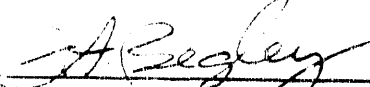
TASK: Measure Mechanical Properties of Irradiated
Stainless Steel, Task 89-023-C-1

APPROVALS



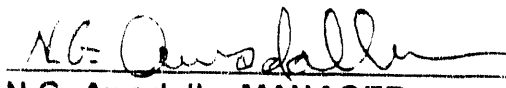
J.K. Thomas, TECHNICAL REVIEWER
SRL - MATERIALS TECHNOLOGY

DATE: 1/31/92



J.A. Begley, TECHNICAL REVIEWER
WEC - SCIENCE & TECHNOLOGY CENTER

DATE: 1/22/92



N.G. Awadalla, MANAGER
MATERIALS TECHNOLOGY

DATE: 1/31/92



T.L. Capeletti, SECTION MANAGER
MATERIALS TECHNOLOGY

DATE: 1/31/92

DISCLAIMER

This report was prepared as an account of work sponsored by an agency of the United States Government. Neither the United States Government nor any agency thereof, nor any of their employees, makes any warranty, express or implied, or assumes any legal liability or responsibility for the accuracy, completeness, or usefulness of any information, apparatus, product, or process disclosed, or represents that its use would not infringe privately owned rights. Reference herein to any specific commercial product, process, or service by trade name, trademark, manufacturer, or otherwise does not necessarily constitute or imply its endorsement, recommendation, or favoring by the United States Government or any agency thereof. The views and opinions of authors expressed herein do not necessarily state or reflect those of the United States Government or any agency thereof.

This report has been reproduced directly from the best available copy.

Available to DOE and DOE contractors from the Office of Scientific and Technical Information, P.O. Box 62, Oak Ridge, TN 37831; prices available from (615) 576-8401, FTS 626-8401.

Available to the public from the National Technical Information Service, U.S. Department of Commerce, 5285 Port Royal Rd., Springfield, VA 22161.

EXECUTIVE SUMMARY

The vessels (reactor tanks) of the Savannah River Site nuclear production reactors constructed in the 1950's are comprised of Type 304 stainless steel with Type 308 stainless steel weld filler¹. Irradiation exposure to the reactor tank sidewalls through reactor operation has caused a change in the mechanical properties of these materials. A database of as-irradiated mechanical properties for site-specific materials and irradiation conditions has been produced for reactor tank structural analyses and to quantify the effects of radiation-induced materials degradation for evaluating reactor service life. The data has been collected from the SRL Reactor Materials Program (RMP) irradiations and testing of archival stainless steel weldment components and from previous SRL programs to measure properties of irradiated reactor Thermal Shield weldments and reactor tank (R-tank) sidewall material. The results from application of the Lower Bound properties to structural and fracture analysis of the tank show ASME² safety margins are maintained for postulated throughwall flaws up to several feet in length at exposure conditions corresponding to 50 years additional operation of the SRS reactor tanks. The continued safe operation of the reactors is not limited by radiation-induced degradation of the tank materials.

Irradiation programs of the RMP are designed to quantify mechanical properties at tank operating temperatures following irradiation to present and future tank wall maximum exposure conditions. The exposure conditions are characterized in terms of fast neutron fluence ($E_n > 0.1$ MeV) and displacements per atom (dpa)³. Tensile properties, Charpy-V notch toughness, and elastic-plastic fracture toughness were measured for base, weld, and weld heat-affected zone (HAZ) weldment components from archival piping specimens (ASTM L-C and C-L orientations) following a Screening Irradiation in the University of Buffalo Reactor (UBR) and following a Full-Term Irradiation in the High Flux Isotope Reactor (HFIR). A total of 81 Charpy V-notch specimens and 12 Tensile specimens were tested at temperatures of 25 and 125°C following irradiation to a fast fluence of 1.1×10^{20} n/cm² (0.065 dpa) in the UBR irradiation. A total of 10 Compact Tension, 5 Charpy V-notch, and 5 Tensile specimens were tested at a temperature of 125°C following irradiation to fast fluences from 1.8 to 3.8×10^{21} n/cm² (1.0 to 2.1 dpa) in the HFIR 4M mechanical specimen irradiation capsule. The qualification capsule, 1Q, for the HFIR irradiation contained mechanical specimens of Type 304L stainless steel. A total of 6 Compact Tension, 4 Charpy V-notch, and 5 Tensile specimens from the 1Q were tested at a temperature of 125°C following irradiation to fast fluences from 0.36 to 0.92×10^{21} n/cm² (0.21 to 0.52 dpa) and are included in the irradiated properties database.

¹The joining process for the reactor tanks (e.g. plates for tank shell or "sidewall") was Inert-Gas-Shielded Metal Arc Welding with a Consumable Electrode. This process is similar to the fabrication process for the reactor primary coolant or Process Water System piping and is termed Gas Metal Arc Welding in the current site specifications for the piping.

²American Society of Mechanical Engineers, Boiler and Pressure Vessel Code, Section XI.

³The exposure unit "displacement per atom" (dpa) is a calculated parameter representing, on average, the number of times an atom in the material being exposed is displaced from a lattice position during the irradiation. Contributions to dpa at the tank wall originate from: scattering and capture (recoil) reactions with fast and thermal neutrons, respectively; helium production (recoil); and gamma irradiation (via Compton Electron production followed by scattering event). The present maximum tank wall exposure of 1.4 dpa occurs at six azimuthal locations at the beltline of K reactor tank. The present maximum tank fast fluence level is 1.86×10^{21} n/cm².

Previous irradiation effects studies at SRL (by Walt Joseph in 1960) produced tensile data of base, weld, and HAZ components for specimens cut from a thermal shield model constructed from Type 304 stainless steel plates and butt welded with Type 308 stainless filler (lime coated "stick weld"). A total of 20 Tensile specimens were tested at room temperature following irradiation in two sets to average fast fluences of 2.9×10^{20} and 1.2×10^{21} n/cm², respectively, and are included in the as-irradiated properties database.

Mechanical specimens of base materials removed from the R-tank sidewall with fast fluence levels of 1 and 7×10^{20} n/cm² were also tested in a previous SRL-sponsored program (Reactor Operability Assurance Program) in 1987. The test results from a total of 9 Tensile and 6 Compact Tension specimens tested at 25°C and 125°C from this program are included in the database.

The reduction in fracture toughness and radiation hardening effects (increase in strength with a loss of work hardening ability) have been quantified. The tensile and fracture toughness results for the irradiation exposure levels investigated show high residual material toughness and ductility for all weldment components with little sensitivity to exposure level. Hardening of the materials reaching a saturation in hardening with exposure is interpreted in terms of the production of extended lattice defect microstructures during irradiation. Radiation hardening of the materials caused an average increase in yield strength between about 20 to 190% of the unirradiated values with a concomitant increase in tensile strength values between about 15 to 30% for all the data sets (categorized by weldment component, orientation, and test temperature). The corresponding total elongations are between 27 and 53%. The range of average absolute strengths is 56 to 96 ksi (yield) and 65 to 106 ksi (tensile or ultimate) for the data sets.

The Charpy V-notch as-irradiated toughness is between 41 and 62% of the unirradiated values for the data sets. The range of absolute values of the average impact toughness is 54 to 94 ft-pounds. The as-irradiated elastic-plastic material toughness, the J value at 1 mm crack extension from the J_{deformation}-R curve analysis, is between 35 to 78% of the corresponding unirradiated material toughness. The range of absolute toughness defined by the J value at 1 mm crack extension is 662 to 2900 in-lbs/in². The range of values for J_{IC} corresponding to a power law fit to the J_{deformation}-R data is 428 to 2092 in-lbs/in². The as-irradiated testing results show a lower (absolute level) fracture resistance with the fracture plane parallel compared to perpendicular to the pipe axis or rolling direction of the original Type 304 stainless steel plate (similar results were obtained in testing of unirradiated companion materials). The low carbon materials, Type 304L (0.030 wt%) and the archival piping 1BB material (0.035 wt%), have higher absolute toughness levels following irradiation than the other base materials.

The application of the as-irradiated properties in a fracture analysis of the reactor tanks is illustrated. Elastic-plastic material toughness parameters are developed from J-R curve analysis from the Compact Tension (CT) specimen test results. Material J-T curves are developed for each of the irradiated CT specimens and a cut-off to the J-T curves is specified. "Nominal" and "Lower Bound" fracture toughness data is defined for tank fracture analyses. A specific case to evaluate tank flow instability with the lower bound toughness data is reproduced from a previous fracture analysis. With the Lower Bound toughness data, postulated throughwall flaws in the tank sidewall over several feet in length meet the ASME BPV Code safety margins.

The as-irradiated database in this report will be supplemented by the results from the HFIR 12M capsule specimens and the K-reactor Surveillance Program specimens upon completion of the irradiated testing in the SRL Reactor Materials Program subtasks.

WSRC-TR-91-11
Table of Contents

<u>Section</u>	<u>Page</u>
1.0 INTRODUCTION.....	1-1
2.0 MATERIAL SOURCES	
2.1 Introduction.....	2-1
2.2 Archive Pipe Sections.....	2-1
2.3 Thermal Shield Model.....	2-2
2.4 R-Reactor Tank Wall.....	2-2
2.5 Reactor Tank Materials and Fabrication.....	2-3
2.6 HFIR IQ Material: Type 304L Stainless Steel.....	2-3
3.0 IRRADIATION PROGRAM OVERVIEW	
3.1 Introduction.....	3-1
3.2 Irradiation Parameters Summary.....	3-1
3.3 Screening Irradiation: University of Buffalo Reactor.....	3-2
3.4 Full-term Irradiation: High Flux Isotope Reactor.....	3-2
3.5 R-Reactor Tank Irradiation.....	3-3
3.6 Thermal Shield Materials Irradiation	3-3
3.7 Surveillance Irradiation: K-Reactor	3-4
4.0 MATERIALS TESTING AND ANALYSIS OF DATA	
4.1 Overview	4-1
4.2 As-Irradiated Test Conditions Summary.....	4-1
4.3 UBR and HFIR Charpy Impact Testing.....	4-2
4.4 UBR and HFIR Tensile Testing.....	4-2
4.5 HFIR Compact Tension Testing.....	4-2
4.6 Thermal Shield Tensile Testing.....	4-3
4.7 R-Reactor Tank Mechanical Testing.....	4-3
5.0 MECHANICAL TESTING RESULTS AND DISCUSSION	
5.1 Overview.....	5-1
5.2 Effect of Irradiation Temperature and Exposure Level on Irradiation Response.....	5-1
5.3 Tensile Data Results.....	5-3
5.4 Charpy Data Results.....	5-3
5.5 Compact Tension Data Results.....	5-4
5.6 Fractography Results.....	5-4
6.0 IRRADIATED MECHANICAL PROPERTIES: ENGINEERING STRUCTURAL ANALYSES	
6.1 Overview.....	6-1
6.1.1 Comparison of RMP, R-Tank, and Thermal Shield Materials to SRS Tanks.....	6-1
6.1.2 Reactor Tank Sidewall Exposure Levels.....	6-1

Table of Contents (cont'd)

<u>Section</u>	<u>Page</u>
6.1.3 As-Irradiated Database: Development of Properties for Engineering Analyses - Summary.....	6-2
6.1.4 Baseline Properties for Irradiation Effects Studies.....	6-2
6.2 Tensile Properties.....	6-3
6.2.1 Tensile Properties for Structural Analysis.....	6-3
6.2.2 Flow Stress Evaluation.....	6-3
6.2.3 Tensile Properties for Fracture Analysis.....	6-3
6.3 Charpy V-Notch Impact Energy.....	6-4
6.4 Fracture Toughness-CT Specimens.....	6-4
7.0 MECHANICAL PROPERTIES: APPLICATION TO TANK FRACTURE ANALYSES	
7.1 Introduction.....	7-1
7.2 SRS Reactor Tank Fracture Analysis.....	7-1
7.2.1 Material J-T Curves	7-3
7.2.2 Applied J-T Curve Formulation.....	7-4
7.2.3 Flaw Stability Analysis: Example Case.....	7-5
8.0 RMP IRRADIATION EFFECTS STUDIES	
8.1 Introduction.....	8-1
8.2 Additional As-Irradiated Testing: 12M & Surveillance Specimens	8-1
8.3 Microstructural Analysis and Mechanical Property Correlation....	8-2
8.4 Microchemical Analysis and Solute Segregation Estimation.....	8-2
9.0 ACKNOWLEDGMENTS.....	9-1
10.0 REFERENCES.....	10-1
APPENDIX 1: IRRADIATED MECHANICAL PROPERTY TEST RESULTS	
APPENDIX 2: IRRADIATED MECHANICAL TEST DATA - DIGITIZED PLOTS	

LIST OF TABLES

<u>Table Number</u>		<u>Page</u>
2-1	Base Metal Chemical Compositions for Archive Pipe.....	2-4
2-2	Weld Metal Chemical Compositions for Archive Pipe.....	2-5
2-3	Average Ferrite Levels for Weld Material of Archive Pipe.....	2-5
2-4	Base Metal Chemical Compositions for R-Tank Disks A,B,C, and D and for the R-Tank plate composition reported by New York Shipbuilding Co.....	2-6
2-5	Base Metal Chemical Compositions for the K and L-Tank plates' composition reported by New York Shipbuilding Co.....	2-6
2-6	Chemical Composition and Heat Treatment of the Type 304L stainless steel material irradiated in the HFIR 1Q capsule.....	2-7
3-1	HFIR 1Q and 4M Specimen Irradiation Parameters.....	3-5
3-2	R-Tank Specimen Irradiation Parameters.....	3-6
3-3	Thermal Shield Material Irradiation in P-reactor.....	3-7
4-1	Irradiated Specimen Test Matrix for the RMP Archive Pipe Weldment Components.....	4-4
4-2	Specimen Test Matrix for the Thermal Shield Weldment Components.....	4-5
4-3	Specimen Test Matrix for the Base Material from R-Tank Disks.....	4-5
4-4	Specimen Test Matrix for the HFIR 1Q Specimens Comprised of Wrought Plate of Type 304L Stainless Steel.....	4-5
5-1A	As-Irradiated Tensile Data.....	5-5
5-1B	As-Irradiated Tensile Data (Average Change from Unirradiated).....	5-6
5-2A	As-Irradiated Charpy Impact Data.....	5-7
5-2B	As-Irradiated Charpy Impact Data (Average Change from Unirradiated).....	5-8
5-3A	As-Irradiated Fracture Toughness Data.....	5-9
5-3B	As-Irradiated Fracture Toughness Data (Average Change from Unirradiated).....	5-10
5-4	Effect of Irradiation Temperature on Room Temperature Tensile Properties.....	5-11

LIST OF FIGURES

<u>Figure Number</u>	<u>Page</u>
1-1 Schematic of the SRS Reactor Tank Wall Evaluation Sequence.....	1-3
1-2 Schematic of the As-Irradiated Mechanical Test Parameter Categories.....	1-4
2-1 Etched Cross Section of Pipe Ring #1 Weld.....	2-8
2-2 Modified Schaeffler Diagram from ASM Metals Handbook	2-9
3-1 Conversions from Thermal and Fast Neutron Fluence to displacements per atom.....	3-8
4-1 Schematic Illustration of Specimen Orientation in the Pipe Ring.....	4-6
4-2 UBR and HFIR Charpy Impact Specimen Dimensions.....	4-7
4-3 UBR and HFIR Tensile Specimen Dimensions.....	4-8
4-4 HFIR 0.4T Compact Tension Specimen Dimensions.....	4-9
4-5A Example of a Typical J-R curve (ASTM E813-81 Format).....	4-10
4-5B ASTM E813-88 Method for Determination of J _{IC}	4-10
4-6 Tensile Specimen Design and Orientation for the Thermal Shield Irradiation Testing.....	4-11
4-7 Sub-Size Tensile Specimen Design for R-Tank Tensile Testing.....	4-12
4-8 0.8T CT Platform Design for the R-Tank Specimens	4-12
5-1A Yield and Tensile Strengths at 25°C as a Function of Fast Fluence...	5-12
5-1B Yield and Tensile Strengths at 125°C as a Function of Fast Fluence..	5-12
5-2A Absorbed Impact Energy at 25°C as a Function of Fast Fluence.....	5-13
5-2B Absorbed Impact Energy at 125°C as a Function of Fast Fluence....	5-13
5-3A Fracture Toughness at 25°C as a Function of Fast Fluence.....	5-14
5-3B Fracture Toughness at 125°C as a Function of Fast Fluence.....	5-14
5-4A Normalized Fracture Toughness at 25°C as a Function of Fast Fluence.....	5-15
5-4B Normalized Fracture Toughness at 125°C as a Function of Fast Fluence.....	5-15
5-5A Effect of Irradiation Temperature on Room Temperature Tensile Test Data.....	5-16
5-5B Effect of Fast Fluence Level on the Change in Yield Strength for Types 304, 316, and 347 Stainless Steel.....	5-16
5-6 Effect of Test Temperature on Impact Energies of Irradiated CVN Specimens.....	5-17
5-7 Fracture Surface of the UBR CVN Specimen 3HA-34 and Unirradiated CVN Specimen 5HB-16.....	5-18
6-1 Material J-T Curves from the HFIR 4M Capsule.....	6-6
7-1 Equivalent J-T, J-a Illustrations of Crack Growth Stability.....	7-5
7-2 Material J-T Curve "Cut-Off" Options to Define Instability.....	7-6
7-3 Example Case of Derivation of Instability Crack Length with J-T Analysis.....	7-7
8-1 Weak Beam Dark Field Transmission Electron Micrograph of the Irradiation-Produced Defect Complex Microstructure of R-Tank Sidewall.....	8-3
8-2 Histogram of the Size/Volume Density of the Defect Complexes in R-Tank Specimen RA3.....	8-4

1.0 INTRODUCTION

The production reactors at the Savannah River Site (SRS) were constructed and began operation in the 1950's. The sidewalls of the reactor tanks have been exposed to neutron irradiation during reactor operation with nearly all of the exposure occurring when the core was configured with fuel assemblies in all of the available positions. The neutron exposure rate to the sidewalls was reduced when blanketed operation began in 1968 [1]. The accumulated exposure is characterized as a "low" temperature (< 130°C at maximum historic full power [2]) neutron irradiation with the present maximum dose to the tank sidewall of 1.4 dpa [3].

The activities for understanding irradiation effects to the reactor tanks, the development of an irradiated property database, and the application of irradiated properties to structural evaluation of the SRS reactor tanks are included under the SRL Reactor Materials Program (RMP) at the Savannah River Laboratory (SRL) [4, 5]. The structural integrity evaluation of the reactor tanks includes evaluation of postulated flaws for acceptability for reactor operation as shown schematically in Figure 1. The irradiated material properties are an important input to flaw evaluation. The RMP studies of service effects to reactor tank materials supports the demonstration for reactor life extension and parallels the intent of Plant Life Extension (PLEX) technological activities required for evaluation of materials' degradation for commercial nuclear power plants. The results and program conclusions from the RMP studies on the Process Water System service life are part of site activities for life extension for the SRS reactors' systems.

The material of construction of the pressure boundary of the reactor primary coolant system (Process Water System) including the reactor tank is American Iron and Steel Institute (AISI) Type 304 stainless steel joined by inert-gas-shielded metal arc welding with Type 308 stainless steel filler wire [6]. Archival piping materials were obtained for irradiation and mechanical testing [7] for the experimentation programs of the RMP. Program studies include measurement of both baseline mechanical/corrosion and irradiated mechanical/corrosion properties for application to engineering analyses of the PWS piping and reactor tanks, respectively. The machining and testing of the irradiated mechanical test specimens were performed by Materials Engineering Associates (MEA) in Lanham, Maryland under the direction of the RMP [8, 9].

This report covers the as-irradiated mechanical testing details, results, and application of mechanical properties to tank structural analyses from the RMP studies to-date. The results from tensile specimen testing at SRL (by Walt Joseph in 1960) [10] at exposures near reactor tank maximum levels [1] and testing of SRS reactor (R-tank) sidewall materials (by Westinghouse Electric Corporation - R&D Center in 1987) [11, 12] are also included to provide a composite as-irradiated property database. The high neutron exposures (2.1 dpa) of the mechanical specimens included in this report meet and exceed the SRS reactor tanks' maximum levels at present exposure and also for an additional 50 years of operation with a blanketed core at a power level of 2400 MW with 66% innage [1, 13].

Section 2 of this report contains a brief description of the materials' source for the RMP irradiation and testing programs and the previous SRL programs. The composition of materials and fabrication details for the SRS reactor tanks are provided for comparison to the weldment components tested in the SRL irradiation programs. Section 3 contains an overview of the SRL mechanical specimen irradiations.

The mechanical test specimen types were tensile (T), Charpy V-notch (CVN), and compact tension (CT) specimens machined from the three different weldment components: base material; weld material; and weld heat-affected-zone (HAZ) material. The test temperatures (25 and 125°C) approximately bound the tank historic operating temperatures. The RMP test specimens

from the archival piping were machined in the ASTM C-L and L-C orientations to allow comparison of the mechanical response for the cases of flaws oriented parallel and perpendicular, respectively, to the pipe axis or rolling direction of the original plate. An overview of the mechanical testing procedures and data analysis procedures is provided in Section 4. Test results and a discussion of the effects of irradiation and irradiation (exposure) level on mechanical properties are provided in Section 5. From the test parameters of temperature (25 and 125°C), orientation (L-C and C-L) and weldment component (base, HAZ and weld), twelve different categories of properties are defined (as shown schematically in Figure 1-2). [The as-irradiated mechanical results in Section 5 show only a slight sensitivity to neutron exposure at fast fluence levels investigated in this study (1×10^{20} to 4×10^{21} n/cm², $E_n > 0.1$ MeV). Therefore, the as-irradiated properties for each category defined in Figure 1-2 are grouped into one "irradiated" set, independent of exposure level].

The mechanical test results from the data sets are compared to evaluate mechanical response dependency on testing condition. The development of as-irradiated mechanical properties for SRS reactor tank structural analyses, including fracture mechanics analyses, is provided in Section 6. "Lower bound" and "nominal" as-irradiated mechanical properties for the reactor tank operating range (25 to 125°C) are selected from the data sets. Application of the mechanical properties to an elastic-plastic fracture analysis of the tank is provided in Section 7. Ongoing RMP studies to characterize the material response to irradiation for SRS tank conditions are discussed in Section 8. Mechanical property test results for the individual mechanical specimens are listed in Appendix 1. Digitized curves summarizing the full mechanical test response are provided in Appendix 2.

The SRL-Reactor Materials Program data collected by Materials Engineering Associates and evaluated in this report have been qualified for critical application as part of the Qualification of LOCA Definition Project [14-17]. The data from the previous SRL programs [10, 11, 12] were not generated under the present NRTSC QA Procedures [18]. The results from the previous SRL programs are consistent with the RMP data and have been added to the RMP data to form the composite as-irradiated database. Therefore, the as-irradiated database, overall results, and conclusions reached in this report may be used in critical applications per the NRTSC QA Procedures [18].

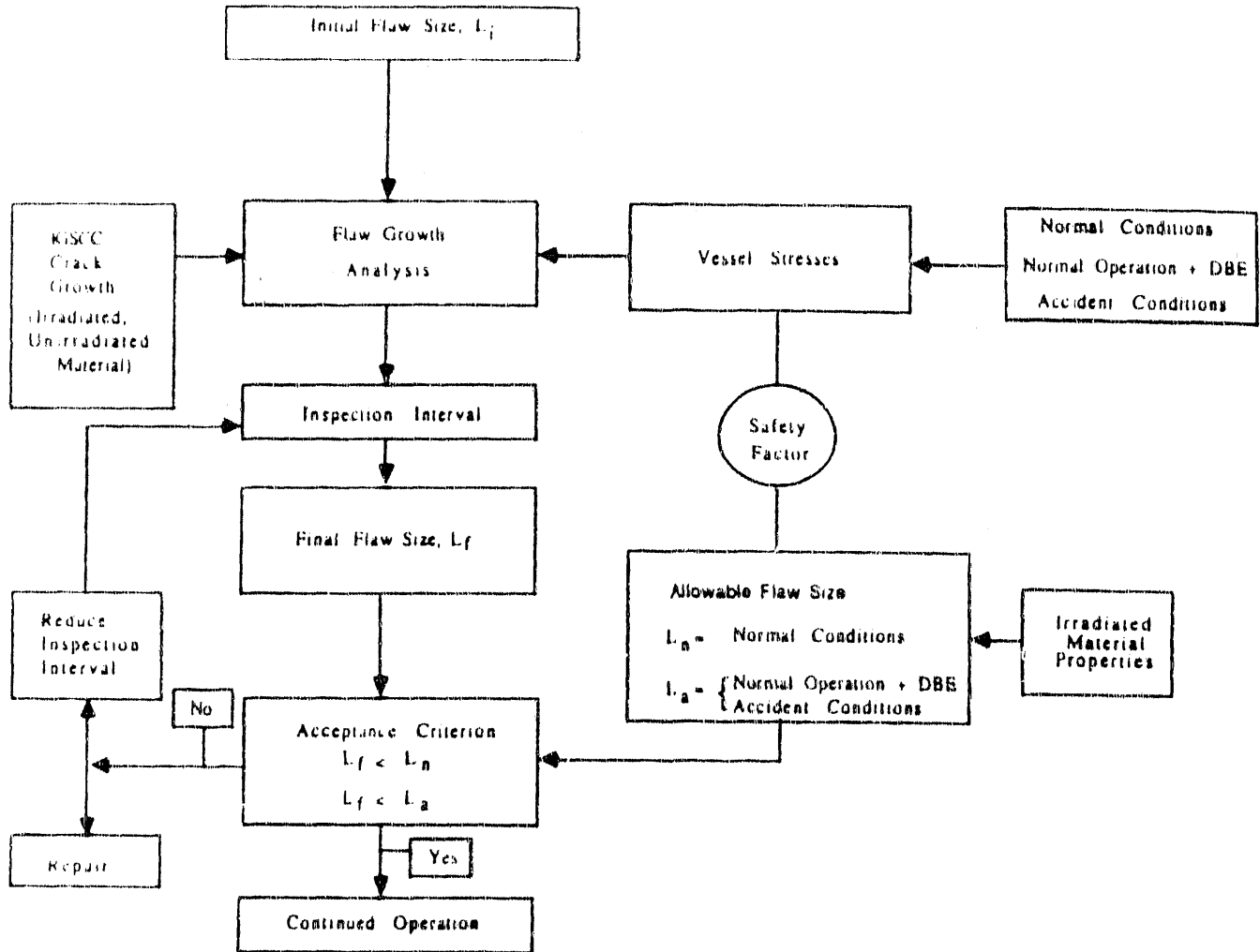


Figure 1-1: Schematic of the SRS Reactor Tank Wall Evaluation Sequence

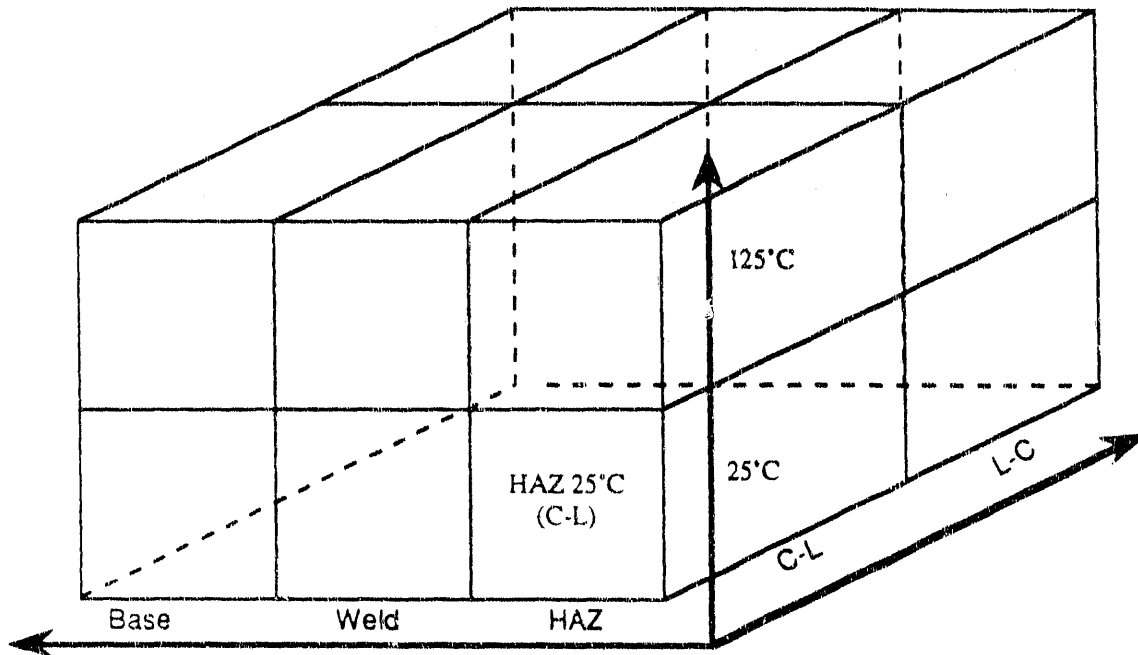


Figure 1-2: Schematic of the as-irradiated mechanical test parameter categories illustrating the twelve sets defined for tensile, Charpy V-notch toughness, and fracture toughness properties for various Material, Temperature and Flaw Orientation combinations (Section 5 of this report). "Nominal" and "lower bound" fracture toughness properties from these sets have been provided in Section 6. [The as-irradiated test results show only a slight sensitivity to neutron exposure level at the fast fluence levels investigated in this study (1×10^{20} to 4×10^{21} n/cm², $E_n > 0.1$ MeV) and therefore the as-irradiated properties are not categorized by exposure level].

2.0 MATERIAL SOURCES

2.1 Introduction

The mechanical property data base for irradiated stainless steel is compiled from tests of materials that were obtained from three sources: pipe sections taken from a decommissioned reactor (R); a model of a reactor thermal shield; and the sidewall of R-reactor. All of these materials are nominally Type 304 austenitic stainless steel and were produced in the 1950's. Specimens from the archive pipe sections were irradiated in the UBR, HFIR, and K-reactor as part of the RMP beginning in 1985 [4, 5]. Specimens from the thermal shield model were irradiated in P-reactor in 1959 [19]. Discs were cut from the sidewall of R-reactor as part of an investigation on weldability of irradiated stainless steel beginning in 1986 [20].

The SRS reactor tank sidewalls (shells) were constructed in the early 1950's by New York Shipbuilding Co. [6] and were transported to the site for final joining. All of the plate materials are nominally Type 304 stainless steel joined with Type 308 stainless steel filler using an inert cover gas of helium. The plate materials' compositions and joining techniques of the tank sidewalls are provided for comparison to the weldment materials investigated in the SRL irradiation programs.

2.2 Archive Pipe Sections

All piping contacting the heavy water moderator was fabricated originally from Type 304 stainless steel per Du Pont Specification SW 304M (Grade 304) as listed in Specification 3018, P39.010 and P39.020, issued November 11, 1951 with latest revision January 24, 1957. The original construction design code of record was American National Standards Institute (ANSI) B31.1. General specifications for process piping components were covered in Specification 3069 issued March 14, 1952 and revised December 18, 1952. Seamless pipe was to be manufactured to ASTM Specification A-269-47 (Grade chromium-nickel) and welded pipe was to be fabricated to ASTM A-312-48T (Grade chromium-nickel).

The archive pipe sections were from rolled and welded Type 304 stainless steel pipe with a 16-inch (406 mm) outer diameter and a nominal wall thickness of 0.5-inch (12.7 mm). Eight pipe sections with approximately six years of service each were removed from the decommissioned R-Reactor [7]. Individual sections have an arbitrarily assigned pipe ring number (1 through 8). Each pipe section contained a circumferential butt weld made by the Metal Inert Gas (MIG) welding process and one or more mill-annealed longitudinal welds. Potentially there were 16 different heats of steel in the eight sections. These pipe sections were located either between the pump and the heat exchanger or between the heat exchanger and the inlet plenum to the reactor [7]. Service temperatures during operation for these two sections were approximately 95 and 40°C, respectively [21].

The mechanical properties of the circumferential welds, associated heat affected zones, and base metal regions were measured in this study. The circumferential weld joint was a single Vee; the joint preparation contained a small land on the inner diameter (ID) side to aid preweld fitup. Figure 2-1 shows an etched cross section of a typical weld joint from ring #1. The joint was filled from the OD side using several weld passes; a root pass made from the ID side is also visible in most joints.

The chemical compositions of the different base and weld metals for the eight pipe rings are given in Tables 2-1 and 2-2. With minor exception, the base material compositions are within the range specified by AISI for Type 304 stainless steel: max 0.08 wt% carbon, max 2.0 wt% manganese.

max 0.045 wt% phosphorous, max 0.03 wt% sulfur, max 1.00 wt% silicon, 8 - 10.5 wt% nickel and 18-20 wt% chromium [22].

Delta-ferrite measurements were taken along the outer surface of the circumferential weld metal around each of the eight pipe sections. The weld filler metal for the SRS reactor process water system piping consists of a delta-ferrite forming Type 308 stainless steel. The ferrite level in specific piping welds is one property that can be used to establish uniformity of welding conditions among different reactor systems throughout the plant. The ferrite measurement results (Laboratory Notebook DPSTN-4321, Copy Series E37276. Measurements with Autotest Model Fe probe) are summarized in Table 2-3. This range of 10 to 15 percent ferrite indicates uniformity in the welding operation and is consistent with commercial piping weldments. Measured ferrite contents are within the range of 1 to 18 percent ferrite predicted by the weld composition and the Schaeffler Diagram (Figure 2-2) [23].

Specimens were machined according to applicable ASTM specifications and assigned a unique identification number that allowed traceability throughout their testing history, as well as identification of their location and orientation with respect to the original pipe ring section. The first number of this code identifies the pipe ring number, and the adjacent letter indicates the material type (W = weld, B = base, and H = heat-affected-zone or HAZ). The second letter (applicable to base and HAZ material only) identifies the side with respect to the circumferential weld from which the specimen came from in the pipe ring (side A or side B) as referenced in the cutting diagrams [see Appendix D of Reference 24].

The sixteen inch diameter pipe from which the specimens were machined was seam welded pipe [7]. A stainless steel plate is cold formed to the pipe diameter and welded lengthwise. Examination of the seam welds indicates that the welds were annealed after welding as there is no evidence of sensitization of the metal next to the welds [Section 3.1.1.2 of ref. 25].

2.3 Thermal Shield Model

Test specimens for the SRL irradiation program in 1959 were machined from a model of a thermal shield that had been made about the same time as the reactor tanks and thermal shields [10]. The model was constructed of 5/8-inch as-rolled plate of Type 304 stainless steel. Plates were joined by butt welding by a manual metal arc process with Type 308 electrodes with a lime coating. The composition of the steel from which the specimens were made is not known. Flat tensile specimens with a 2-inch gauge length were machined from base metal, weld metal, and the weld heat affected zones (see Figure 4-6).

2.4 R-Reactor Tank Wall

Four discs were cut from the sidewall of R-reactor with a hole saw [26] as part of the diagnostic program to assess the reasons for the poor weldability of the knuckle in C-reactor [20]. The main tank shell was fabricated from five different heats of Type 304 stainless steel, two heats in the upper section and three heats in the lower section, Table 2-4 [27]. The top and bottom halves of the tank shell each contained three steel plates; therefore, there were three vertical welds in each half and a circumferential weld to join the upper and lower sections. Access to the tank wall was through six inch diameter instrument ports that penetrate the concrete biological shield and the steel thermal shield. These ports are located 5-feet-6.5-inches above the bottom of the reactor tank and are evenly spaced 90° from one another. All four discs were cut from the lower half of the reactor tank and came from plates 3, 4, and 5 as listed in Table 2-4. According to mill analyses included in the construction records, all of the steel in the tank shell was low carbon stainless steel, ≤ 0.03 weight percent, as shown in Table 2-4 [27]. However, chemical analyses of the discs yielded

carbon contents of >0.05 weight percent for three of the four discs. Nickel and chromium analyses on the discs were also slightly lower than those reported in the mill analyses. Concentrations of the other constituents were consistent between the two analyses. In both cases, the analyses fall within the specifications for Type 304 stainless steel.

2.5 Reactor Tank Materials and Fabrication

The mechanical properties were measured on irradiated specimens taken from archive SRS piping (Section 2.2) and are applicable to structural assessments of K- and L-reactor tanks. [The SRS R-reactor was permanently shutdown in 1964, C-reactor in 1986, and P-reactor in 1991]. The materials of construction of the tanks and piping were purchased to the same codes and standards in the period from 1950 to 1958 and were of comparable quality. Chemical analyses of K and L reactor tanks, Table 2-5, are similar to those of R tank, Table 2-4, and the piping, Table 2-1. All compositions fall within the specifications for Type 304 stainless steel.

All manual and automatic machine welding for both the pipe and tanks was inert gas shielded tungsten arc with bare Type 308 filler rod. In the case of the pipe, single Vee welds were oriented with the weld root at the inner surface of the pipe. In contrast, tank welds were usually double Vee. This difference should not affect the mechanical properties of the weld or heat affected zones, although residual stress patterns and sensitization levels would be expected to differ in the pipe and tanks.

The main tank shell was fabricated from either four or six plates which were partially welded, roll formed to the tank radius, and finish welded. The first weld became the circumferential girth weld near the middle of the tank wall and was cold worked during roll forming. Vertical seam welds in the tank wall were made after the plates were roll formed to the tank radius. Detailed descriptions of the reactor fabrication procedures are found in the activities and fabrication manuals from New York Ship [27].

2.6 HFIR 1Q Material: Type 304L Stainless Steel

Materials Engineering Associates supplied a wrought plate (MEA Code F50) of Type 304L stainless steel for specimens irradiated in the HFIR 1Q capsule assembly [ref. 24, Appendix V]. These specimens, identical in mechanical design to the 4M specimens, were irradiated and tested as part of the RMP (see Section 3 to 5). Table 2-6 lists the chemical composition and heat treatment of the F50 plate material.

Table 2-1: Base metal chemical compositions (wt%) for archive pipe

		Composition (wt-%)											
		C	Mn	Si	P	S	Ni	Cr	Mo	B	Co	Cu	N
1	A	0.079	1.60	0.79	0.031	0.011	9.36	18.79	0.41	0.001	0.11	0.29	0.047
	B	0.035	1.56	0.58	0.024	0.016	9.19	18.44	0.25	0.002	0.10	0.24	0.036
2	A	0.079	1.50	0.34	0.031	0.024	9.65	18.27	0.45	0.002	0.13	0.42	0.043
	B	0.052	1.41	0.38	0.031	0.025	8.50	19.40	0.39	<0.001	0.15	0.42	0.036
3	A	0.063	1.30	0.31	0.028	0.024	9.38	18.59	0.40	0.001	0.12	0.38	0.044
	B	0.048	1.33	0.39	0.027	0.025	9.13	18.67	0.36	0.002	0.13	0.39	0.034
4	A	0.053	1.81	0.33	0.026	0.017	8.75	18.97	0.35	0.002	0.11	0.28	0.033
	B	0.083	1.75	0.74	0.033	0.017	9.60	18.88	0.46	0.002	0.13	0.32	0.043
5	A	0.041	1.39	0.67	0.026	0.024	9.64	19.05	0.52	0.002	0.12	0.28	0.035
	B	0.080	1.25	0.32	0.026	0.016	10.0	18.88	0.44	0.001	0.13	0.41	0.043
6	A	0.058	1.44	0.49	0.027	0.017	9.65	19.05	0.43	0.001	0.15	0.62	0.044
	B	0.046	1.46	0.66	0.026	0.024	8.48	18.88	0.22	0.001	0.13	0.17	0.034
7	A	0.052	1.30	0.55	0.028	0.016	9.35	18.65	0.38	0.002	0.12	0.26	0.039
	B	0.047	1.33	0.34	0.027	0.019	9.15	18.50	0.21	0.001	0.08	0.20	0.037
8	A	0.055	1.30	0.40	0.030	0.026	8.72	19.05	0.42	0.002	0.16	0.45	0.036
	B	0.078	1.75	0.40	0.033	0.018	8.30	19.66	0.44	0.003	0.54	0.34	0.043

Table 2-2: Weld metal chemical compositions (wt%) for archive pipe

Composition (wt-%)											
	C	Mn	Si	P	S	Ni	Cr	Mo	B	Co	Cu
1	0.038	1.39	0.41	0.023	0.018	9.65	20.15	0.23	0.002	0.11 0.11 ^a	0.21 0.20 ^a
2	0.052	1.45	0.41	0.022	0.019	10.50	19.20	0.20	0.005	0.10	0.22
3	0.039	1.25	0.39	0.020	0.017	10.16	19.56	0.21	0.004	0.20	0.21
4	0.047	1.41	0.43	0.022	0.018	10.75	19.29	0.17	0.005	0.094	0.20
5	0.048	1.52	0.42	0.023	0.010	10.15	19.96	0.26	0.001	0.16 0.17 ^a	0.23 0.18 ^a
6	0.050	1.56	0.49	0.024 0.022 ^a	0.008 0.010 ^a	10.12	19.87	0.24	<0.001	0.18	0.19 0.19 ^a
7	0.042	1.47	0.43	0.020	0.009	9.88	19.47	0.24	0.003	0.15	0.21
8	0.045	1.52	0.37	0.022	0.018	9.70	20.15	0.21	0.002	0.22	0.18 0.16 ^a

^a Duplicate Analysis Using Separate Stock

Table 2-3: Average Ferrite Levels for Weld Material of Archive Pipe

Ring #	Weld Reference	Ferrite (%)
1	2PW216W3	13.6
2	6PW1816W3	10.0
3	4PW16W5	15.0
4	1P1W1316W3	10.7
5	2PW1716W2	11.7
6	3PW1516W5	11.2
7	4PW416W4	14.2
8	2PW216W5	14.3

Table 2-4: Base metal chemical compositions (wt%) for R-Tank Disks A,B,C, and D and for the R-Tank plate composition reported by New York Shipbuilding Co.

		Composition (wt-%)											
		C	Mn	Si	P	S	Ni	Cr	Mo	B	Co	Cu	N
RA	3	0.050	1.02	0.60	0.027	0.015	8.54	17.2	0.076	<0.005	0.05	0.121	0.009
RB	3	0.016	1.15	0.54	0.008	0.013	8.79	18.2	<0.01	<0.005	0.058	0.046	0.070
RC	3	0.054	1.24	0.57	0.017	0.022	9.28	18.2	0.35	<0.001	0.027	0.069	0.080
RD	3	0.077	1.26	0.55	0.020	0.022	9.73	18.7	0.34	<0.001	0.026	0.075	0.045
R*	1	0.028	0.95	0.55	0.027	0.015	9.10	18.47	NA	NA	NA	NA	NA
	2	0.026	1.17	0.60	0.023	0.011	9.47	18.42	NA	NA	NA	NA	NA
	3	0.023	1.20	0.63	0.015	0.024	9.12	19.00	NA	NA	NA	NA	NA
	4	0.025	1.05	0.60	0.027	0.011	9.15	18.49	NA	NA	NA	NA	NA
	5	0.030	1.28	0.48	0.015	0.024	9.32	18.48	NA	NA	NA	NA	NA

* Tank plates 1 and 2 were in the upper half of the tank wall and plates 3, 4, and 5 were in the lower half of the tank wall.

Table 2-5: Base metal chemical compositions (wt%) for the K and L-Tank plates' composition reported by New York Shipbuilding Co.

		Composition (wt-%)											
		C	Mn	Si	P	S	Ni	Cr	Mo	B	Co	Cu	N
K	1	0.066	1.02	0.62	0.025	0.015	9.10	18.41	NA	NA	NA	NA	NA
	2	0.07	0.66	0.54	0.024	0.011	9.14	18.60	NA	NA	NA	NA	NA
L	1	0.055	0.77	0.58	0.026	0.013	9.28	18.43	NA	NA	NA	NA	NA

Table 2-6: Chemical composition and heat treatment of the Type 304L stainless steel material irradiated in the HFIR 1Q capsule [ref. 24, Appendix V].

Composition (wt-%)												
	C	Mn	Si	P	S	Ni	Cr	Mo	B	Co	Cu	N
F50 Plate	0.025	1.71	0.85	0.015	0.023	10.63	19.8	0.09	NA	0.11	NA	NA

Plate thickness: 1/2 inches.

Heat Treatment: Solution annealed at 1950-2000°F for 1/2 hour, water quenched.

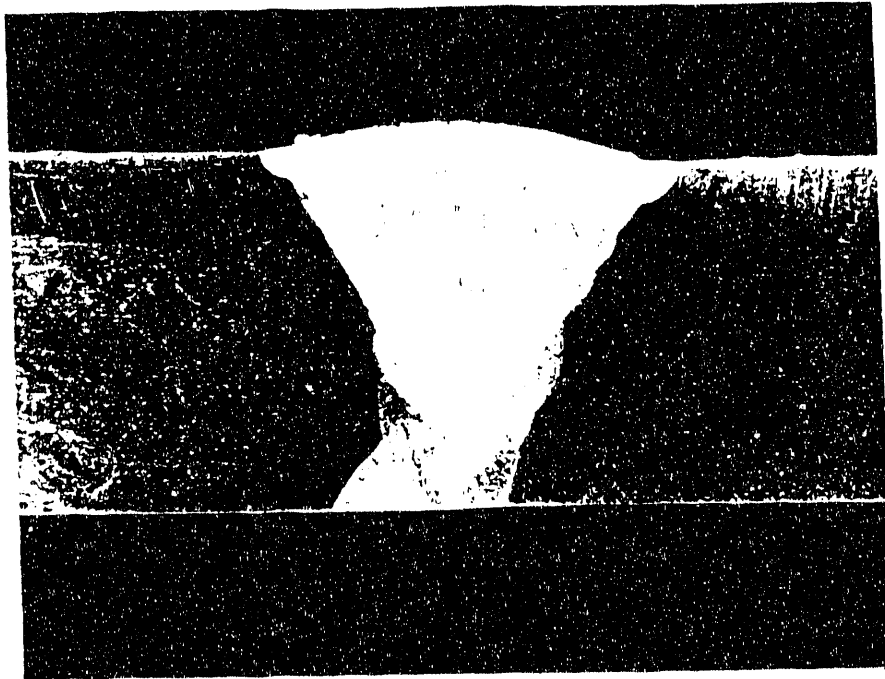


Figure 2-1: Etched cross section of pipe ring # 1 weld (4X)
(12.7 mm base plate thickness)

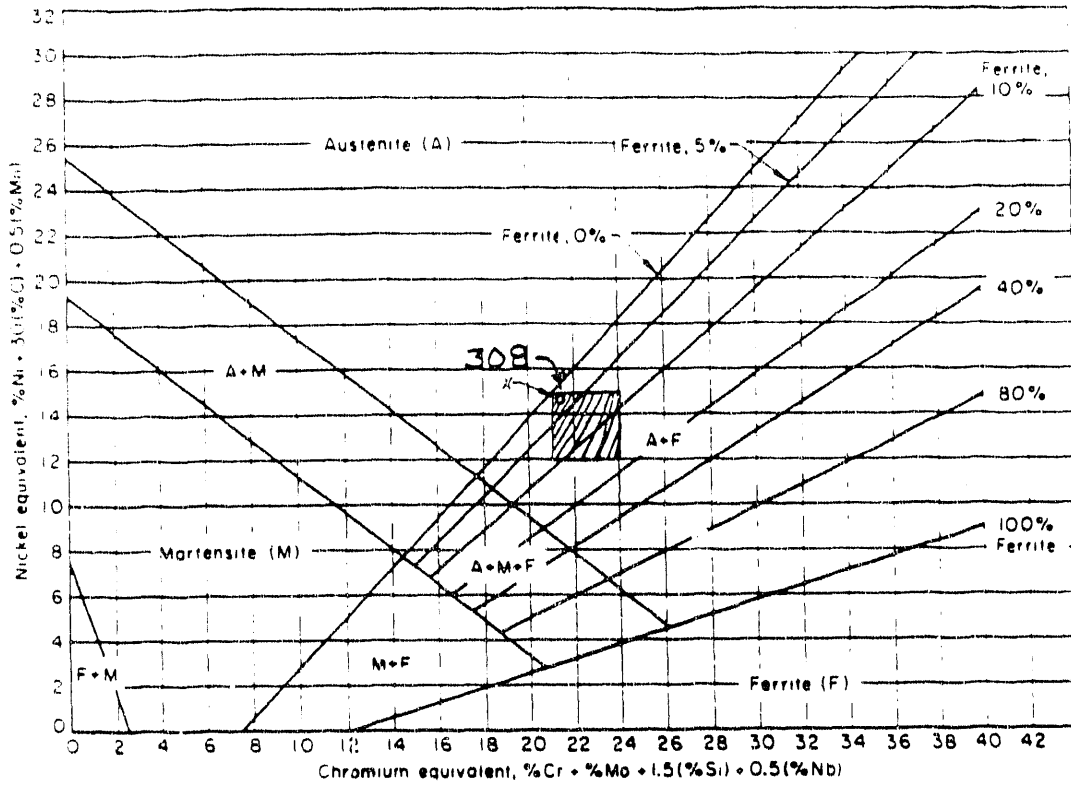


Figure 2-2: Modified Schaeffler Diagram from ASM Metals Handbook [23]

3.0 IRRADIATION PROGRAM OVERVIEW

3.1 Introduction

The irradiations of the Reactor Materials Program [4, 5] are the Screening Irradiation conducted in the University of Buffalo Reactor (UBR), Buffalo Materials Research Center, at the State University of New York at Buffalo, the Full-Term Irradiation conducted in the Removable Beryllium position in the High Flux Isotope Reactor (HFIR) at Oak Ridge National Laboratory, and the Surveillance Irradiation conducted in the K reactor at SRS. The Screening Irradiation of mechanical specimens was performed in 1985 and the testing of all specimens has been completed with the results reproduced in this report. Irradiations in the HFIR included: the 4M and 12M mechanical specimen capsules containing the archival piping weldment materials, as part of the Full-Term Irradiation; and the 1Q qualification capsule, containing mechanical specimens of Type 304L stainless steel plate material. The as-irradiated testing of all specimens from the 1Q and 4M capsules has been completed with the results reproduced in this report. Testing of the 12M capsule will be performed in accordance with RMP Specification SRP-SL-1111, Rev. 2 [28].

The RMP Surveillance Irradiation capsules containing mechanical and corrosion specimens [29] were loaded in K reactor [30] and began irradiation in March 1986. The target irradiation level for the initial testing was to match the tank wall fast fluence ($E_n > 0.1$ MeV). At historic full power levels (2400 MW), an irradiation period of 4 years would have been required; however extended shutdowns and reactor power reductions have reduced the exposure rate and therefore increased the time required to reach tank wall maximum exposure levels in the Surveillance Irradiation. Revised target exposures and a testing plan for the K specimens will be developed in a future RMP report [5].

Mechanical specimens were cut from discs removed from the R-tank sidewall at four separate tank wall locations, with two disks each exposed to the same exposure conditions [26] and were tested as part of the Reactor Operability Assurance Program [20]. The R-Reactor reached initial criticality on December 28, 1953 and operated continuously from that date, with the exception of normal reactor shutdowns and shutdowns for facility improvements, until June 17, 1964, at which time reactor operations were permanently terminated. The exposure history of the R-tank sidewalls are contained in reference 1.

An irradiation of tensile specimens of weldment components of a thermal shield model was performed in P reactor in 1959 [19] for four one-month cycles (P-8 through P-11). The specimens were tested by SRL in 1960 [10].

The testing procedures of the mechanical specimens from the UBR, HFIR, R-Tank, and P-reactor (thermal shield model) irradiations are reported in Section 4. The individual specimen mechanical testing results are contained in Appendix 1 with the results summarized in Section 5 of this report.

3.2 Irradiation Parameters - Summary

Tables 3-1 to 3-3 lists the irradiation parameters for the set of specimens from the HFIR, R-Tank, and P-reactor (thermal shield model) irradiations from which as-irradiated test results are included in this report. The irradiation parameters include specimen identification, weldment type and orientation, fast neutron fluence ($E_n > 0.1$ MeV), thermal neutron fluence, dpa, and irradiation temperature.

All of the UBR specimens were irradiated to a nominal thermal fluence of 1.1×10^{19} n/cm² and fast fluence of 1.1×10^{20} n/cm², $E_n > 0.1$ MeV and a displacement damage level of 0.065 dpa [24]. The parameters for the UBR specimens are not listed individually.

The as-irradiated database will be supplemented by results from the HFIR 12M and K-Reactor Surveillance. Several specimens from the 4M and 1Q capsules were reserved for thermal-cycle testing [5, 9]; these specimens, testing conditions, and results are not reported herein.

3.3 Screening Irradiation: University of Buffalo Reactor

The UBR is a 2 MW light-water-cooled and moderated reactor located in the Buffalo Materials Research facility. The 81 Charpy V-notch and 12 Tensile specimens (see Appendix 1) were contained in three, independently temperature-controlled capsules designated A, B, and C, which together formed one irradiation assembly. Capsule A was placed over capsule B which itself was placed over capsule C for irradiation in the B-4 position in the fuel lattice of the UBR. The B-4 facility had been previously benchmarked for neutron spectra conditions for the Nuclear Regulatory Commission irradiation studies.

To achieve fluence balancing of the specimens, capsule B, which bisects the peak neutron flux plane, was removed and replaced with a dummy capsule prior to the end of the irradiation. The experiment was loaded into the core on May 31, 1985 and the neutron exposure was completed September 6, 1985.

Thermocouples welded to specimen midsections were used for temperature monitoring. The target temperature for each capsule was $120^\circ\text{C} \pm 15^\circ\text{C}$. Actual minimum and maximum thermocouple readings from twenty-two thermocouples were 113 and 132°C , respectively. Uncertainty in dosimetry analysis was reported from $\pm 5\%$ to $\pm 8\%$ at the 1σ confidence level for the fast fluences and $\pm 10\%$ for the thermal fluences. These estimates did not include any uncertainties that would be associated with the actual averaged cross sections of the irradiation fields or the burn-out of the reaction products of interest. Additional details of the Screening Irradiation are contained in reference 24.

3.4 Full-Term Irradiation: High Flux Isotope Reactor

The HFIR is a 85 MW (100 MW prior to November 1986 extended shutdown) pressurized water research reactor at the Oak Ridge National Laboratory. The SRL irradiations in the HFIR were specified in RMP Specification SRP-SL-1107 [31] and planned through the Engineering Technology Division at ORNL [32]. The 1Q capsule, the Qualification capsule (prototype for the 4M and 12M capsules) for the SRL irradiations, was instrumented with thermocouples, Removable Dosimeter Tubes, Backbone Dosimeter Sets, and Small Gradient Monitors to characterize the irradiation conditions in the SRL capsules. The 1Q irradiation ran one HFIR irradiation cycle beginning June 6 and ending June 28, 1986. The 4M irradiation ran four HFIR cycles beginning July 23, 1986 to October 23, 1986.

The 12M irradiation began July 23, 1986 and ran for five cycles at 100 MW until November 14, 1986. At that time, the HFIR was shutdown for extensive reviews of containment, operation, and other issues. The shutdown lasted until June 1990. The 12M irradiation recommenced July 17, 1990 and ran four cycles at 85 MW until December 12, 1990. The 12M experiment was taken out of the reactor at that time for reactor maintenance and subsequently a capsule weld was broken. The 12M capsule was repaired and ran the remaining 3 irradiation cycles from June 20,

1991 to September 17, 1991. The cycle length at 85 MW was increased so that the fluence per cycle at 85 and 100 MW was approximately equal.

Exposure conditions were assumed constant across the capsule cross section in calculating the specimen fluence and dpa levels [13]. Analysis of the 1Q and 4M dosimeter sets is provided in reference 33. Irradiation temperatures recorded at seven specimen locations in the 1Q irradiation [results directly applicable to the 4M irradiation] included mid-specimen and specimen surface temperatures for the T, CVN, and CT specimens at each end of the capsule and at capsule mid-plane. The temperature ranges were 75 to 95°C for the T specimens, 100 to 140°C for the CVN specimens, and 110 to 150°C for the CT specimens [13]. Full details including an uncertainty analysis of individual specimens exposures and irradiation temperatures for the HFIR irradiations (including the 12M) will be provided in a future RMP report [5]. The 12M as-irradiated testing will be performed in 1992 and the results will be added to the database at a future date.

Specimen selection for the HFIR 1Q, 4M, and 12M capsules is discussed in reference [34]. The 1Q and 4M specimen complements are given in Table 3-1. The HFIR 4M specimens included base, weld, HAZ components in both the L-C and C-L for each component except for the weld material, which is oriented in the L-C direction only. The specimen set included material with the highest carbon content available, 4BB, and the lowest carbon content available, 1BB. In addition, the weldment component and piping material with the lowest fracture toughness from the baseline testing program [35], (7HA, C-L), was included in the HFIR 4M capsule.

3.5 R-Reactor Tank Irradiation

R-tank sidewalls were irradiated during reactor operation from 1953 to 1964. The fast and thermal neutron exposure levels of the R-Tank sidewalls are provided in reference 1. Conversion from neutron fluence (thermal and fast) to dpa for the SRS reactor spectrum is based upon the multigroup displacements cross sections of Doran [36] and two-step neutron reaction with Ni-58 given by Greenwood [37] as modified for the SRS reactor spectrum by Baumann [see ref. 3]. A chart to convert from fluence to dpa for the SRS reactor spectrum is shown in Figure 3-1.

Four disks (labelled A, B, C, and D) approximately 6 inches in diameter were cut from R-tank in 1986 as part of the Reactor Operability Assurance Program [20, 26]. The disks A & C and B & D were irradiated to fast fluence ($E_n > 0.1$ MeV) levels of 1 and 7×10^{20} n/cm² [1, 20, 26] with corresponding thermal fluences of 6×10^{21} and 3.5×10^{21} n/cm² [13], respectively. Table 3-2 contains the individual irradiation parameters of the R-tank disk specimens. The R-tank D disk also contained a maximum helium level (measured) of 34 appm and the A disk contained a maximum of 12 appm [1]. [Note that the labeling of A & C and B & D disk locations in Figure 1 of ref. 1 is reversed].

3.6 Thermal Shield Materials Irradiation

Twenty tensile specimens sectioned from base, weld, and heat-affected zone were irradiated in the P reactor in 1959 (reactor cycles P-8 through P-11) and were tested in the SRL High Level Caves in 1960. Details of the irradiation are in the Test Authorization TA 1-757 [19]. The irradiation parameters (fast fluence, $E_n > 0.1$ MeV) and test results in this report were reproduced from reference 10. An irradiation temperature of 119°C was calculated as the maximum temperature of the tensile specimens during the irradiation [38]; . Two different nominal fluence levels, 2.9×10^{20} and 1.2×10^{21} n/cm² ($E_n > 0.1$ MeV), were achieved in the irradiation. Specimen fluences were determined by flux traverses near the specimens; uncertainty was

estimated at $\pm 35\%$ [38, 39]. Table 3-3 contains the individual specimen irradiation parameters of the specimens of the thermal shield model.

3.7 Surveillance Irradiation: K-Reactor

The K-Surveillance program contains 180 mechanical specimens of CT, T, CVN and Wedge Opening Loaded (WOL) design [29, 30, 40] loaded in 12 separate specimen holders with 4 holders per specimen rod. The specimen rods are located in the far side spargers at positions X35-Y57, X29-Y33, and X20-Y54. The 3 specimen rods or irradiation assemblies were changed to K-Reactor at the start of K-12.1 which began in March 1986. The irradiation plan and testing plan for the specimens in the Surveillance Irradiation will be updated [41] from the previous plan [29, 30] in a future RMP report [5].

Table 3-1 HFIR 1Q and 4M Specimen Irradiation Parameters [13].

Specimen ID	Specimen Type	Orientation	Thermal Fluence, 10^{21} n/cm ²	Fast Fluence, $E_n > 0.1$ MeV, 10^{21} n/cm ²	dpa
1Q Capsule					
F50-12	T	L-T	1.2	0.36	0.21
F50-9	T	L-T	2.1	0.60	0.34
F50-1	T	L-T	2.7	0.77	0.43
F50-6	T	L-T	3.1	0.89	0.50
F50-8	T	L-T	3.2	0.92	0.52
F50-13	CVN	L-T	1.2	0.36	0.21
F50-19	CVN	L-T	2.1	0.60	0.34
F50-14	CVN	L-T	2.7	0.77	0.43
F50-23	CVN	L-T	3.1	0.89	0.50
F50-17	CT	L-T	1.2	0.36	0.21
F50-18	CT	L-T	2.0	0.58	0.33
F50-12	CT	L-T	2.3	0.67	0.38
F50-19	CT	L-T	3.0	0.88	0.50
F50-13	CT	L-T	3.1	0.90	0.51
F50-8	CT	L-T	3.2	0.92	0.52
4M Capsule					
3HA8	T	L-C	6.2	1.8	1.0
1BB1	T	L-C	9.3	2.7	1.5
5BA5	T	C-L	11.4	3.3	1.9
4BB2	T	C-L	12.8	3.7	2.1
1BB4	T	L-C	13.1	3.8	2.1
6W1	CVN	L-C	6.2	1.8	1.0
6HA6	CVN	L-C	9.3	2.7	1.5
3HB1	CVN	L-C	11.4	3.3	1.9
4BB9	CVN	C-L	12.8	3.7	2.1
1BB5	CVN	L-C	13.1	3.8	2.1
3HA5	CT	L-C	6.2	1.8	1.1
1BB8	CT	L-C	7.6	2.2	1.3
1BB16	CT	L-C	9.0	2.6	1.5
2W2	CT	L-C	10.0	2.9	1.7
5BA7	CT	C-L	11.0	3.2	1.8
3HB4	CT	L-C	11.7	3.4	1.9
7HA5	CT	C-L	12.4	3.6	2.1
7HA7	CT	C-L	12.4	3.6	2.0
1BB9	CT	L-C	12.8	3.7	2.1
4BB10	CT	C-L	13.1	3.8	2.1

Table 3-2 R-Tank Specimen Irradiation Parameters [1, 13, 26]. The temperature during irradiation was below 130°C. The R-disk A was cut at a tank azimuthal position near the peak fast fluence sector; the R-disks B & D were cut from tank azimuthal positions near the gas port. [Note that the labelling of A & C and B & D disk locations in Figure 1 of ref. 1 is reversed].
Dpa levels are calculated from Figure 3-1.

Specimen ID	Specimen Type	Orientation	Irradiation Temp (°C)	Thermal Fluence, 10 ²¹ n/cm ²	Fast Fluence, E _n >0.1MeV, 10 ²¹ n/cm ²	dpa
RA3 Disk						
3A1c	Sub T	-	< 130	3.5	0.7	0.5
3A2a	Sub T	-	< 130	3.5	0.7	0.5
3A3c	Sub T	-	< 130	3.5	0.7	0.5
RA37	0.8T CT	-	< 130	3.5	0.7	0.5
RA38	0.8T CT	-	< 130	3.5	0.7	0.5
RD3 Disk						
4E	Sub T	-	< 130	6	0.1	0.21
4B	Sub T	-	< 130	6	0.1	0.21
5I	Sub T	-	< 130	6	0.1	0.21
3F	Sub T	-	< 130	6	0.1	0.21
RD37	0.8T CT	-	< 130	6	0.1	0.21
RD39	0.8T CT	-	< 130	6	0.1	0.21
RD314	0.4T CT	-	< 130	6	0.1	0.21
RD313	0.4T CT	-	< 130	6	0.1	0.21
RB3 Disk						
1F5	Sub T	-	< 130	6	0.1	0.21
1F3	Sub T	-	< 130	6	0.1	0.21

Table 3-3 Thermal Shield Materials Irradiation in P-reactor [10, 19, 38]. The thermal fluence is approximately 10X the fast fluence. Dpa levels are calculated from Figure 3-1.

Specimen ID	Specimen Type	Orientation	Irradiation Temp (°C)	Thermal Fluence, 10^{21} n/cm ²	Fast Fluence, $E_n > 0.1$ MeV, 10^{21} n/cm ²	dpa
Weld, Longitudinal (see Figure 4-6)						
1	T	Long.	< 119°C	2.5	0.25	0.2
2	T	Long.	< 119°C	3.0	0.30	0.2
3	T	Long.	< 119°C	10	1.0	0.6
4	T	Long.	< 119°C	12	1.2	0.6
Weld, Transverse						
1	T	Trans.	< 119°C	2.7	0.27	0.2
2	T	Trans.	< 119°C	3.0	0.30	0.2
3	T	Trans.	< 119°C	11	1.1	0.6
4	T	Trans.	< 119°C	12	1.2	0.6
Heat-Affected-Zone, Longitudinal						
1	T	Long.	< 119°C	2.8	0.28	0.2
2	T	Long.	< 119°C	11	1.1	0.6
Heat-Affected-Zone, Transverse						
1	T	Trans.	< 119°C	2.9	0.29	0.2
2	T	Trans.	< 119°C	11	1.1	0.6
Plate, Longitudinal						
1	T	Long.	< 119°C	2.9	0.29	0.2
2	T	Long.	< 119°C	3.0	0.30	0.2
3	T	Long.	< 119°C	12	1.2	0.6
4	T	Long.	< 119°C	12	1.2	0.6
Plate, Transverse						
1	T	Trans.	< 119°C	2.9	0.29	0.2
2	T	Trans.	< 119°C	3.0	0.30	0.2
3	T	Trans.	< 119°C	11	1.1	0.6
4	T	Trans.	< 119°C	12	1.2	0.6

Neutron Radiation Damage Ranges for P Reactor Midplane

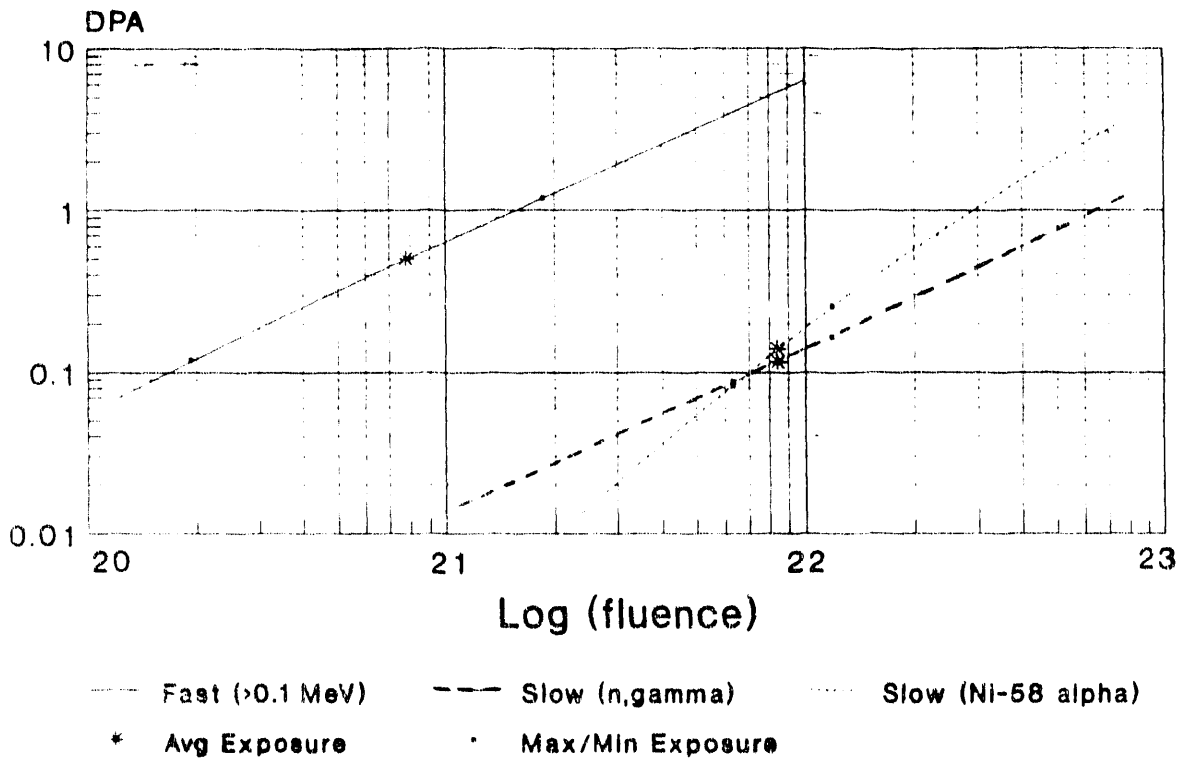


Figure 3-1 Conversions from thermal and fast neutron fluence to displacements per atom for the SRS reactor spectrum [3]. The thermal fluence contributions to dpa include the two-step thermal neutron reaction with Ni-58 with the cross sections provided by Greenwood [37].

4.0 MATERIALS TESTING AND ANALYSIS OF DATA

4.1 Overview

Mechanical properties and corrosion characteristics of the weldment components (Base, Weld, and weld Heat-Affected-Zone (HAZ) materials) are measured with Charpy-V notch (CVN), tensile (T), compact tension (CT), constant extension rate tensile (CERT), and wedge-opening-loaded (WOL) specimens [4, 5, 7]. The source materials for the irradiated mechanical property studies are described in reference 7 and summarized in Section 2 of this report. The RMP irradiations (Screening in the University of Buffalo Reactor and Full-term in the High Flux Isotope Reactor) contained CVN, T, and CT specimens identical in design and material type to specimens tested in the baseline (unirradiated) program of the RMP [35] providing a one-to-one specimen match and allowing computation of the radiation-induced change in mechanical properties. Specimens in the RMP included base, weld, and weld heat-affected-zone components tested at temperatures of 25 and 125°C, approximately bounding the tank sidewall operating temperatures for power levels up to 2400 MW operation [2].

Tensile tests of specimens cut from a model of the thermal shield (see Section 2.3) and irradiated in P-reactor [38] were also performed. The Thermal Shield irradiation materials included Base, Weld, and HAZ components. The specimens were tested in two orientations, longitudinal (parallel to the weld) and transverse (perpendicular to the weld), which correspond to the C-L and L-C orientations, respectively, of the RMP tensile specimens.

Base material of the R-tank was tested from the R-tank discs (see Section 2.4). Subsize T specimens and two separate CT planforms (0.8T and 0.4T) were tested at temperatures of 25 and 125°C. Other test temperatures, outside of the range 25 to 125°C, were investigated in the R-tank testing program [11, 12] but are not listed in this report.

4.2 As-Irradiated Test Conditions Summary

The RMP specimen designs for CVN, T, and CT specimens, the R-tank disk CT and T specimen designs, and the Thermal Shield T specimen design are described below. Final design for the CT specimens was based on an evaluation of the effects of substandard (ASTM E399) specimen size, load hole size and position, and side-grooves, as described in reference 35. The final specimen CT design (E399 SR) [35, 42] was used in the HFIR 1Q and 4M irradiated specimen testing. The testing results for the individual specimens at the conditions recorded below are listed in Appendix 1 and summarized in Section 5.

The RMP specimens were machined to the applicable ASTM specifications (including the CT E399 SR design), and assigned a unique identifier number that allowed traceability throughout their testing history, as well as identification of their location and orientation with respect to the original pipe ring section. The first number of this code identifies the pipe ring number, and the adjacent letter indicates the material type (W = weld, B = base, and H = heat-affected-zone or HAZ). The second letter (applicable to base and HAZ material only) identifies the side with respect to the circumferential weld from which the specimen came from in the pipe ring (side A or side B) as referenced in the cutting diagrams [see Appendix D of Reference 24]. The RMP specimens also included irradiation of Type 304L stainless steel in the HFIR 1Q capsule. The Type 304L stainless steel was from wrought plate supplied by MEA (Code F50) [24, 43]. The RMP irradiated specimen tests (from UBR and HFIR 4M irradiations) were conducted at temperatures of 25 and 125°C controlled to $\pm 5^\circ\text{C}$ [5] and included both the ASTM L-C and C-L specimen orientations (see Figure 4-1) [24, 42]. The specimen configuration and testing of the

1Q specimens was identical to the UBR (CVN and T) and HFIR 4M (CVN, T, and CT) materials testing.

Table 4-1 contains the mechanical specimen test matrix indicating the specimen material origin (ring number), mechanical specimen type, orientation and test temperature for the RMP (UBR and HFIR 4M) specimens. Table 4-2 contains the T specimen test matrix for the Thermal Shield specimens, and Table 4-3 contains the test matrix for the CT and T specimens cut from the R-tank disks. Table 4-4 contains the test matrix for the Type 304L stainless steel material (F50 plate) irradiated in the HFIR 1Q capsule.

Sections 4.3 to 4.5 describe the specimen design and testing of the (CVN, T and CT) for the UBR and HFIR specimens. An overview of the thermal shield materials testing (Section 4.6) and the R-tank materials testing (Section 4.7) is also provided and references are given for additional testing details.

4.3 UBR and HFIR Charpy Impact Testing

The CVN specimen design for notch toughness testing for the UBR and HFIR irradiations is shown in Figure 4-2. The dimensions conform with those of the standard size Type-A specimen identified in ASTM E 23-81, "Standard Methods for Notch Bar Impact Testing of Metallic Materials." The impact tests were conducted in accordance with this standard at the Buffalo Materials Research Center. The baseline specimen test matrix shown in Table 4-1 lists the number of specimens for each material melt tested at 25 or 125°C. The test results of absorbed energy and lateral expansion for each specimen are contained in Appendix 1.

4.4 UBR and HFIR Tensile Testing

The tensile test specimen design (Figure 4-3) conforms to ASTM standards E8-81 and E21-79. Test results of yield (0.2% offset) and tensile strengths (engineering), uniform elongation, and percent reduction in area at specimen failure for each specimen are contained in Appendix 1. All stress-strain curves were recorded over the entire range of load, up to failure and are recorded as both engineering and true stress strain curves (Task Files 89-023-C-1).

4.5 HFIR Compact Tension Testing

Fracture toughness was evaluated by analysis of J-R curves obtained from specimens tested by procedures that were in general conformance to ASTM E 813-81 (also E813-88) and ASTM 1152. Due to piping size constraints, the CT specimens were limited to a 0.4T-CT thickness, that is, a 0.394-in (10 mm) thick specimen was the maximum that could be machined from the pipe considering the curvature of the large diameter pipe stock. The diameter and location of the loading holes were modified slightly to produce consistent and conservative J-R curves. All specimens were side-grooved (10% on each side or 20% total) to reduce crack tunneling and to provide an even, parallel crack front to assess crack extension. The final specimen design, shown in Figure 4-4, was based upon extensive testing and comparison with specimens of standard design [35].

A conventional load cell was used to measure the applied load to the CT specimen during testing. Specimen load-line displacement was measured with an outboard clip gage. Crack extension was calibrated with single-specimen compliance techniques. J-integral resistance (J-R) curve analysis was performed for both the modified-J (J_M) and deformation-J (J_D) approach from the load versus crack extension data. Flow stress values, $(s_y + s_u)/2$ (where s_y and s_u are the engineering yield and ultimate tensile strengths, respectively) were obtained from corresponding

tensile data or from estimated flow stress properties in the cases where no corresponding data existed [42]. A power-law of the form $J = C(\Delta a^n)$ was fit to the data between the exclusion lines (ASTM E 813-81, E 813-88) with the power law toughness corresponding to the onset of stable tearing, J_{IC} , defined as the intersection of the power law curve with the 0.15 mm (0.006 in) exclusion line (see Figures 4-5A and 4-5B). The power law formulation of the J-R curve was employed to facilitate construction of the material J-T curve discussed in Sections 6 and 7. Values for J_{IC} were also obtained as specified in ASTM E813-81 with results similar to those from the power law formulation [24, 42, 44].

4.6 Thermal Shield Tensile Testing

Tensile specimens cut from the thermal shield model were 8-inches long with a gauge length of 2-inches, a width of 0.500-inches, and a thickness of 0.375-inches as shown in Figure 4-6. Tensile tests were performed at room temperature on a 60,000 pound capacity tensile machine with a strain rate of 0.005 inch/inch/minute [38, 39]. Strains were measured with a high magnification extensometer and recorded to a strain of 0.8%. The extensometer was then removed. Total elongation was calculated from the original and final specimen lengths. Yield and ultimate strengths were based on the original cross sectional area. These tests were conducted in the high level caves at SRL.

4.7 R-Reactor Tank Mechanical Testing

Tensile tests of sub-sized specimens, Figure 4-7, were conducted on an Instron tensile machine according to pertinent sections of ASTM specifications E8 and E21 [12]. Tensile specimens were taken from discs RA3, RB3, and RD3 and thus sampled the full range of irradiation damage levels and helium contents. Initial and final specimen diameters were measured by micrometer and from 2.5X photographs, respectively. Errors in diameter measurements were ± 0.0001 and ± 0.003 -inch, respectively. Specimen elongation and strain rate were calculated from cross-head travel assuming a stiff machine and hence are approximate but allow comparison among the specimens as they were treated alike. Tests at 25 and 125°C were conducted in air. Specimens were held at temperature for 15-minutes before testing.

The J-integral tests for fracture toughness were all performed on compact tension specimens of the dimensions shown in Figures 4-4 or 4-8 at 25 or 125°C [11]. The four larger specimens (RA3-7A, RA3-8, RD3-7 and RD3-9) had a plan form of 0.8T-CT, but were only 0.45-inches thick. The specimen thickness and plan form were limited by the thickness and curvature of the tank wall. The four smaller specimens machined from disc RD3 were 0.394-CT specimens with 20% sidegrooves (0.315-inch thick net section). Sidegrooves promote straight crack fronts and facilitate crack extension measurement.

The CT specimens were tested on a 20,000 pound capacity screw driven Instron tensile machine. Crack lengths were determined by the unloading compliance method with load line clip gauges to measure displacements. Rotation corrections were made to the crack length measurements. Load-displacement data were collected and stored by computer for analysis by both J-deformation and J-modified procedures.

Table 4-1: Irradiated Specimen Test Matrix [Mechanical Test / Orientation/ Temperature (°C)]
 for the RMP archive pipe weldment components (UBR and HFIR 4M Irradiation)

Material Heat	Tensile				Charpy-V Impact				CT-Toughness				
	L-C		C-L		L-C		C-L		L-C		C-L		
	25	125	25	125	25	125	25	125	25	125	25	125	
1BB	-	2	-	-	-	1	-	-	-	-	3	-	-
3BA	-	-	-	-	3	3	3	3	-	-	-	-	-
4BB	-	-	-	1	-	-	-	1	-	-	-	-	1
5BA	-	-	-	1	-	-	-	-	-	-	-	-	1
1HA	-	-	-	-	3	-	-	-	-	-	-	-	-
1HB	-	-	-	-	3	-	-	-	-	-	-	-	-
2HA	-	-	-	-	3	-	-	-	-	-	-	-	-
2HB	-	-	-	-	3	-	-	-	-	-	-	-	-
3HA	-	1	-	-	3	3	3	3	-	1	-	-	-
3HB	-	-	-	-	-	1	-	-	-	1	-	-	-
4HA	-	-	-	-	3	-	-	-	-	-	-	-	-
4HB	-	-	-	-	3	-	-	-	-	-	-	-	-
5HA	-	-	-	-	3	-	-	-	-	-	-	-	-
5HB	-	-	-	-	3	-	-	-	-	-	-	-	-
6HA	-	-	-	-	3	1	-	-	-	-	-	-	-
6HB	-	-	-	-	2	-	-	-	-	-	-	-	-
7HA	-	-	-	-	-	-	-	-	-	-	-	-	2
1W	-	-	-	-	4	2	-	-	-	-	-	-	-
2W	-	-	-	-	2	1	-	-	-	1	-	-	-
3W	-	-	-	-	3	-	-	-	-	-	-	-	-
4W	-	-	-	-	3	-	-	-	-	-	-	-	-
5W	2	1	-	-	3	-	-	-	-	-	-	-	-
6W	2	1	-	-	3	1	-	-	-	-	-	-	-
7W	-	-	2	1	-	-	-	-	-	-	-	-	-
8W	-	-	2	1	3	3	-	-	-	-	-	-	-

Table 4-2: Specimen Test Matrix [Tensile Specimens in longitudinal or transverse orientation (see Figure 4-6)] for the Thermal Shield Weldment Components (Base, Heat-Affected-Zone, and Weld). The specimens were all tested at room temperature (25°C) [10].

Material Type	Orientation (see Figure 4-6)	
	Longitudinal	Transverse
Base	4	4
Heat-Affected-Zone	2	2
Weld	4	4

Table 4-3: Specimen Test Matrix [Mechanical Test/Temperature (°C)] for the base material from R-Task Disks [11, 12].

R-Task Disk (Base Material)	Tensile		CT-Toughness	
	25	125	25	125
A	3	-	2	-
D	1	3	-	4
B	2	-	-	-

Table 4-4: Specimen Test Matrix [Mechanical Test] for the HFIR 1Q specimens comprised of wrought plate of Type 304L stainless steel. The specimens were all tested at 125°C.

Material Type 304L Plate (F50)	Tensile	Charpy	CT-Toughness
	5	4	6

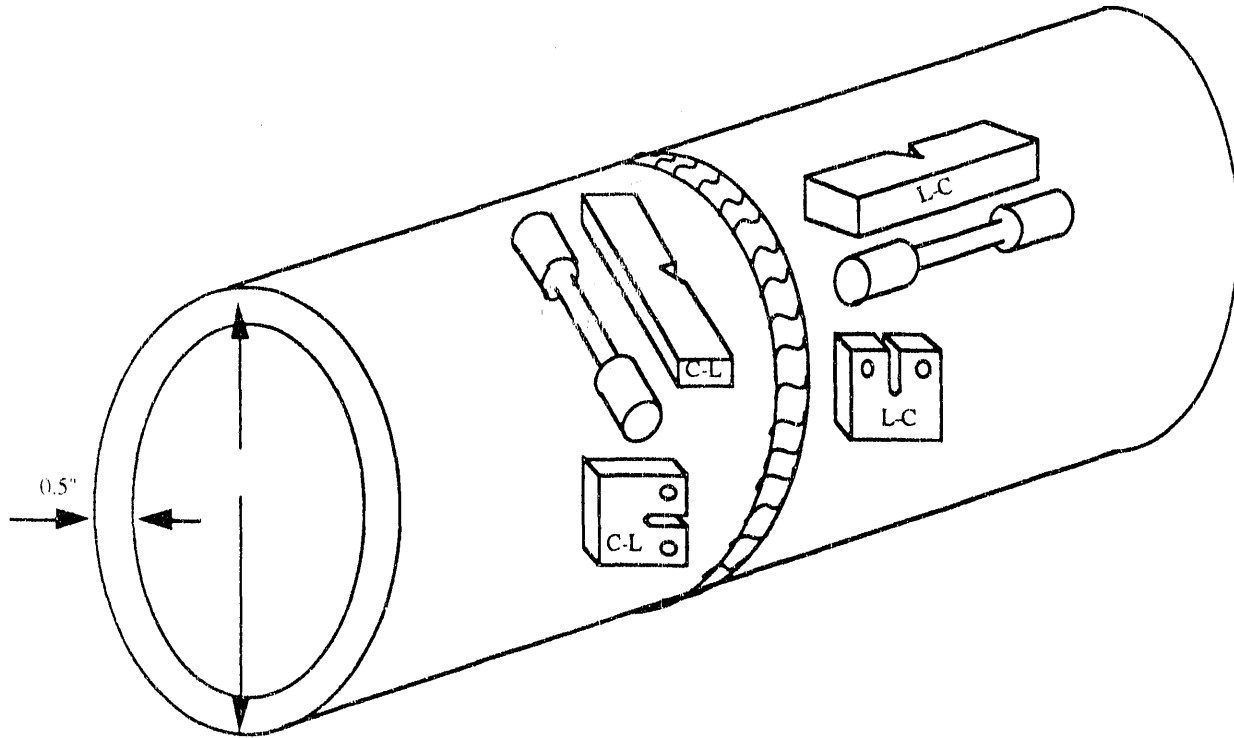


FIGURE 4-1: Schematic illustration of specimen orientation in the pipe ring (archive RMP Materials [7]). The rolling direction of the original plate used to make the piping is parallel to the pipe axis. The rolling direction of the plate materials used to make the tank sidewalls is presumed to be parallel to the original plate length, along the tank circumferential direction.

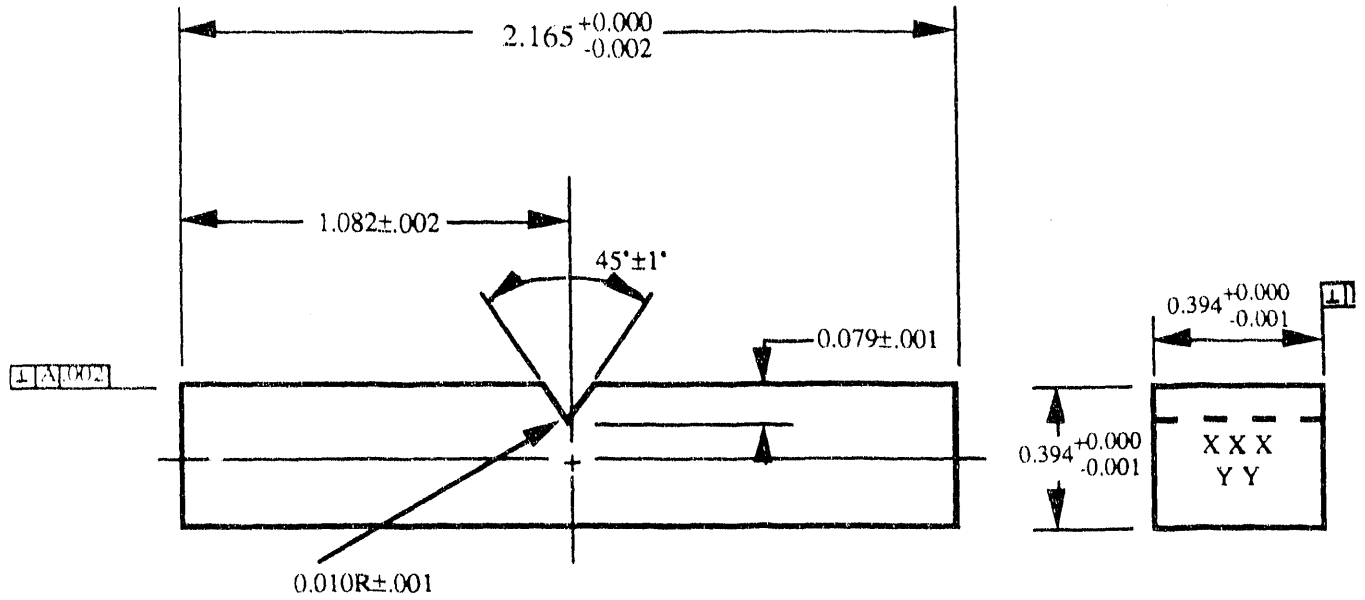


FIGURE 4-2: UBR and HFIR Charpy Impact Specimen Dimensions (inches).

Type	DIM "A"	DIM "B"
1	7/16 - 14 UNC	0.340 TYP
2	5/16 - 18 UNF	0.235 TYP

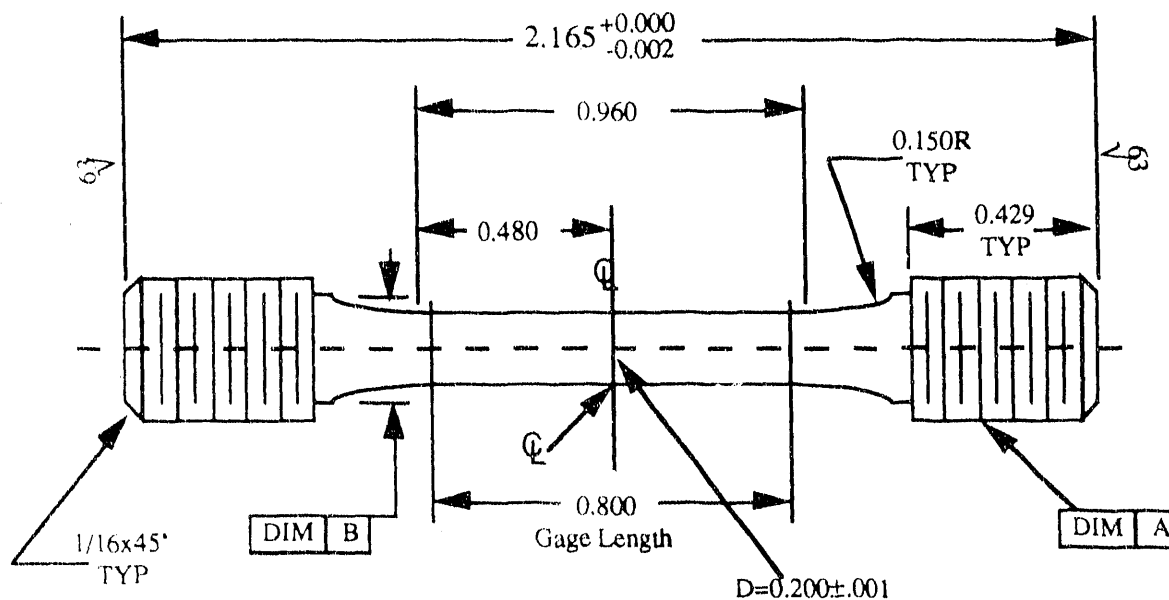


FIGURE 4-3: UBR and HFIR Tensile Specimen Dimensions (inches) [Type 2].

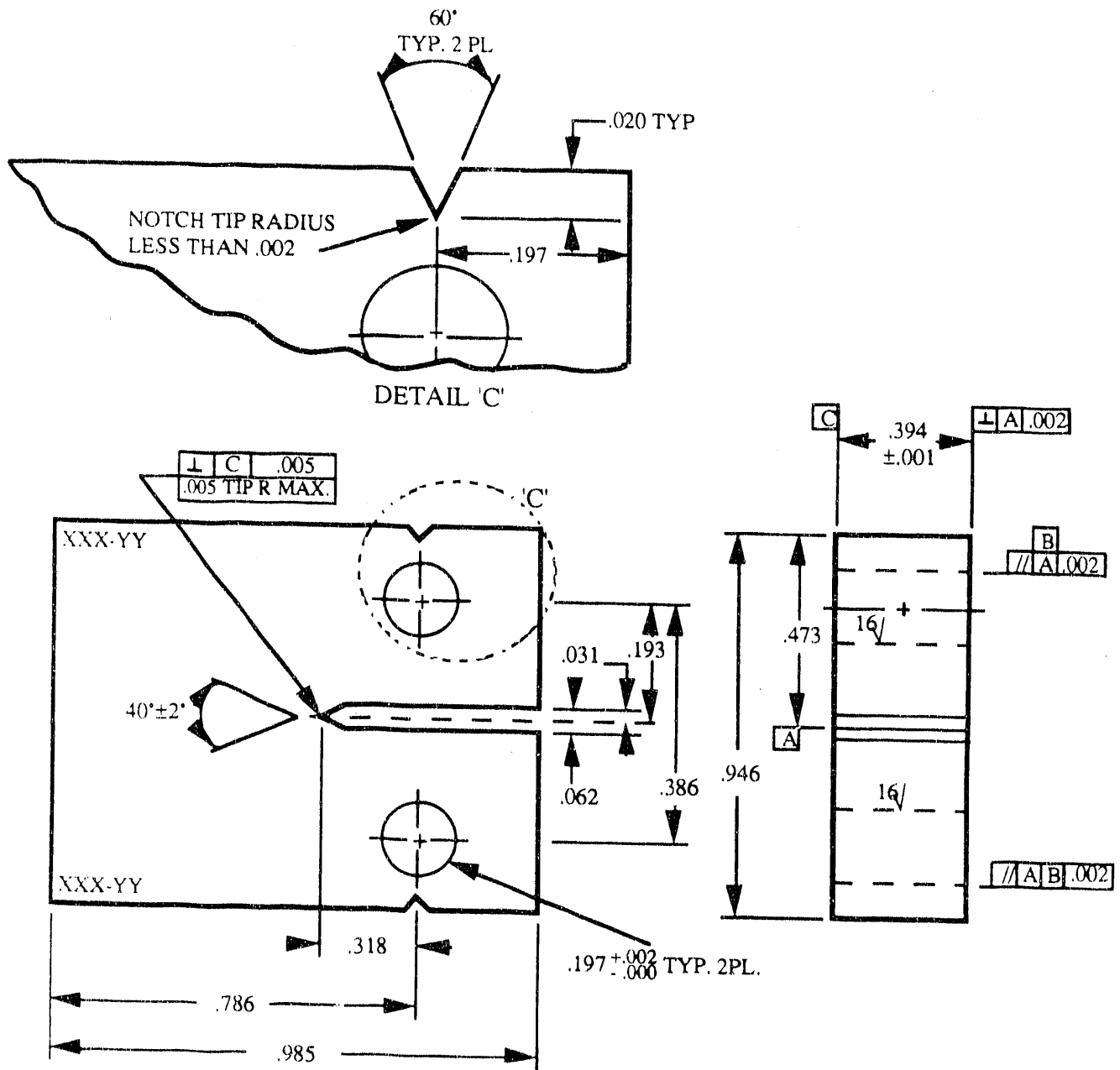


FIGURE 4-4: HFIR 0.4T Compact Tension Specimen Dimensions (inches). The final specimen design included 20% (10% each side) sidegrooving of the notch plane. R-tank CT specimen designs also included this 0.4T design and a 0.8T planform design [11].

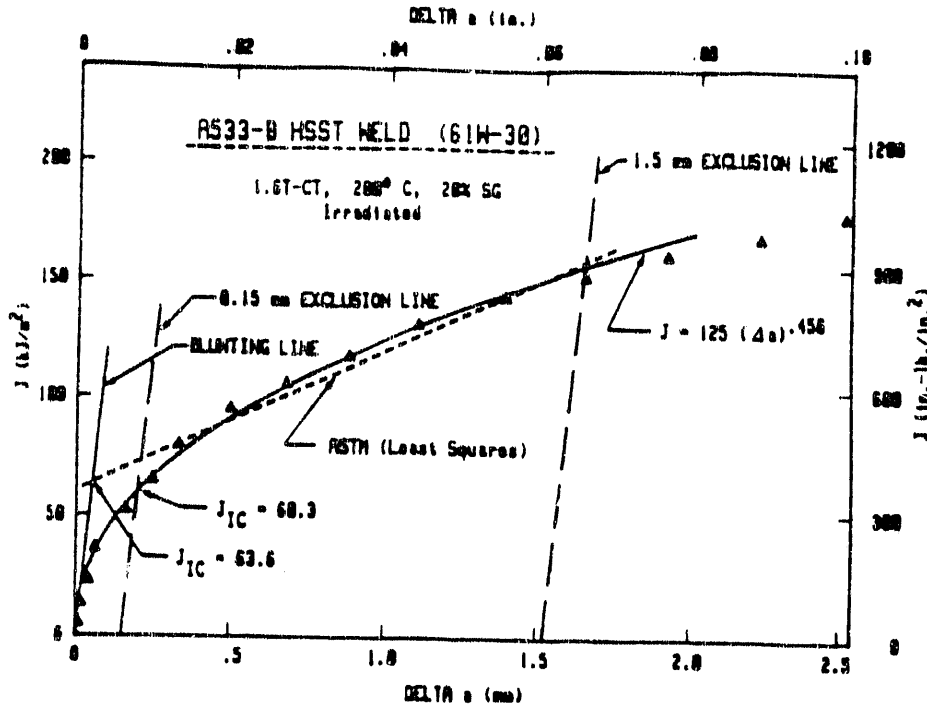


Figure 4-5A: Example of a typical J-R curve. The ASTM E813-81 is the "ASTM least squares fit" to the data between the exclusion lines.

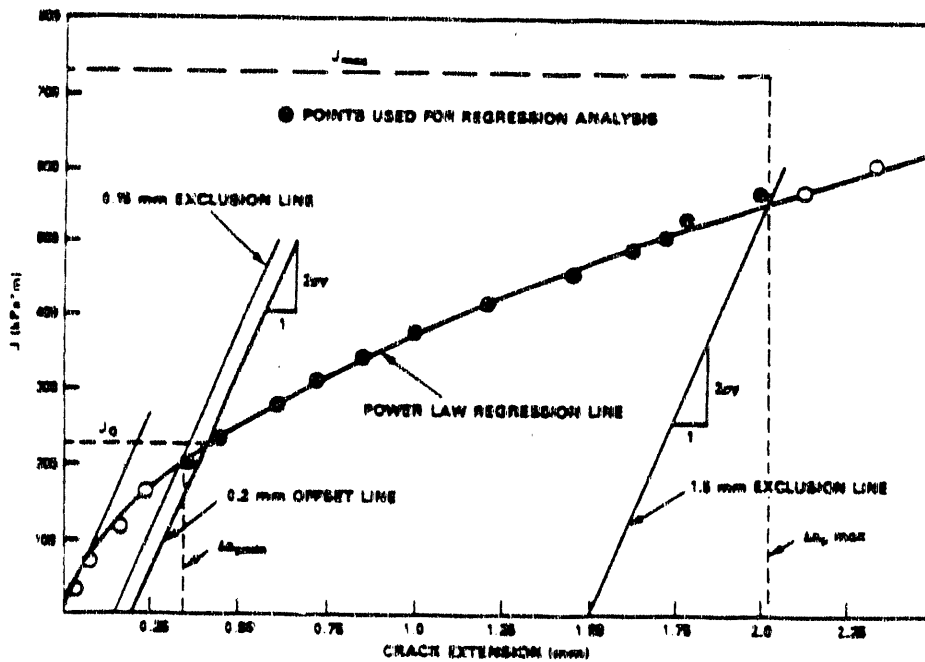


Figure 4-5B: ASTM E813-88 method for determination of J_{IC} (J_Q). The J_{IC} reported for the baseline data (Section 5) determined by the MEA power law method, corresponds to the intersection of the power law fit with the exclusion line (0.15 mm offset) of Figure 4-5A and thereby yields to lowest J_{IC} of the three methods (ASTM E813-81, -88, and the MEA power law) to calculate J_{IC} (J_Q)

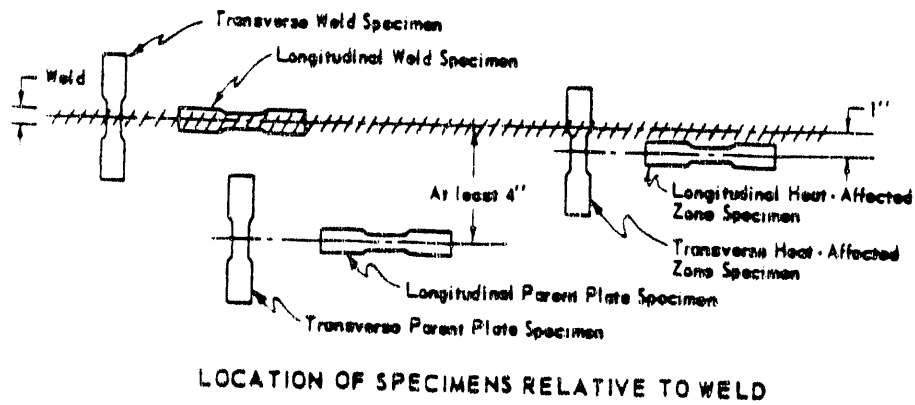
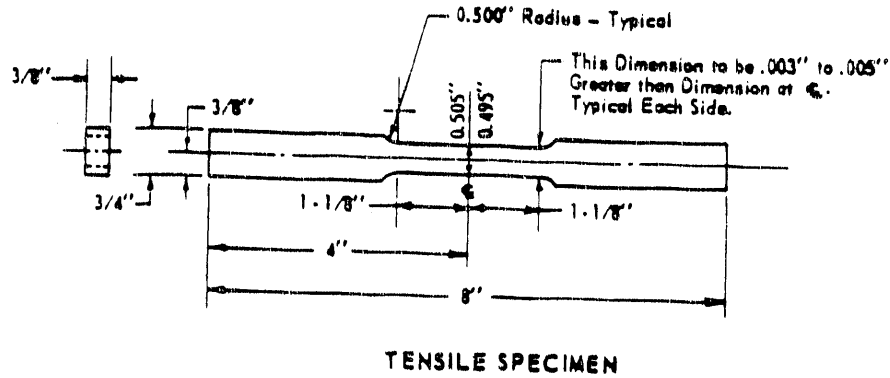


FIGURE 4-6: Tensile specimen design and Orientation for the Thermal Shield Irradiation testing [10].

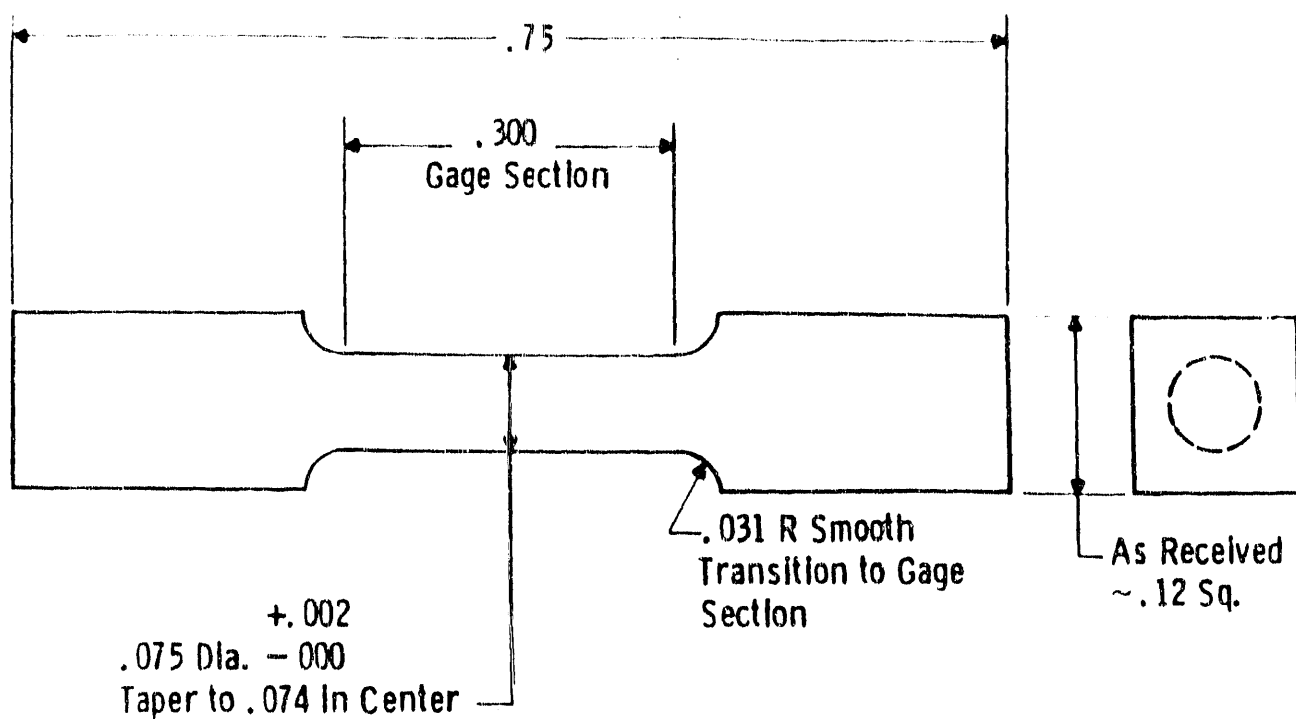


FIGURE 4-7: Sub-size tensile specimen design for R-tank tensile testing [12].

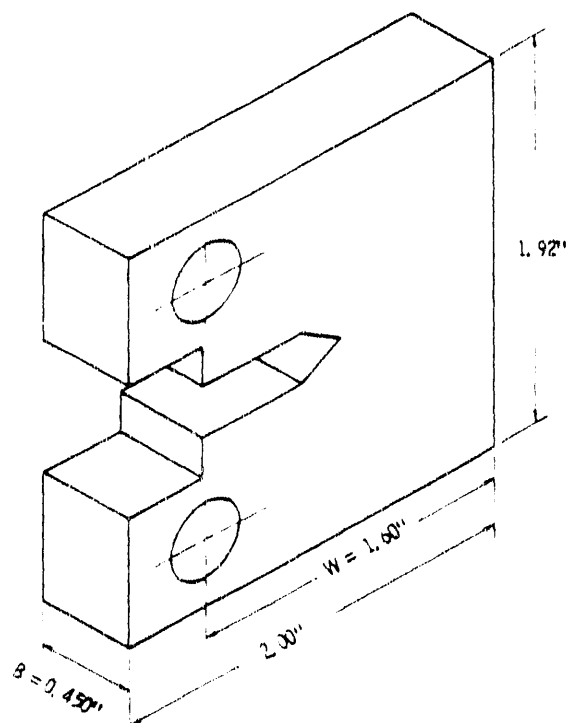


FIGURE 4-8: 0.8T CT Planform Design for the R-Tank Specimens [11]

5.0 MECHANICAL TESTING RESULTS and DISCUSSION

5.1 Overview

The effects of irradiation on the mechanical properties of Type 304 stainless steel weldments are quantified in terms of the absolute values of tensile and fracture toughness irradiated properties and, also, of the change from the unirradiated property values. The as-irradiated database includes many experimentation variables including irradiation conditions (temperature, exposure level, exposure rate, and neutron energy spectrum), weldment component (base, weld, or HAZ), orientation, material source (product form and composition), mechanical specimen configuration, and test conditions (strain rate, temperature, and testing apparatus). Categories were constructed (shown in Figure 1-2) to differentiate factors of major importance in evaluating irradiation effects (ie, weldment component, test temperature, and orientation). Selection of lower bound and nominal as-irradiated mechanical properties from these categories to be applied to structural assessment of the reactor tank sidewalls is discussed in Section 6. Effects of irradiation temperature, exposure level, and composition are discussed separately below.

Exposure rate and neutron spectral effects can influence the evolution of irradiation damage effects. Under SRS reactor tank sidewall irradiation conditions, exposure rate effects are unimportant because the irradiation temperature is low ($< 160^{\circ}\text{C}$). Neutron spectrum effects are unimportant at high exposure levels since the mechanical response of the austenitic stainless steel is not strongly sensitive to fluence above a fluence of approximately $1 \times 10^{20} \text{ n/cm}^2$ ($E_n > 0.1 \text{ MeV}$), i.e., the degradation in properties has "saturated". Further discussions of fluence or dose rate and neutron spectral effects will be presented in the future RMP report updating the K-Surveillance Irradiation Program (5, 41).

Appendix 1 contains the individual results of the irradiated mechanical specimen testing for the UBR, HFIR (1Q & 4M), R-tank, and Thermal Shield specimens measured at 25 and 125°C. Figures 5-1A (25°C), -1B (125°C) to 5-3A, -3B show the tensile test results (yield and tensile strengths), Charpy V-notch results (absorbed energy), and fracture toughness results (J at 1 mm) as a function of fast fluence exposure levels (see Tables 3-1 to 3-3) for each of specimens. Figures 5-4A and -4B show the 25 and 125°C fracture toughness (J at 1 mm) data for each specimen normalized by the its respective unirradiated value.

The average tensile, fracture toughness and impact mechanical properties and the change from the average unirradiated values are listed in Tables 5-1A (absolute value), -1B (change from unirradiated value) to 5-3A, -3B for the twelve categories defined by Figure 1-2. The properties in these tables were obtained by averaging the combined set of individual irradiated property results from Appendix 1 as noted in the tables.

The stress-strain data plotted in a Ramberg-Osgood format and $J_{\text{deformation-R}}$ curves for the R-Tank and HFIR 4M irradiations are provided in Appendix 2. The original sources for the UBR and HFIR irradiated specimen testing data are references 24, 42, 43, 44, 45, and 46. The original source documents reporting the fracture toughness and tensile data for the R-tank specimens are references 11 and 12.

5.2 Effect of Irradiation Temperature and Exposure Level on Irradiation Response

The SRS reactor tank sidewalls were irradiated at temperatures $\leq 130^{\circ}\text{C}$ [2], corresponding to the historic reactor full power level of 2400 MW. The specimens in the database were irradiated at temperatures from 75 to 150°C (Sections 3-2, 3-3). A comprehensive study of the effect of irradiation temperature on the room temperature tensile properties of Type 304 stainless steel had

been conducted by Bloom, et al [47]. The irradiation was conducted in the B-8 position of the Oak Ridge Research Reactor and the specimens were irradiated to a common thermal fluence of 9×10^{20} n/cm² and fast fluence ($E_n > 1$ MeV) of 7×10^{20} n/cm². [In the ORR experiment position A-9, adjacent to the B-8 position, the fast fluence ($E_n > 0.1$ MeV) is approximately 2.5 times the fast fluence ($E_n > 1$ MeV) or fission spectrum]. The irradiation temperatures in the Bloom experiments [47], 93 to 454°C, span the temperatures of the specimens in this as-irradiated database. The results of that study [47] showed that irradiation at 93 to 300°C produced a high density of defect clusters on the order of 10 nm diameter and that the yield and ultimate strengths were of approximately 90 to 100 and 115 ksi, respectively. The results of Bloom's study, reproduced in Figure 5-5A and Table 5-4, show that the mechanical properties would be insensitive to temperature under the irradiation conditions for the as-irradiated database.

The effect of fast fluence level (fluence) on the tensile properties of Type 304, 316 and 347 stainless steels for a low temperature (< 100°C) was conducted in the High Flux Reactor at Petten Holland by Higgy and Hammad [48]. Yield points in the stress-strain curves for the stainless steels were observed at fluences of 1.3×10^{19} n/cm² ($E_n > 1$ MeV) and above. A saturation of radiation hardening (increase in yield strength) was reported [48] at a fast fluence level of 4×10^{19} n/cm² ($E_n > 1$ MeV) (see Figure 5-5B). A correlation was developed showing the change in yield strength to be linear with (fast fluence)^{1/2} from the minimum investigated fluence of 1.15×10^{18} n/cm² ($E_n > 1$ MeV) to the saturation fluence.

Although the change (from initial or unirradiated) in the tensile properties of austenitic stainless steels with fluence appears constant above a "saturation" fluence level, "saturation" of the irradiated properties or a saturation exposure level are not rigorously defined in the literature. A trend of a slight increase in radiation hardening (yield strength) or change in other mechanical properties may occur at fluences above the "saturation fluence." [Note that plotting mechanical property data on a graph that is linear in fluence may appear to "show" a saturation in properties whereas a plot on a log scale shows a slight change in properties, especially when the data spans one or more decades of exposure].

Several of the data in the as-irradiated database are of the same material (e.g. 1BB material), allowing an assessment of "saturation" in changes in mechanical properties. The Thermal Shield data, corresponding to fast fluence levels of 2.9×10^{20} and 1.2×10^{21} n/cm² ($E_n > 0.1$ MeV) (see Figures 4 and 5 in reference 10 and also Figure 5-1A) indicate that a "saturation" in the ultimate tensile and yield strengths of base, weld, and HAZ components, each of common material source, occurs at a fluence level of approximately 2.9×10^{20} n/cm² ($E_n > 0.1$ MeV). Similarly, the R-tank T specimens irradiated to 1 and 7×10^{20} n/cm² ($E_n > 0.1$ MeV) also show no strong dependency of hardening with fluence at this exposure range although there is significant scatter in the yield strength data (see Figure 5-1A).

The 1Q material (F50 code Type 304L stainless steel) irradiated to fast fluence levels from 3.6 to 9.2×10^{20} n/cm² ($E_n > 0.1$ MeV) has similar strength values (from T specimens) and toughness values (from CVN and CT specimens) (see Figures 5-1B to 3B and also Appendix 1 data). Also the data from the 4M CT specimens of 1BB material irradiated to fast fluences of 2.2, 2.6, and 3.7×10^{21} n/cm² ($E_n > 0.1$ MeV) with fracture toughness values (J @ 1mm) of 2621, 2641, and 2346 in-lb/in², respectively, do not show any significant decrease with fluence. The toughness data (J @ 1mm) from R-tank specimens RD37 and RD39 at 1×10^{20} n/cm² (tested at 125°C) are 2700 and 2500 in-lb/in², similar to the values from RA37 and RA38 at 7×10^{20} n/cm² (tested at 25°C), 2900 in-lb/in² for both. Thus, the change in toughness with fluence is not significant at the exposure levels of the as-irradiated database.

The average results from the as-irradiated database in Appendix 1, representing irradiated mechanical data at exposures from 0.1 to 4×10^{21} n/cm² ($E_n > 0.1$ MeV), are categorized in Tables 5-1A,B to 5-3A,B independent of exposure level. It is noted, however, that the irradiated results from the UBR tensile data (125°C) suggest that "saturation" in hardening for weld components tested at 125°C has not occurred at 1.1×10^{20} n/cm² ($E_n > 0.1$ MeV).

5.3 Tensile Data Results

Tensile results (strengths and ductility) for each tensile specimen in the UBR, HFIR (1Q and 4M), R-tank, and Thermal Shield specimen irradiations are listed in Appendix 1. The HFIR 4M tensile data are presented graphically in a Ramberg-Osgood format Appendix 2. The average of the tensile data for the UBR, HFIR 4M, and Thermal Shield categorized by temperature and orientation (see Figure 1-2) is provided in Table 5-1A. The average R-Tank and HFIR 1Q data are also listed separately in Table 5-1A.

As expected for Type 304 stainless steel, strength properties at the higher test temperature (125 °C) were slightly lower than the strength properties at the lower temperature (25 °C). Ductility as measured by either elongation or reduction in area showed little temperature dependence. The room temperature (25°C) average tensile property data exceed the ASME Section II required values of 70 ksi for tensile strength, and 30 ksi for yield strength. No orientation effect on material tensile properties was observed for the L-C and C-L test directions. The average longitudinal (L-C) and transverse (C-L) elongations of the base, weld, and HAZ material are also consistent with the required levels of 35 and 25%, respectively, although several individual data at the lower bound data range were measured at 15% elongation. Therefore, based on the composite database for SRS specific materials and irradiation conditions, the tensile properties of the reactor tank walls current and projected irradiation conditions are predicted to meet the material property requirements of the ASME BPV code.

Hardening due to irradiation is evident in all of the test data except for the tensile strength of the weld metal at 125°C. The observed decrease in tensile strength (- 6%) for the irradiated 5W material (irradiated specimen 5W24) of L-C orientation was not accompanied by any unusual changes in yield strength or ductility. Data from the 6W52, 7W9, and 8W7 specimens also show low (~ 65 ksi) tensile strengths; no corresponding unirradiated tests were conducted for these materials. Irradiation induced changes in yield strength and ductility for the remaining weld specimens (UBR and Thermal Shield weld specimens tested at 25°C) show expected results and are consistent with all data for the base and HAZ specimens.

5.4 Charpy Data Results

Test results for each Charpy specimen are listed in Appendix 1. Table 5-2A summarizes the average Charpy impact energy data. The average energy absorption exceeded 50 ft-lbs for base metal, weld metal and HAZ material at both 25 and 125°C. These impact test results corroborate the high toughness of Type 304 stainless steel for the temperature range of operation for all three material types (base, weld, and HAZ), and both ASTM specimen orientations.

Regardless of test temperature, orientation, or weld component, irradiation reduced the energy absorption under impact loading, as seen in Figure 5-6. All three material types (base, weld, and HAZ) show a slight temperature dependence with lower impact energies at the lower temperature, an effect reported earlier for irradiated Type 304L and 347 stainless steels [43]. Irradiation effects in the base and HAZ specimens were more pronounced at 125°C than at 25°C.

The lowest impact energies were for the C-L orientation at both test temperatures. These observations suggest that segregation, ferrite stringers, or texture effects associated with pipe

forming operations are particularly sensitive to irradiation. Comparison of the UBR and 4M data indicates no statistically significant decrease in impact energies with increased fast fluence ($E_n > 0.1 \text{ MeV}$) from $1.1 \times 10^{20} \text{ n/cm}^2$ to $3.8 \times 10^{21} \text{ n/cm}^2$.

5.5 Compact Tension Data Results

The test results including the fracture toughness parameters from each compact tension specimen are listed in Attachment 1. The $J_{\text{deformation}}$ -R curves for the 0.4T planform R-Tank and HFIR 4M specimens are shown graphically in Attachment 2. Average fracture toughness properties for the three weldments (base, weld and HAZ) are shown in Table 5-3A. The deformation-J values shown in Table 5-3A were derived using a power law fit to the J-R curve data between the 0.15 and 1.5 mm exclusion lines. A linear analysis per the requirements of ASTM E 813-81 yields similar results [5] which are included in the Appendix 1 data set.

Reductions in fracture toughness due to irradiation depended on both the weldment component and the specimen orientation, as seen in Table 5-3A. The largest reductions in toughness occurred for the HAZ specimens and the smallest for the base metal. The C-L orientation, where the crack runs parallel to any stringers or segregation in the steel, was especially sensitive to irradiation, an effect seen also in the CVN data. This observation is discussed further in connection with fractography of the specimens in Section 5.6.

The fracture toughness data for the 0.8T compact specimens from R-tank illustrate the effect of test temperature on fracture toughness. Both the J-integral value at crack initiation and at 1-mm crack extension are lowered as the test temperature is raised. This temperature dependence of fracture toughness is common to the austenitic stainless steels. Note also that the smaller size (0.4T) specimen with sidegrooves has a lower fracture toughness than the larger (0.8T) specimens and provides a conservative fracture toughness for structural assessments.

5.6 Fractography Results

Fracture surfaces of selected specimens were examined by scanning electron microscopy. Materials selected for examination included: base, weld, and heat-affected-zone (HAZ); CVN specimens irradiated in UBR and tested at 25 and 125°C; and a base metal tensile specimen from R-tank wall tested at 25°C.

All CVN test specimens and all three material types exhibited ductile fracture at both test temperatures. A typical fracture, Figure 5-7, shows microvoids and associated inclusions for unirradiated and irradiated specimens. Energy dispersive X-ray spectroscopy analysis of the unirradiated specimen fracture surfaces was applied to obtain a chemical assay of selected precipitates. The analysis suggests the precipitates to be chromium and titanium carbides, calcium-aluminum silicates and manganese sulfides. A bimodal microvoid size distribution was found in the HAZ specimen from ring 3. In all other cases the microvoid size was uniform. Transverse cracking was observed in one weld metal specimen and one HAZ specimen. In the HAZ specimen with the lowest impact energy, banding was evident on the fracture surface. Metallographic examination of this specimen showed thin borders of a second phase around some austenite grains. This phase were identified as delta-ferrite and probably formed as a result of the thermomechanical processing. The cracks appear to be associated with inclusion stringers or short bands of segregation leading to weakened areas aligned parallel to the surfaces during forming.

The tensile test results for specimens machined from the R-tank discs A and D indicated ductile fracture at both 25 and 125°C. Scanning Electron Microscopy analysis of the fracture surface of the specimens tested at 25°C showed microvoid coalescence (dimpled rupture fracture mode).

Table 5-1A: As-Irradiated Tensile Data

Material	Test Temperature (°C)	Sample ASTM Orientation	Engineering Yield (0.2%) Strength (ksi)	Engineering Tensile Strength (ksi)	Total Elongation* (%)	Reduction in Area (%)
Base	25	L-C	87.4	102.5	34.5	NR
		C-L	86.2	101.7	41.5	NR
R-Tank	125	-	74.8	104.9	52.3	68.7
		L-C	72.9	85.0	52.6	68.5
R-Tank	125	C-L	74.5	86.4	37.2	73.5
		-	64.3	90.3	42.1	65.0
Type 304L	25	L-T	65.6	79.2	33.6	60.8
		HAZ	L-C	88.4	102.5	32.0
HAZ	125	C-L	89.5	103.1	40.5	NR
		L-C	81.2	88.6	NR	NR
Weld	25	C-L	-	-	-	-
		L-C	90.1	104.2	36.5	60.8
	125	C-L	96.0	105.5	27.4	52.7
		L-C	55.9	64.6	36.0	72.6
		C-L	60.2	65.2	32.0	59.3

Notes: 1) The results for the **Base**, **HAZ**, and **Weld**, L-C and C-L orientations are comprised of the average of the properties from the UBR, HFIR 4M and Thermal Shield individual specimens (see Appendix 1). [The "longitudinal" orientation of the thermal shield specimens is taken as equivalent to the C-L orientation of the RMP piping specimens; the "transverse" orientation is taken as equivalent to the L-C orientation].

2) The number of mechanical specimens in the various test categories are listed in Tables 4-1 to 4-4 (summed from the specimens listed in Appendix 1).

3) Specimens from a plate of Type 304L SS were irradiated in the HFIR 1Q capsule.

4) The range of the Modulus of Elasticity (Young's Modulus) for the Thermal Shield specimens is 24.4×10^6 to 30.4×10^6 psi (page A1-3). The range of Young's Modulus for the HFIR 4M specimens is 27.3×10^6 to 36.1×10^6 psi (ref. 46).

*: Total Elongation in respective gage lengths
NR = Not Reported

**Table 5-1B: As-Irradiated Tensile Data
(Average Change from Unirradiated Strengths)**

Material	Test Temperature (°C)	Sample ASTM Orientation	Δ Yield Strength (ksi)	Δ Tensile Strength (ksi)	Yield: Δ Irr/Unirr (%)	Tensile: Δ Irr/Unirr (%)
Base	25	L-C	53.3	19.3	156	23
		C-L	52.1	18.2	153	22
R-Tank	125	-	36.3*	12.9*	97*	14*
		L-C	47.5	19.2	187	29
R-Tank	125	C-L	44.3	18.2	147	27
		-	35.3*	19.3*	122*	27*
Type 304L HAZ	25	L-T	36.8	10.4	128	15
		L-C	49.3	18.4	126	22
HAZ	125	C-L	50.4	19.3	129	23
		L-C	-	-	-	-
Weld	25	C-L	-	-	-	-
		L-C	40.0	15.6	80	18
Weld	125	C-L	38.5	17.4	67	20
		L-C	10.0	-6.2	22	-9
		C-L	-	-	-	-

*Unirradiated values for R-Tank assumed equivalent to the average (L-C & C-L) baseline properties at 25 and 125°C (from reference 35)

**Table 5-2A: As-Irradiated
 Charpy Impact Data**

Material	Test Temperature (°C)	Sample ASTM Orientation	Energy Absorption (ft-lbs)	Lateral Expansion (mils)
Base	25	L-C	83	67
		C-L	63	50
Type 304L HAZ	125	L-C	94	80
		C-L	71	66
	125	L-T	83	79
	25	L-C	80	59
Weld		C-L	54	43
	125	L-C	84	66
		C-L	63	56
	25	L-C	64	50
		C-L	-	-
	125	L-C	87	77
	C-L	78	65	

The results for the **Base**, **HAZ**, and **Weld**, L-C and C-L orientations are comprised of the average of the properties of the UBR and HFIR 4M data. Specimens from a plate of Type 304L SS were irradiated in the HFIR 1Q capsule.

**Table 5-2B: As-Irradiated
Charpy Impact Data (Average
Change from Unirradiated
Impact Energy)**

Material	Test Temperature (°C)	Sample ASTM Orientation	Energy Absorption (Decrease) Δ ft-lbs; Δ Irr/Unirr (%)	Lateral Exp. (Decrease) Δ mils; Δ Irr/Unirr(%)
Base	25	L-C	66; 44	13; 16
		C-L	53; 46	43; 52
	125	L-C	135; 59	7; 8
		C-L	57; 44	11; 14
Type 304L HAZ	25	L-T	92; 53	7; 8
		L-C	56; 41	21; 26
	125	C-L	41; 43	30; 41
		L-C	104; 55	19; 22
Weld	25	C-L	38; 38	25; 31
		L-C	49; 43	34; 40
	125	C-L	-	-
		L-C	87; 50	2; 2
		C-L	97; 55	18; 22

**Table 5-3A: As-Irradiated Fracture Toughness Data
(Deformation-J, Power law)**

Material	Test Temperature (°C)	Sample ASTM Orientation	J _{IC} - Deformation (in-lb/in ²)	J @ Δa = 1mm (in-lb/in ²)	Ave Tearing Modulus
Base	25	L-C	-	-	-
		C-L	-	-	-
R-Tank	125	-	2092 (0.8T)	2900	125
		L-C	1730	2547	127
R-Tank	125	C-L	942	1502	70
		-	1730 (0.8T)	2500	125
Type 304L HAZ	25	-	1122 (0.4T)	1800	95
		LT	1513	2107	108
HAZ	125	L-C	-	-	-
		C-L	-	-	-
Weld	25	L-C	982	1662	76
		C-L	428	662	18
Weld	125	L-C	-	-	-
		C-L	-	-	-
Weld	125	L-C	805	1542	77
		C-L	-	-	-

*R-Tank 25°C data from 0.8T planform specimens; R-Tank 125°C data from 0.4 and 0.8T planform specimens

The results for the **Base, HAZ, and Weld, L-C and C-L** orientations are comprised of the average of the properties of the HFIR 4M data. Specimens from a plate of Type 304L SS were irradiated in the HFIR 1Q capsule.

**Table 5-3B: As-Irradiated Fracture Toughness Data
(Deformation-J, Power law) (Average Change from
Unirradiated Values)**

Material	Test Temperature (°C)	Sample ASTM Orientation	J @ 1mm Irr/Unirr (Ratio;%Δ)	Ave Tearing Modulus Irr/Unirr (Ratio;%Δ)
Base	25	L-C	-	-
		C-L	-	-
R-Tank*	125	-	(0.8T) 0.83; -17%	0.62; -38%
		L-C	0.74; -26%	0.48; -52%
R-Tank*	125	C-L	0.73; -27%	0.30; -70%
		-	(0.8T) 0.90; -10%	0.53; -47%
Type304L HAZ	25	-	(0.4T) 0.65; -35%	0.40; -60%
		L-T	0.78; -22%	0.45; -55%
HAZ	125	L-C	-	-
		C-L	-	-
Weld	25	L-C	0.50; -50%	0.40; -60%
		C-L	0.35; -65%	0.12; -88%
Weld	125	L-C	-	-
		C-L	-	-
Weld	125	L-C	0.59; -41%	0.31; -69%
		C-L	-	-

*Unirradiated values for R-Tank assumed equivalent to the average (L-C & C-L) baseline properties at 25 and 125°C (from reference 35)

Table 5-4: Effect of irradiation temperature on room temperature tensile properties [Table reproduced from Reference 47].

TABLE 1
Room-temperature tensile properties of irradiated type 304 stainless steel.

Irradiation temperature (°C)	Yield stress (psi)			Ultimate tensile strength (psi)		Fracture stress (psi)	True uniform strain (%)	True strain at fracture (%)	Elongation at fracture (%)
	offset	upper	lower	Engi- neering	True				
	$\times 10^3$	$\times 10^3$	$\times 10^3$	$\times 10^3$	$\times 10^3$	$\times 10^3$			
93	86.8	90.7	85.4	112.2	170.9	288.2	42.0	141.0	58.8
121	94.3	96.7	90.2	115.5	169.3	246.0	38.2	119.5	52.8
149	99.2	100.8	93.5	118.9	171.8	228.4	36.8	111.0	50.4
177	95.1	96.7	92.3	113.8	169.1	247.0	39.6	122.0	54.4
300	91.5			113.8	147.5	296.7	25.9	139.0	36.5
343	51.2			99.2	133.0	230.0	29.4	134.0	40.4
371	40.7			97.7	142.5	283.8	37.7	154.0	52.0
398	45.5			95.9	150.0	245.0	44.6	141.0	63.0
454	43.5			96.8					66.6

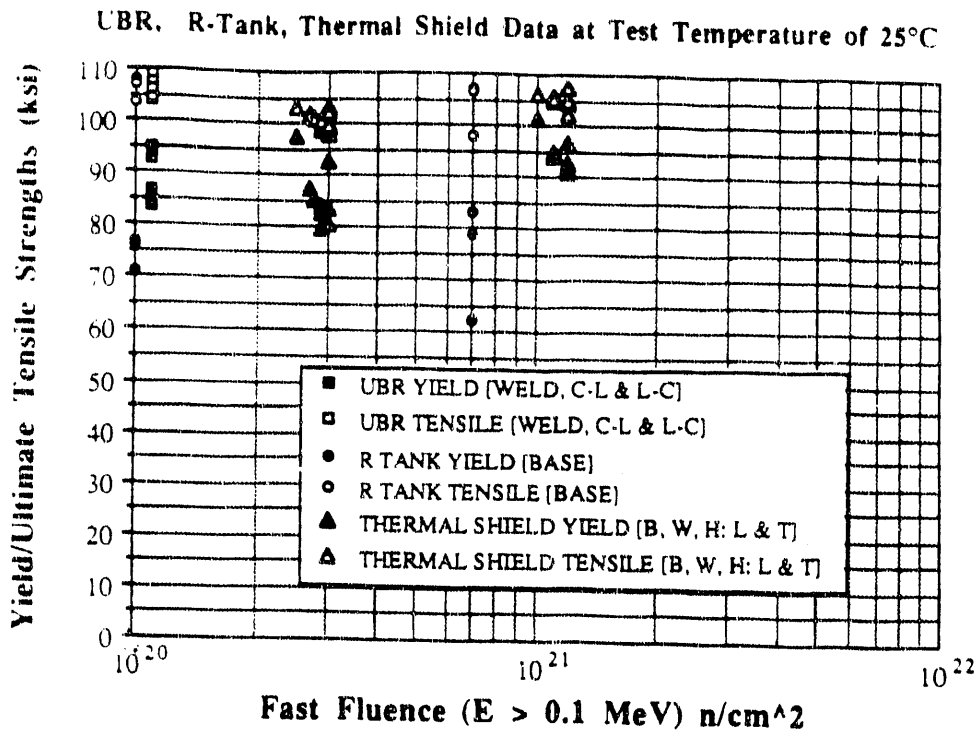


Figure 5-1A: Yield and Tensile Strengths at 25°C as a function of Fast Fluence ($E_n > 0.1$ MeV) for the UBR, R-Tank, and Thermal Shield Specimens

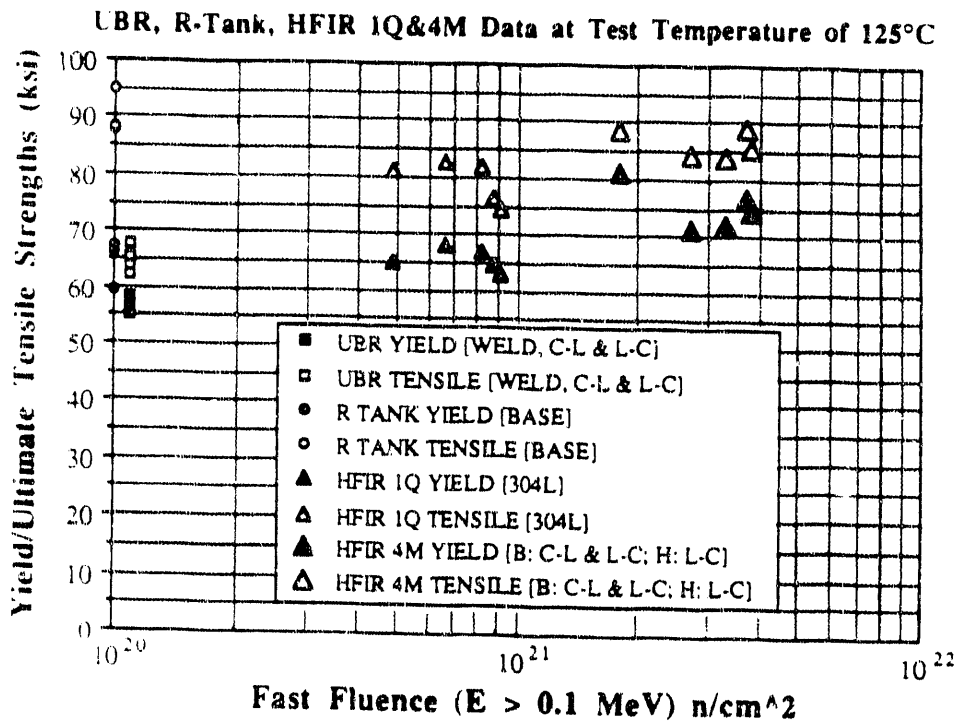


Figure 5-1B: Yield and Tensile Strengths at 125°C as a function of Fast Fluence ($E_n > 0.1$ MeV) for the UBR, R-Tank, and HFIR 1Q & 4M Specimens

UBR Data at Test Temperature of 25°C

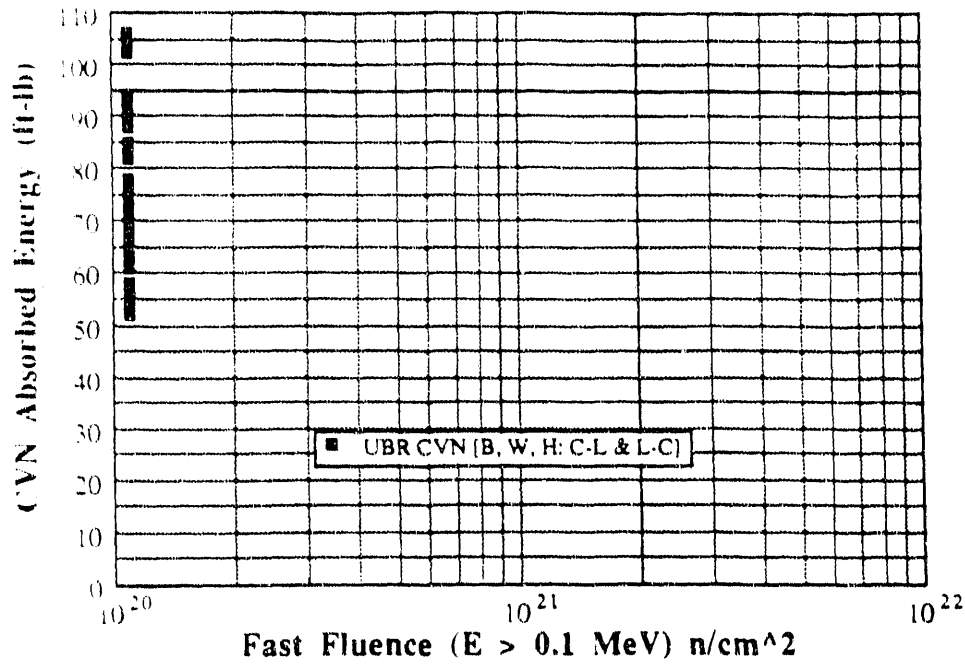


Figure 5-2A: Absorbed Impact Energy at 25°C as a function of Fast Fluence ($E_n > 0.1$ MeV) for the UBR Specimens

UBR, HFIR 1Q & 4M Data at Test Temperature of 125°C

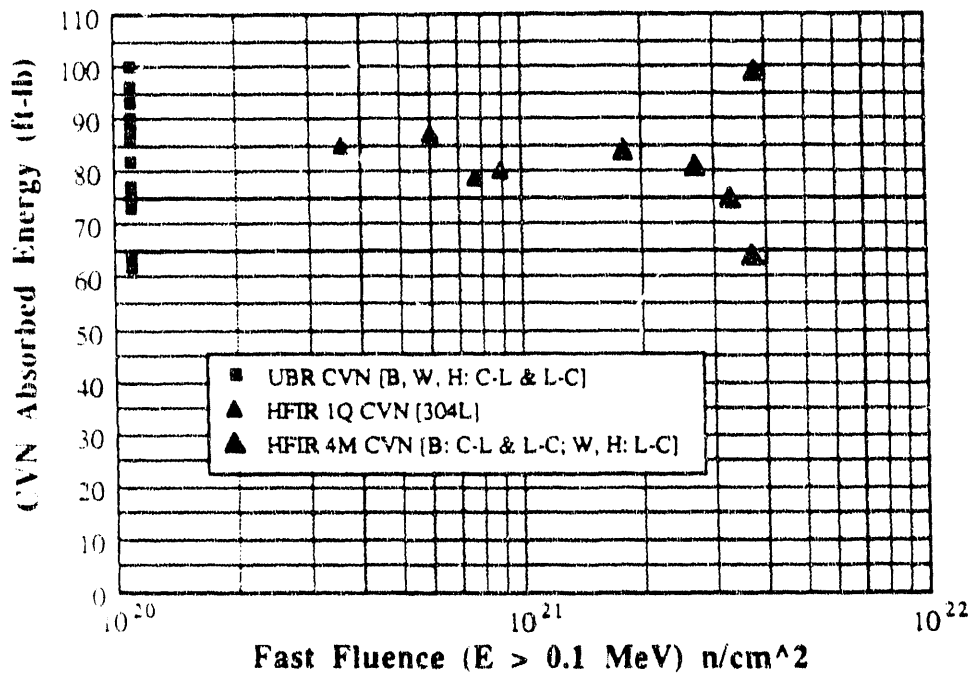


Figure 5-2B: Absorbed Impact Energy at 125°C as a function of Fast Fluence ($E_n > 0.1$ MeV) for the UBR and HFIR 1Q & 4M Specimens

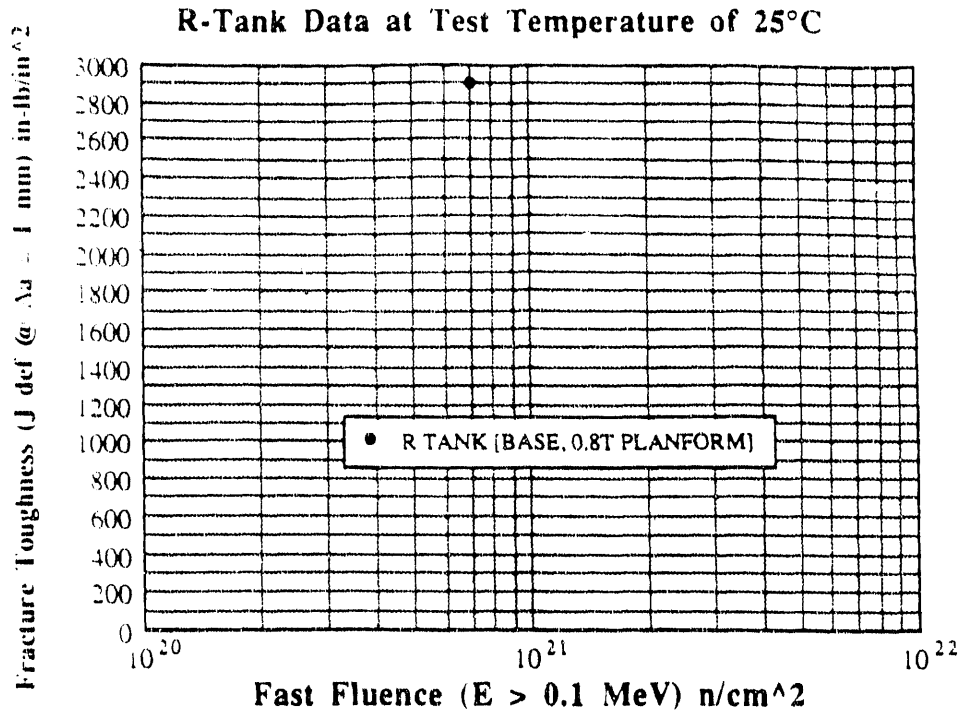


Figure 5-3A: Fracture Toughness at 25°C as a function of Fast Fluence ($E_n > 0.1$ MeV) for the R-Tank Specimens

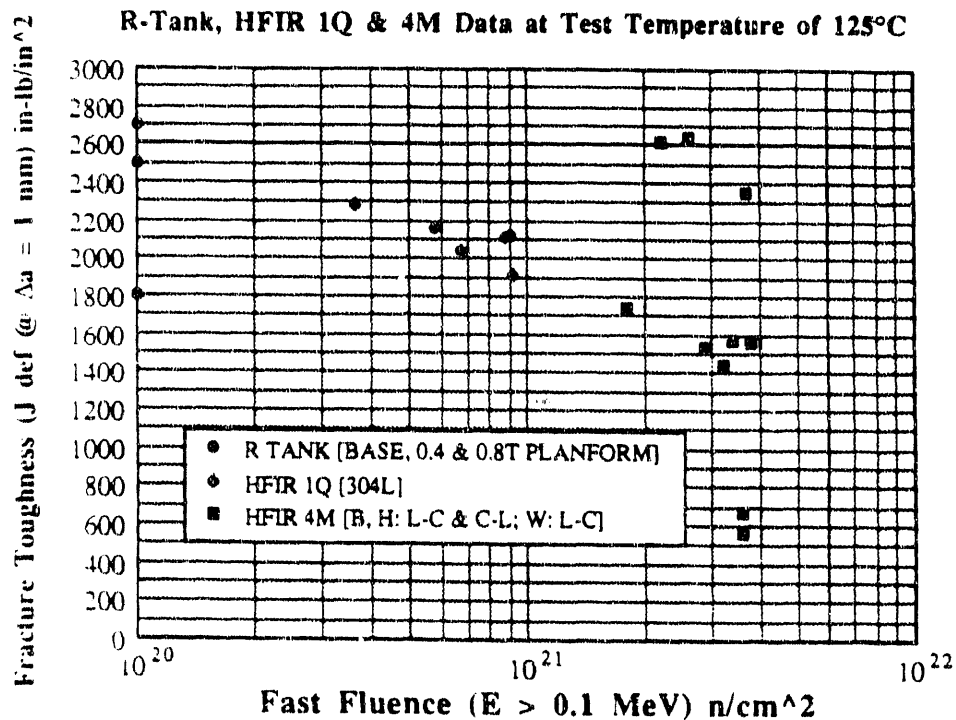


Figure 5-3B: Fracture Toughness at 125°C as a function of Fast Fluence ($E_n > 0.1$ MeV) for the R-Tank and HFIR 1Q & 4M Specimens

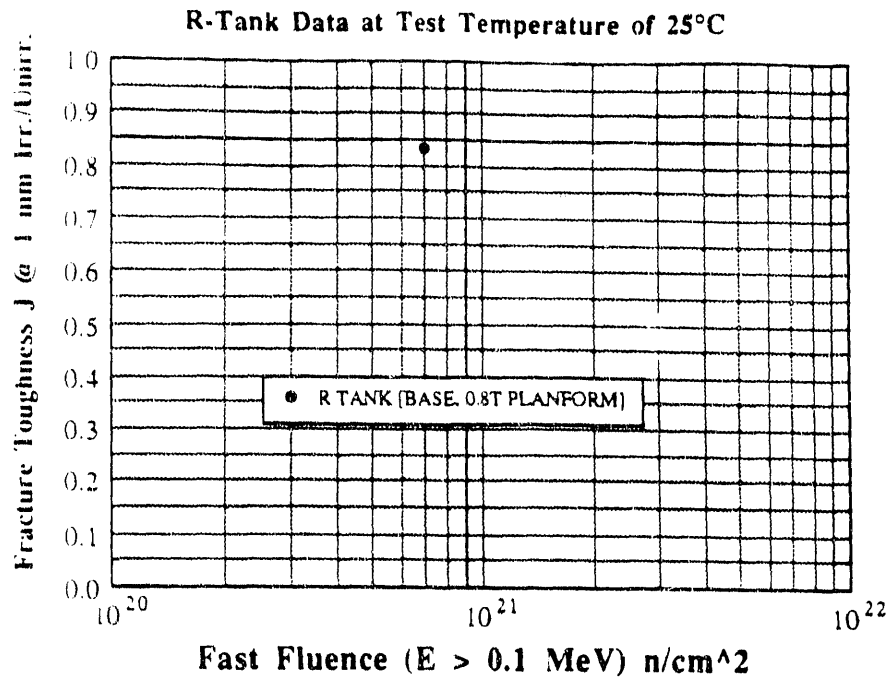


Figure 5-4A: Normalized (Irr./Unirr.) Fracture Toughness at 25°C as a function of Fast Fluence ($E_n > 0.1$ MeV) for the R-Tank Specimens. The unirradiated fracture toughness is taken as the average of the L-C and C-L results from the 25°C Base material properties [ref. 35].

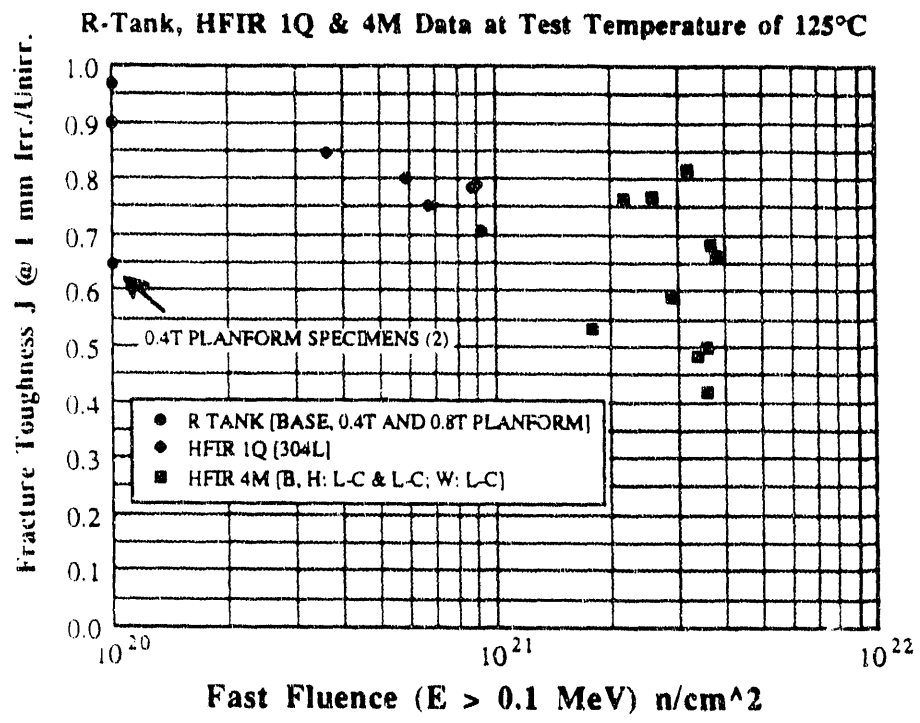


Figure 5-4B: Normalized (Irr./Unirr.) Fracture Toughness at 125°C as a function of Fast Fluence ($E_n > 0.1$ MeV) for the HFIR 1Q&4M and R-Tank Specimens (the unirradiated fracture toughness is taken as the average of the L-C and C-L results from the 125°C Base material properties for the R-Tank Specimens [ref. 35]).

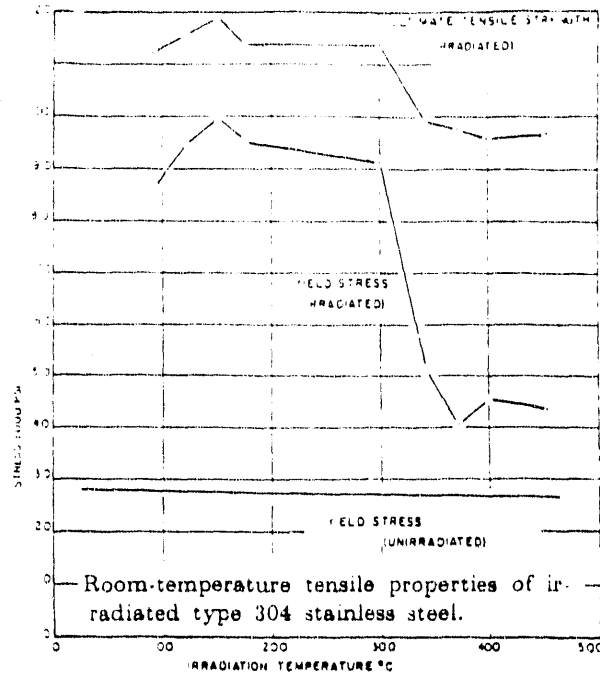


Figure 5-5A: Effect of irradiation temperature on room temperature tensile test data [Figure reproduced from Reference 47].

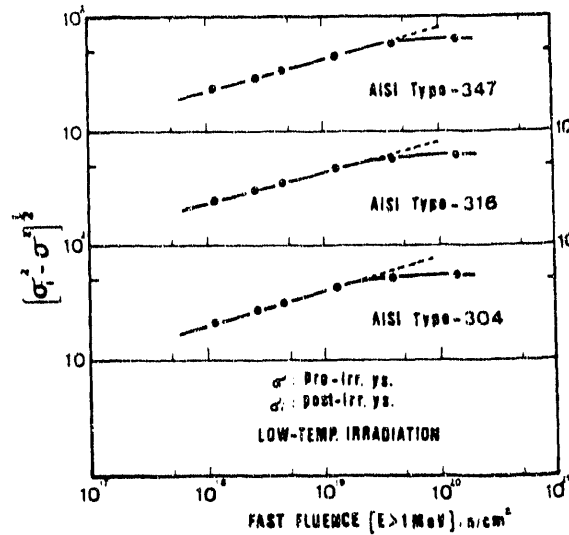


Fig. 8. The effect of fast fluence on the increment $(\sigma_1^2 - \sigma_2^2)^{1/2}$ of AISI Types 304, 316 and 347.

Figure 5-5B: The effect of fast fluence level ($E_n > 1 \text{ MeV}$) on the change in yield strength for Types 304, 316, and 347 stainless steel. Reproduced from reference 48.

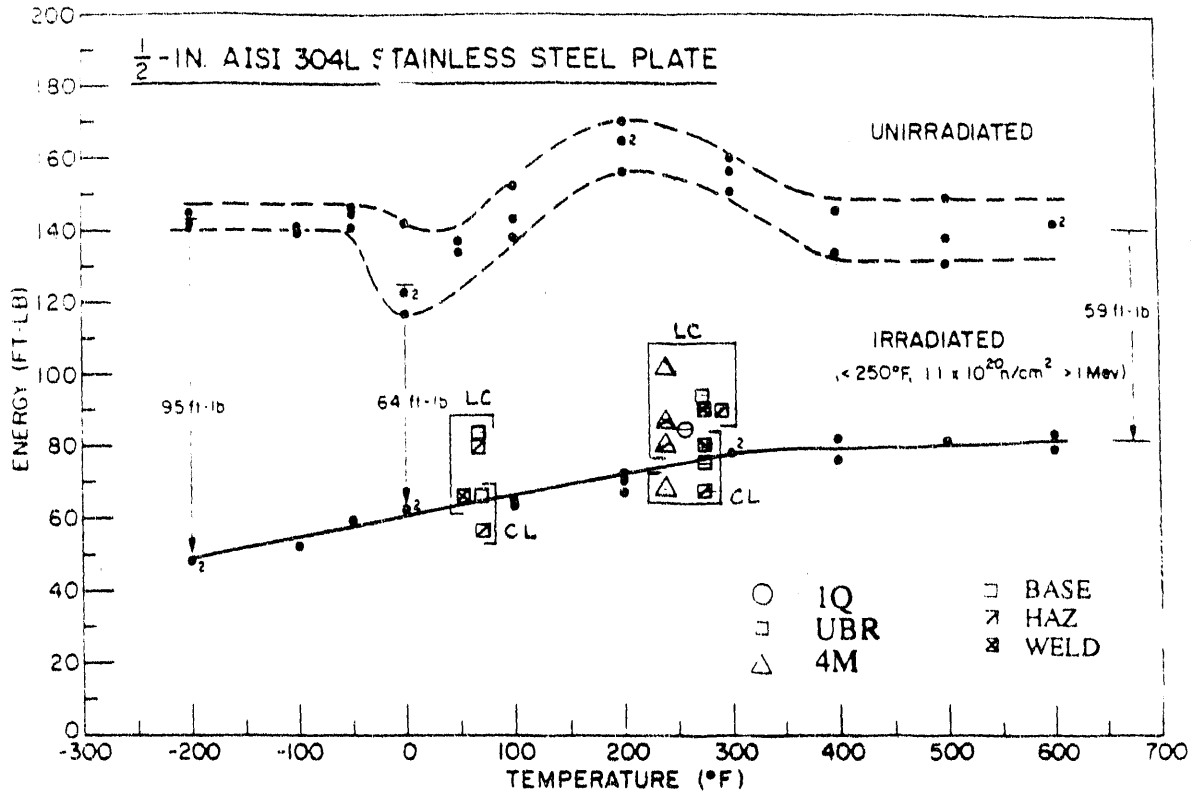


Figure 5-6: Effect of test temperature on impact energies of irradiated CVN specimens [figure copied from Reference 43].

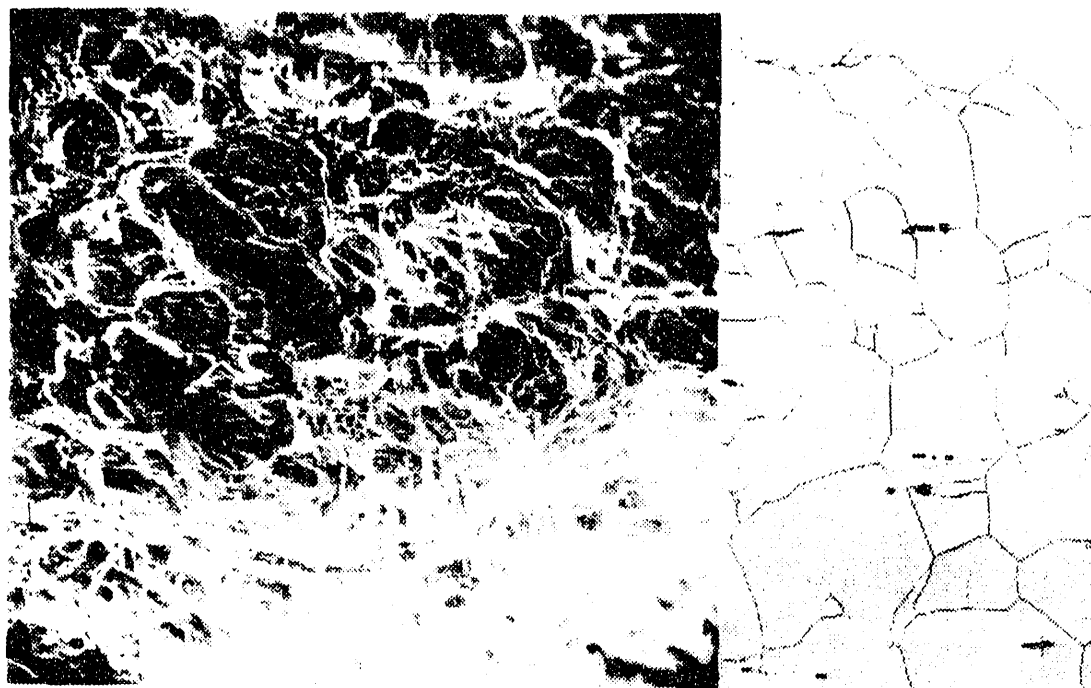


Fig. 19 [24] Charpy impact fracture surface and companion microstructure of heat-affected zone specimen 5HB-16 (L-C orientation). Fractograph-260X magnification. Micrograph-195X.

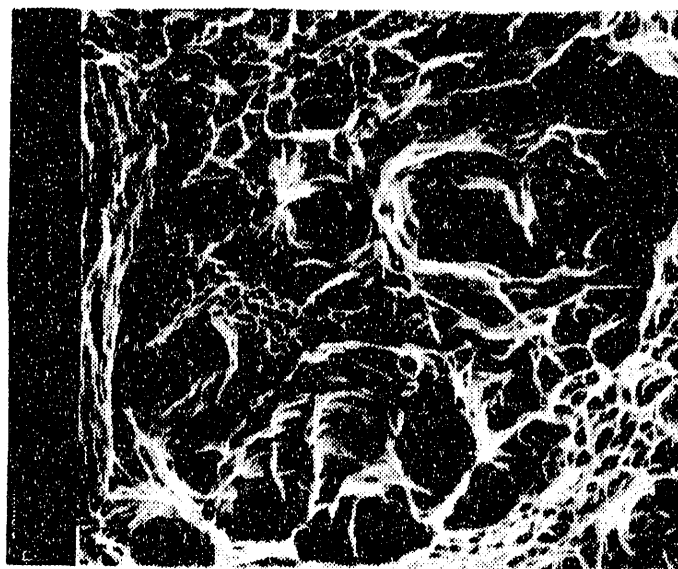


Fig. 48 [24] Scanning electron microscope photomicrograph of the Charpy fracture surface of irradiated specimen 3HA-34, 650X magnification. This figure shows the combination of large and small voids which comprise the fracture surface.

Figure 5-7: Fracture surface of the UBR CVN specimen 3HA-34 and unirradiated CVN specimen 5HB-16 (reproduced from reference 24, Appendix U)

6.0 IRRADIATED MECHANICAL PROPERTIES: ENGINEERING STRUCTURAL ANALYSES

6.1 Overview

6.1.1 Comparison of RMP, R-Tank, and Thermal Shield Materials to SRS Tanks

The material and irradiation conditions of the mechanical specimens in the as-irradiated database are similar to the SRS reactor tank sidewalls. The properties of the specimens, therefore, may be applied in estimating the mechanical properties of the tank sidewalls in engineering analyses. The SRS reactor tanks were constructed [27] and began operation in the 1950's. The tank sidewalls were produced from 0.5 inch thick plate rolled and joined by Inert-Gas-Shielded Metal Arc Welding with bare Type 308 filler wire. Additional fabrication details and materials' composition for the tank are provided in Section 2.5 and in the original tank construction records [27].

The materials for the RMP irradiation and mechanical testing programs were eight separate rings of 16 inch diameter, schedule 40 (0.5 inch thick) Process Water System piping from the R-reactor [7]. The piping installed in 1957 (the materials source) was fabricated per site specifications governing the manufacturing and installation of the piping. All piping contacting the heavy water moderator was fabricated originally from Type 304 stainless steel per Du Pont Specification SW 304M (Grade 304) as listed in Specification 3018, P39.010 and P39.020, issued November 11, 1951 with latest revision January 24, 1957. The construction design code of record was American National Standards Institute (ANSI) B31.1. The piping was joined with Inert-Gas-Shielded Metal Arc Welding with bare Type 308 filler wire. The initial materials of the RMP were therefore typical of the initial tank materials. Additional details of the RMP piping materials irradiated in the UBR and HFIR capsules is discussed in Section 2.2 and reference 7.

The materials from the Thermal Shield model are also similar to the materials in the SRS reactor tanks. The R-Tank disks provide actual tank sidewall material irradiated during reactor operation to fluence levels of 1 and 7×10^{20} n/cm² ($E_n > 0.1$ MeV) (Section 2.4). The base weldment component of the Thermal Shield specimens is 1950's vintage Type 304 stainless steel. The HAZ and Weld components of the Thermal Shield model (Section 2.3) were not prototypic of the reactor tank weldment components but are representative to the weldment components of reactor construction (thermal shield) and the irradiated properties are consistent with the R-tank and RMP irradiated property results; therefore the Thermal Shield irradiated property results are added to the database for selection of properties for engineering structural analyses. The Type 304L material from the HFIR 1Q capsule is part of the as-irradiated database contained in this report, but is not applied in the selection of properties for structural analyses since the tank materials are not Type 304L stainless steel.

6.1.2 Reactor Tank Sidewall Exposure Levels

The reactor tank sidewalls were exposed to a complex neutron irradiation during reactor operation which involved several types of reactor charges and periods of operation. The cumulative reactor tank average and peak exposure levels in terms of fast and thermal neutron fluence were calculated by Gorrell [49] with a four-group diffusion code applied to reactor operation with several types of reactor charges. Baumann refined these calculations by applying azimuthal flux distribution maps to the fast and thermal fluences and re-calculated the level of thermal neutron exposure based on helium assay results from tank wall scrapings [1].

The tank sidewalls have been exposed to fast fluence levels between $\sim 10^{20}$ n/cm² and 2×10^{21} n/cm² ($E_n > 0.1$ MeV) [2] except for regions at the tank bottom (T-weld), tank top (expansion

ring), and tank nozzles outside the plane of the sidewall which have been exposed to much smaller fast fluences. The properties in this report were collected from specimens irradiated from 1×10^{20} to 4×10^{21} n/cm² ($E_n > 0.1$ MeV) (Section 3). Since the response to irradiation is not highly sensitive to the exposure level at these conditions (see Section 5.1), the properties are representative of the tank sidewall properties. Furthermore, blanketed operation has greatly reduced the rate of additional fast fluence accumulation [1] and the highest fast fluence exposure level (4×10^{21} n/cm²) bounds the maximum tank wall future level for at least 50 additional years of operation at 2400 MW with 66% innage or 1600 MW [1, 13]. Thus the irradiated database is applicable to structural analyses for the remaining service life. Additional details of the tank wall irradiation history including fluence rate and tank wall thermal to fast fluence exposure levels will be provided in a future RMP report [5].

6.1.3 As-Irradiated Database: Development of Properties for Engineering Analyses - Summary

The as-irradiated results were produced at temperatures approximately bounding reactor tank wall temperatures including the maximum sidewall temperature at historic full power (~ 130°C) [2] and are applicable to analyses of the tank materials for these temperature conditions. Structural (stress) analyses of the reactor tank are not affected by the increase in the yield and tensile strengths for loading conditions below design yield. For loading conditions resulting in stress levels above design yield, but below the irradiated yield strengths, the tank sidewalls would not undergo plastic deformation.

Furthermore, irradiated tensile results reported by Joseph [10] (see Appendix 1) show that the modulus of elasticity is not significantly changed as a results of irradiation. Therefore the application of code design values for Types 304 plate materials and Type 308 weld material properties are valid in the stress analysis of the reactor tank [50].

Commercial nuclear codes do not specify fracture toughness properties for irradiated austenitic stainless steel weldment components in either design or flaw evaluation criteria. Material fracture toughness parameters for elastic-plastic fracture mechanics analysis of postulated flaws have been developed from the as-irradiated test results. "Nominal" and "Lower Bound" material toughness parameters have been defined.

Digitized J-R curve data and tensile curve data for the individual specimens from the R-tank testing and RMP testing are retained in the RMP Task Files (SRL-NRTSC Task 89-023-C-1). Selected J-R curves and tensile data are shown in Appendix 2. Material fracture toughness and tensile properties for tank fracture analysis are discussed in Sections 6.2.3 and 6.4, respectively.

6.1.4 Baseline Properties for Irradiation Effects Studies

The as-irradiated results (Section 5) were presented in terms of both absolute average property level and change from unirradiated property level. The corresponding baseline (unirradiated) mechanical properties for most of the RMP as-irradiated materials (e.g. HFIR 4M specimen 2W2) were measured and are reported in reference 35.

Several irradiated sample categories (e.g. HAZ, C-L, 125°C) are comprised of one or two specimens. The percent change in the mechanical property from these categories could be applied to the baseline properties database [35] to provide additional confidence in the absolute property level of that category. For example, the as-irradiated category "Weld, L-C, 125°C" for elastic-plastic fracture toughness was based on the one specimen 2W2. A total of 5 specimens comprise this category for the baseline testing [35]. A reduction of 41% (see Table 5-3B)

applied to the average baseline result of 3220 in-lb/in² for J at 1 mm [35] yields an absolute toughness of 1900 in-lb/in².

Application of the unirradiated results to the irradiated database has been done qualitatively to identify the Lower Bound material fracture toughness (Section 6.4). The category HAZ, C-L, 125°C yields the lowest baseline toughness [35]. Furthermore, material 7HA yields the lowest toughness in this category.

6.2 Tensile Properties

6.2.1 Tensile Properties for Structural Analysis

The tensile data in this testing program were generated in conformance to ASTM testing specifications and are applicable to engineering analyses. The average irradiated yield and tensile strengths for the base and heat-affected-zone materials and elongations are equivalent to or superior to the ASME Boiler Pressure Vessel Code Section II (Material Specifications) and Section III (Design) values for Type 304 stainless steel plate. The ASME BPVC, Section II yield and tensile strength design values (A240) for Type 304 stainless steel plate are 30 and 75, respectively with minimum elongations of 35% (longitudinal) and 25% (transverse). The irradiated strength results (Section 5) exceed these specifications and the irradiated material elongations meet the code-specified elongations. Similarly, the tensile strengths of the archival weld materials (Type 308 stainless steel) are superior to ASME-required (SA-358) values for welded pipe. It is thus demonstrated that the ASME code tensile property values (strengths) are conservative to the irradiated property results. Therefore structural (stress) analyses of the reactor tank are not affected by the change in tensile properties.

6.2.2 Flow Stress Evaluation

The flow stress is applied in the development for both applied and material J-T curves. The Tearing Modulus (see Section 7) is a function of the flow stress. The flow stress is defined as $(S_y + s_u)/2$, where S_y is the 0.2 percent offset yield strength (Engineering) and s_u is the ultimate tensile strength (Engineering) [24]. The application of either Engineering or True strengths could be applied in the J-T instability analysis (Section 7); the instability criteria or the results of the analysis are equivalent. Note that the yield strength (0.2 percent offset, True) is applied in the development of the Ramberg-Osgood formulation of the True stress-strain curves for the irradiated material (Section 6.2.3).

6.2.3 Tensile Properties for Fracture Analysis

Parameters from true stress-strain curves are input into calculation of applied J in the fracture mechanics analysis of the tanks (Section 7). The tensile parameters include the yield strength and Ramberg-Osgood parameter for the True stress-strain curves. The tensile curve characterization in the Ramberg-Osgood format is:

$$\frac{\epsilon}{\epsilon_y} = \frac{\sigma}{\sigma_y} + \alpha \left(\frac{\sigma}{\sigma_y} \right)^n \quad (13)$$

where σ_y is the yield stress (True) and ϵ_y is equal to σ_y/E with Young's modulus, E (taken as 28×10^6 psi).

Ideally, Ramberg-Osgood parameters should be obtained from the tensile data for a T specimen from the identical material and orientation as a corresponding CT from which the fracture toughness is measured. The 4M specimen 7HA5 (HAZ, C-L orientation), the Lower Bound toughness specimen, did not have a companion tensile specimen in the 4M capsule. The tensile properties (Ramberg-Osgood parameters) from the 4M HAZ, L-C tensile specimen was applied instead since the tensile properties are not dependent on orientation.

The Ramberg-Osgood values for the as-irradiated categories are contained in Appendix 2.

6.3 Charpy V-Notch Impact Energy

Charpy V-notch results are not applied in either structural analyses or fracture analyses for the reactor tanks. The results of CVN impact tests indicate relative toughnesses among materials. Consequently, an evaluation can be made of the effects of processing variables, heat treatment, test temperature, and sensitivity to irradiation on the toughness of a material type. The UBR irradiation program was developed to provide a survey of the piping ring material [7] to compare the base, weld and heat-affected zone weldment components for the L-C and C-L orientations at test temperatures spanning the operating conditions of the reactor tanks. The results of the UBR CVN tests (Section 5) show no particular sensitivity of material type to irradiation. [The evaluation of sensitivity to irradiation should be performed after normalization with the unirradiated absorbed energy results]. As discussed in Section 5, the Charpy impact energy results (absolute values) indicate a directional dependency (C-L vs. L-C) consistent with the CT fracture toughness results (J values) from the HFIR 4M specimens.

Additional data analysis of the UBR results is provided in reference 24.

6.4 Fracture Toughness - CT Specimens

The commercial nuclear construction code, ASME BPV code Section III, and requirements for in-service inspection, ASME BPV code Section XI, do not specify fracture toughness properties for irradiated austenitic stainless steel weldment components in either design or flaw evaluation criteria. The fracture toughness data generated in this study provide site-specific fracture toughness parameters for elastic-plastic fracture analyses of the SRS reactor tank sidewalls.

The comparison of the as-irradiated toughness results and selection of "nominal" and "lower bound" properties for engineering analyses is based on the J value at a crack extension (Δa) of 1 mm from the J-R curve. The average J at $\Delta a = 1$ mm of crack extension for each category is listed in Table 5-3A with individual specimen results listed in Appendix 1. The onset of stable tearing [44], denoted by J_{IC} (Table 5-3A), calculated from the J-deformation formulation, is not used as a basis for selection of engineering properties. The parameter J_{IC} , a calculated parameter and the associated average tearing modulus, T, are subject to uncertainty because of the approaches to deal with regression analyses of unloading compliance data, selection of different effective elastic moduli, and treatment of blunting line data; also, the ASTM definition of J_{IC} has recently changed (see Section 4).

From the results of J at $\Delta a = 1$ mm listed in Table 5.3A, the lower bound toughness category is the HAZ, C-L category with J @ 1mm of 662 in-lb/in². The remaining categories have J @ 1mm values from 1502 to 2900 in-lb/in². As noted in Section 5, a clear directionality effect for the Base and HAZ materials exists for the absolute as-irradiated toughnesses with the L-C orientation having higher toughness than the C-L orientation. [The C-L orientation provides a crack plane along the pipe axis or rolling direction of the original plate material].

Characterization of the material resistance to fracture is given by J-R curves and the associated material J-T curves developed from the power law fit to the J-R curve data to represent the material resistance to fracture. The J-R curve is the proper format since all the specimens exhibited a ductile fracture mode and the elastic-plastic deformation mode is appropriate for the compact tension specimen design (and for fracture characterization of postulated tank flaws). The material J-T curve from the J-R data is given by:

$$J_D \left[\frac{\text{in}\cdot\text{lb}}{\text{in}^2} \right] = C\Delta a^N, \text{ with } \Delta a \text{ in inches}$$

and,

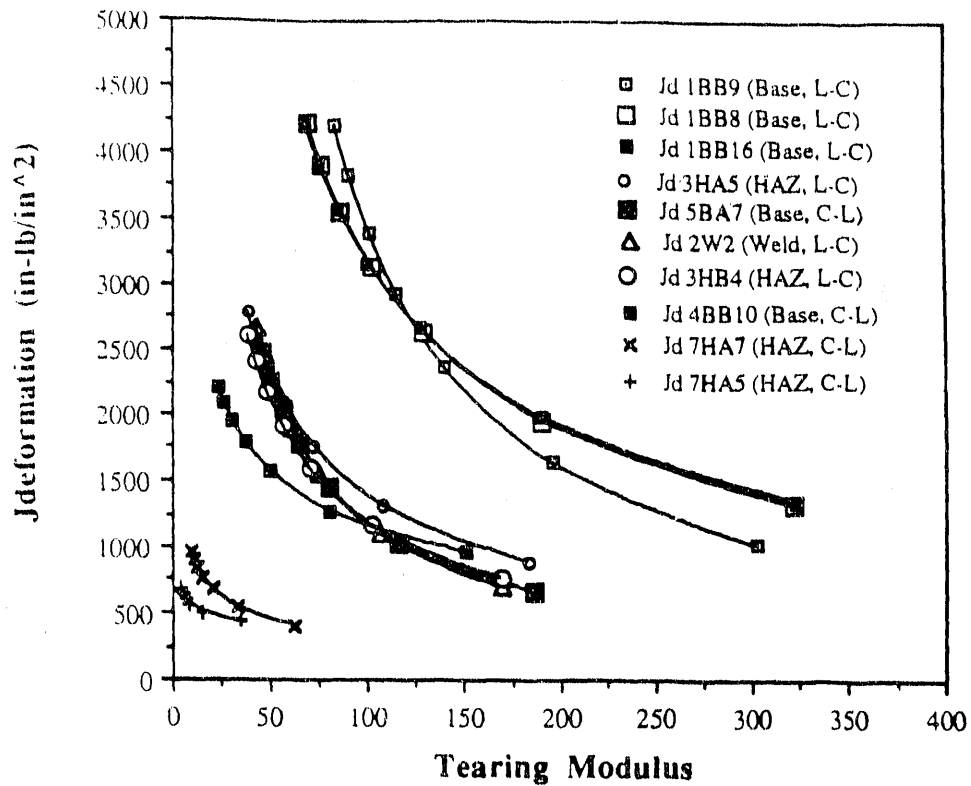
$$T = \left(\frac{C(N)}{\Delta a^{N-1}} \right) \left(\frac{E}{s_f^2} \right)$$

where the expression for J_D (J-deformation) is the power law formulation of the J-R curve data with the coefficient parameter, C, and the exponent parameter, N [Note that the power law parameters for the RMP CT data are contained in Appendix 1 for J in units of kJ/m^2].

Figure 6-1 shows the material J-T curves from the HFIR 4M CT specimens; the equations describing the J-T curves are contained in Appendix 2. The 4M materials included at least one specimens from each category (Figure 2-1) at 125°C except for the Weld, C-L category. It is seen in Figure 6-1 that the 7HA specimens (7HA5 and 7HA7) are the lower bound results to the 4M data. Alternatively, the low carbon (0.035%) 1BB specimens (Base, L-C category) had the highest toughnesses of the 4M specimens. The remaining 4M specimens possess J-T curves at similar toughness levels.

For the purpose of identifying material toughness for elastic-plastic fracture analysis (Section 7), the J-T curve from the 7HA5 specimen is ascribed as the "lower bound" irradiated material toughness, and the J-T curve from the 2W2 specimen is ascribed as the "nominal" irradiated material toughness. The corresponding Ramberg-Osgood parameters from the 125°C HAZ, L-C category (specimen 3HA8) may be applied to calculate J_{applied} (Section 7).

Material J-T Curves - HFIR 4M Specimens



Lower Bound Material Fracture Toughness Parameters (from Appendix 2)

The J-T curve (7HA5) equations are:

$$J_D \left[\frac{\text{in-lb}}{\text{in}^2} \right] = 949 \Delta a^{0.1600}, \text{ with } \Delta a \text{ in inches}$$

and,

$$T = \frac{0.5901}{\Delta a^{0.8400}}$$

for $s_f = 84.9$ ksi, with the limit on Δa of 0.1181 inches corresponding to $J = 674$ in-lb/in².

The Ramberg-Osgood parameters from corresponding tensile data (3HA8) are: $\alpha = 5.52$; $n = 10.8$; with $\sigma_y = 81.2$ ksi.

Figure 6-1: Material J-T curves from the HFIR 4M capsule. The curves represent as-irradiated property categories from each category at 125°C except for the Weld, C-L category. The J-T curve from specimen 7HA5 is the Lower Bound material fracture toughness and the curve from specimen 2W2 is ascribed as the Nominal material fracture toughness for elastic-plastic analysis of tank flaw postulates (Section 7).

7.0 AS-IRRADIATED MECHANICAL PROPERTIES: APPLICATION TO TANK FRACTURE ANALYSES

7.1 Introduction

The results in Section 5 demonstrate that the SRS reactor tank sidewall materials, irradiated weldment components of Type 304 stainless steel with Type 308 stainless steel filler, remain tough, ductile materials at test temperatures and exposure conditions corresponding to current and anticipated future operating conditions of the SRS reactors. The CT testing results show that with increasing load applied to a pre-cracked specimen, the material undergoes significant plastic deformation and crack tip blunting prior to initiation of crack growth by ductile tearing [Section 5.6 and references 11, 42, 45, and 46]. With this material characteristic and under increasing load, crack growth initiation is followed by stable growth by tearing prior to unstable tearing. Hence, the maximum load that a flawed section can carry may be appreciably greater than the load that causes the initiation of flaw growth. Under these conditions, a safety analysis of a flawed component should give explicit consideration to crack tip plasticity and stable crack growth by tearing that precedes fracture instability.

Fracture mechanics can be broadly divided into several general categories, namely linear-elastic (LEFM), elastic-plastic (EPFM), plastic or limit load analysis, and combinations thereof. Linear elastic fracture mechanics (LEFM) techniques ignore crack tip plasticity. LEFM methods can take into account a rising crack resistance during stable growth, but its predictions may give inaccurate estimates of the load carrying capability of the component.

The evaluation of flaw stability or fracture analysis of a structure requires mechanical property data, stress analysis, and a fracture mechanics methodology. A fracture analysis of the SRS tanks, applying an elastic-plastic fracture mechanics methodology, was previously performed [50]. Estimated as-irradiated properties had been applied to calculate tank flaw instability lengths. Subsequently, irradiated property data became available from the RMP irradiation programs. "Nominal" and "lower bound" as-irradiated mechanical properties including elastic-plastic fracture toughness properties for the tank fracture mechanics analysis were provided in Section 6. Several of these results have been applied in recent analyses of the SRS reactor tanks [51, 52]. A fracture handbook for the SRS reactor tanks will be prepared as part of the RMP [5] allowing material-specific properties to be applied to evaluate flaw stability. An overview of the elastic-plastic fracture mechanics methodology for the tanks, the J-T instability criterion, and an example of the application of the as-irradiated properties to flaw stability evaluation are provided in Section 7.2.

7.2 SRS Reactor Tank Fracture Analysis

The elastic-plastic fracture mechanics approach, based on the J-integral and the associated tearing modulus, T , instability criterion [53, 54], has been applied to determine the load capacity and calculate safety margins for postulated flaws in the reactor tanks [50, 51, 52]. Figure 7-1 shows schematically the definition of flaw instability for evaluation of flaws. There are several considerations in the J-T approach to assess flaw stability. The first consideration requires equilibrium between the potential to extend an existing crack, J_{applied} , and the material resistance to crack extension, J_{material} or J-R curve. The quantification of the irradiated material fracture resistance is given in Section 7.2.1.

The J-integral (J_{applied}) is a measure of the elastic-plastic stress-strain field around the crack tip field for any specified crack geometry and loading; J_{applied} is dependent on the material stress-

strain relationship. The J_{applied} formulation for the SRS reactor tank analysis is discussed in Section 7.2.2.

By combining the crack driving force solution for a specific crack/structure geometry (J_{applied}) with the experimentally determined material J-R curve, it is possible to predict the critical load (or displacement) at which unstable crack propagation occurs. This determines the amount of stable crack growth achievable prior to instability. Specifically, the J-R curve is superimposed on the J_{applied} diagram at the appropriate initial crack length, a_0 . Equilibrium requires that the J driving force be equal to the material's resistance to crack growth at each applied load level. Crack instability occurs at the crack length corresponding to the tangency between J_{applied} and J_{material} as shown in the diagram at the bottom of Figure 7-1. A convenient means to define the margin against instability involves plotting J versus T for the applied and material resistance values. A schematic diagram showing crack instability as the intersection of the two J-T curves is given in the top diagram of Figure 7-1.

This point of instability is expressed by [53, 54]:

$$\begin{aligned} J_{\text{applied}} &= J_{\text{material}} \\ T_{\text{applied}} &= T_{\text{material}} \end{aligned} \quad (2)$$

where T_f (nondimensional) is the tearing modulus defined as:

$$\begin{aligned} T_{\text{applied}} &= \frac{E}{s_f^2} \left(\frac{dJ_{\text{applied}}}{da} \right) \\ T_{\text{material}} &= \frac{E}{s_f^2} \left(\frac{dJ_{\text{material}}}{da} \right) \end{aligned} \quad (3)$$

and where: E = the elastic modulus (28×10^6 psi), and
 s_f = flow stress (Section 6.2.2).

The second consideration in the J-T approach is that proportional loading of the crack tip field must be satisfied during crack growth. The condition for the proportional loading (J-controlled growth) is:

$$\omega = \left(\frac{dJ}{da} \right) * \left(\frac{b}{J} \right) \gg 1, \quad (1)$$

where b is the remaining ligament, and a is the crack length. Generally, only small amounts of crack growth are allowed under the strict requirements of J-controlled growth. It has been previously reported that J-controlled growth requirements are satisfied when ω is greater than 10 [55], but recent studies show that crack extension to $\omega = 1$ meets the proportional loading criteria [35]. The large (1T) vs. small (0.4T) specimen testing performed in the RMP baseline program (Section 5.5 of reference 35) provide justification for a cut-off in the J-R data up to at least $\Delta a = 3$ millimeters. Since the crack growth in the large (1T) specimen, in which ω is greater than 10 at $\Delta a = 3$ mm, yielded results equivalent to the small (0.4T) specimen up to at least 3 mm, crack extension in the 0.4T planform specimen apparently occurred under J-controlled growth

(remaining ligament in the small specimen sufficient to allow J-controlled growth up to 3 mm). The ω at $\Delta a = 3$ mm for the 0.4T planform specimen is 1 (RMP Calculation Set #91-03, Part 2). The parameter ω at $\Delta a = 3$ mm for the irradiated specimens is also approximately 1 and therefore a cutoff at $\Delta a = 3$ mm (0.118 inches) is recommended for the irradiated J-T curves (Section 6). The equations for the irradiated material J-T curves are provided in Appendix 2.

Section 7.2.1 outlines the approach in development of the as-irradiated material properties in the J-T instability criterion analysis for the tanks. [The application of material toughness properties from this testing program to the tank is discussed for the J-deformation material fracture toughness results which are similar to the J-modified results for crack extension (Δa) of approximately 1 mm and lower bound to the J-modified results at crack extensions greater than approximately 1 mm (see ref. 35, Figure 4-4). The testing results for the J-modified formulation are contained in the final reports by Materials Engineering Associates and Westinghouse Electric Corporation [11, 42, 45, and 46]].

Section 7.2.2 provides references for the approach and methodology in the definition of the applied J-T for the tank fracture analysis.

Section 7.2.3 provides an example of the application of the as-irradiated properties to a flaw stability analysis (reproduced from reference 51).

7.2.1 Material J-T Curves

The J-resistance (J-R) curves developed in this work provide the material fracture toughness for the SRS reactor tank sidewall weldment components.

The J-R curve defines the material resistance to crack extension. J-R curves for each of the CT specimens are contained in Appendix 2 to this report. The lower bound toughness for the irradiated material (7HA5) bounds the material toughnesses for the specimens tested in the SRL irradiation programs (Section 6).

The equations describing the material J-T curve formulation are provided in Section 6.4. The J-T curves from the 4M specimens are shown in Figure 6-1. The data range corresponds to Δa of 0.2 mm up to the limit of J-controlled crack extension, with the upper limit of J validity taken at the J value at $\Delta a = 3$ mm of crack extension. Alternate "cut-off" options are presented schematically in Figure 7-2.

7.2.2 Applied J-T Curve Formulation

As shown schematically in Figure 7-1, elastic-plastic fracture mechanics analyses are based on a comparison of the J-integral crack driving force (J_{applied}), which reflects the crack configuration and applied loads, and the crack growth resistance in a given material [53, 54]. An estimation procedure for calculating the J crack driving force for several cracked configurations has been established [58]. The J_{applied} formulation for axial and circumferential flaw postulates in the SRS reactor tanks for pressure loadings, thermal gradient loadings, and residual stresses are discussed in detail in reference 50 and summarized in reference 51. The following discussion provides an overview of the development of the applied J-T for the reactor tank fracture analysis.

The J_{applied} formula for pressure loadings are calculated from the formulas for a crack in an infinite plate with suitable shell correction factors to account for the curvature effects [53, 54]. Standard formulas [56] for calculating stress intensities for bending stresses due to thermal

gradient loadings were applied. The stress intensity for residual stresses are calculated by applying a residual stress distribution with a peak stress of 45 ksi in the form of nodal loads on the nodes at the crack surface in a finite element model of the tank. The stress intensities from the pressure loadings, thermal gradient loadings, and residual stresses were added linearly and converted into J_{applied} with the expression $J_{\text{applied}} = K^2/E$ where K was the sum of the stress intensities and E is Young's Modulus (given above).

The set of J_{applied} values as a function of crack length (a) is formed and the applied tearing modulus (T) is calculated with the expression shown above.

7.2.3 Flaw Stability Analysis: Example Case

For the development of UT Acceptance Criteria for the inspection of the SRS reactor tanks [51], the elastic-plastic J-T instability criteria was applied to postulated flaws. The lower bound material J-T curve from the 7HA5 specimen together with the applied J-T from normal operation plus accident or seismic loadings were applied to the J-T instability analysis. The most limiting instability crack length of 25 inches is seen as the intersection of the material and applied J-T curve construction shown in Figure 7-3. The loading cases, including a safety factor of 1.4 on the accident pressure loading, are noted at the top of the figure.

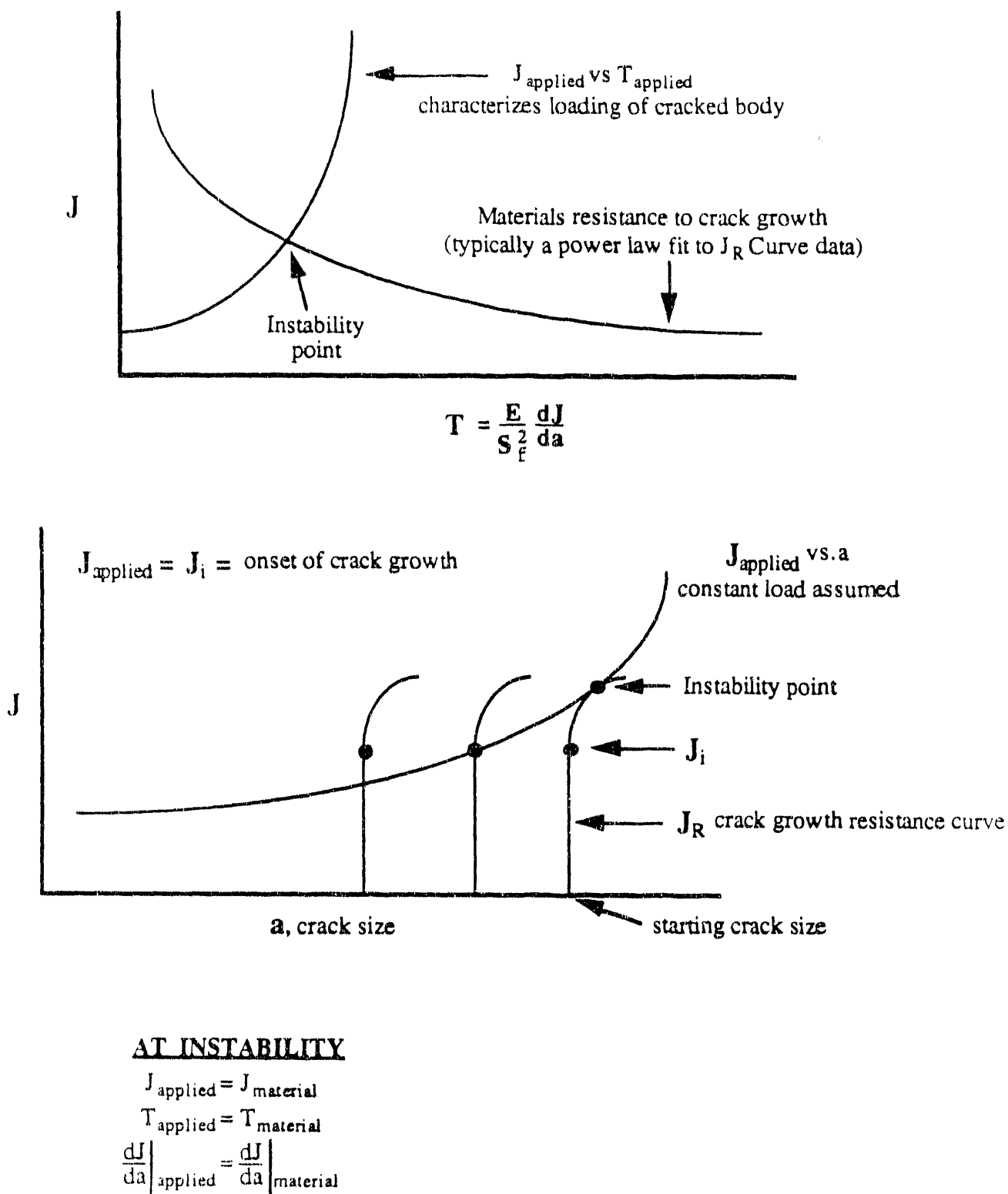


Figure 7-1: Equivalent J-T, J-a Illustrations of Crack Growth Stability [51].

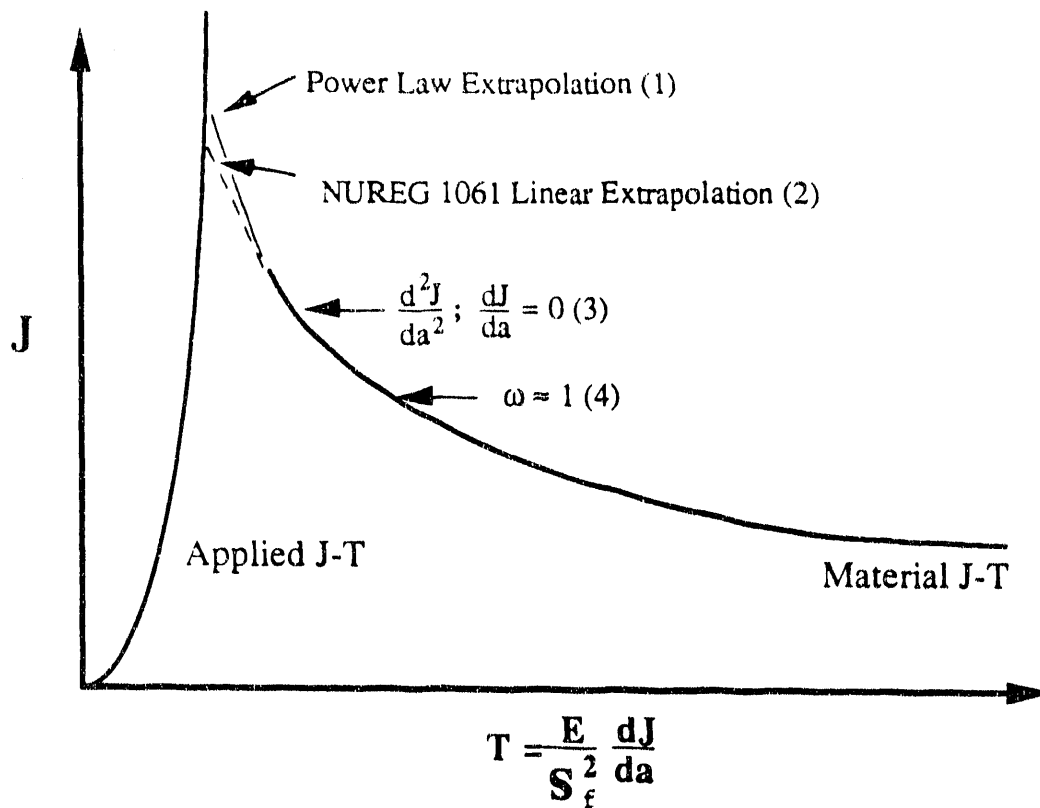


Figure 7-2: Material J-T Curve "Cut-off" Options to define instability:

- (1) Power-law extrapolation of the material J-T curve to intersect the applied J-T curve;
- (2) Linear extrapolation of the material J-T curve to intersect the applied J-T curve;
- (3) Horizontal cut-off at $d^2J/(da)^2$ or $dJ/da = 0$; and
- (4) Horizontal cut-off at $\omega = 1$ (recommended, see Section 5-5 of Reference 35).

ALLOWABLE CRACK LENGTH - LOCATION A

ACC. COND. PRESS. * 1.4† + TG + RESID

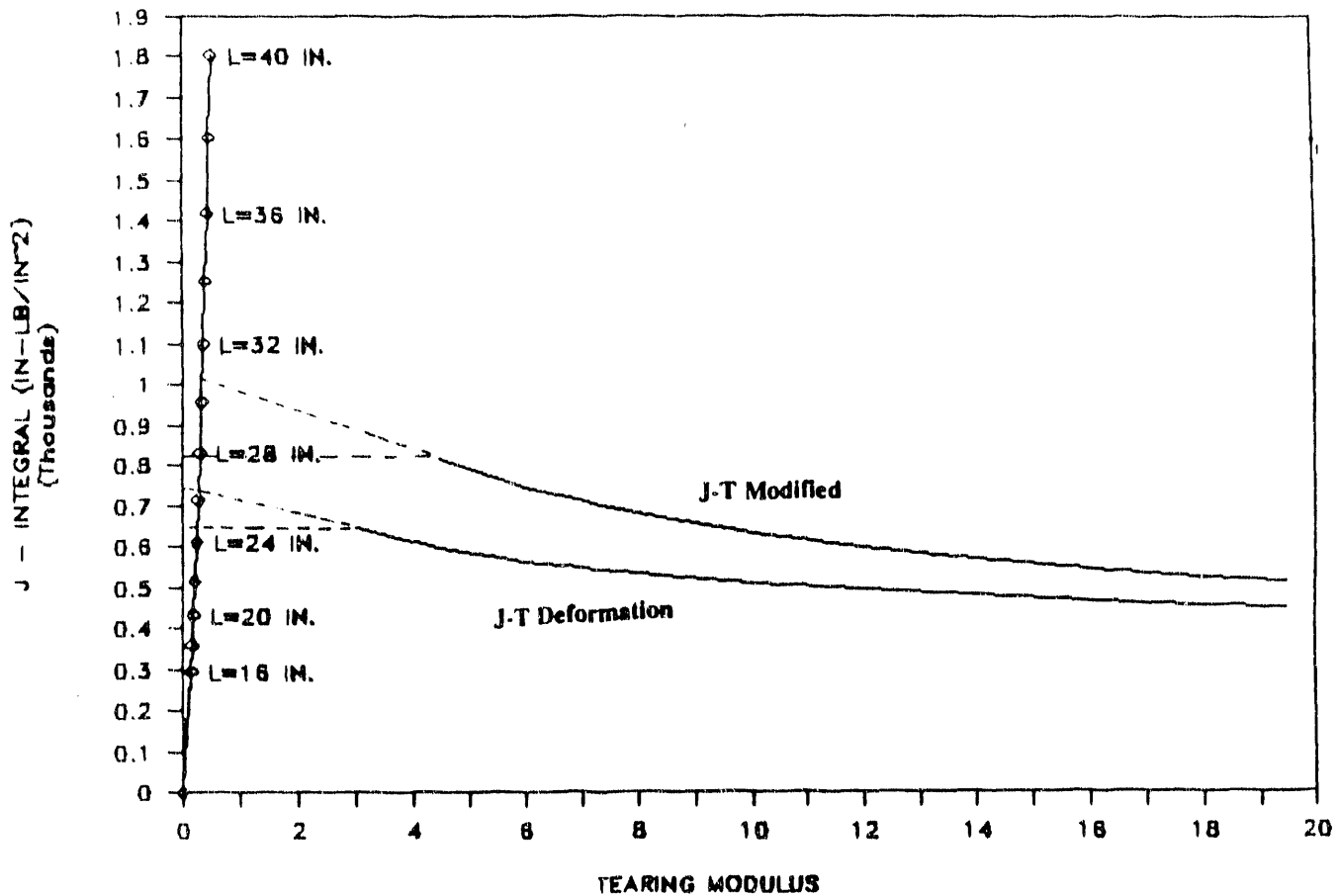


Figure 7-3: Example case of derivation of instability crack length with J-T analysis. The case is the most limiting case (shortest instability crack length) for the reactor tank. The example is reproduced from reference 51.

8.0 RMP IRRADIATION EFFECTS STUDIES

8.1 Introduction

The Reactor Materials Program (RMP) activities to study irradiation effects on the mechanical and corrosion properties of the archival materials are listed in the RMP Action Plan [5]. The studies include both as-irradiated mechanical and corrosion testing and mechanical testing of specimens having been post-irradiation, thermally-cycled to evaluate helium embrittlement effects. This report provides the results of the as-irradiated mechanical testing. Additional activities to analyze irradiation effects to material properties have been completed or are in progress and are briefly described in this section. These studies provide improved understanding of the irradiation effects to the tank sidewalls and support the technical evaluation of SRS reactor tank service life.

Additional mechanical testing of specimens from the HFIR 12M capsule [28] and the K-surveillance capsules are planned under the RMP. The as-irradiated database provided in this report will be supplemented by the mechanical test results from the HFIR 12M specimens and the K-surveillance specimens. The as-irradiated database will be applied as material input data to the tank fracture handbook [5].

Microstructural and microchemical studies of Type 304 and 304L stainless steel from the sidewall of R tank and the RMP irradiation programs are being performed as part of material characterization studies to provide improved understanding of the mechanical and corrosion property response to irradiation at SRS reactor tank wall conditions. The scope of the investigations has been previously planned and specified [28] and activities are in progress.

Fractography analysis of the broken mechanical test specimen surfaces have been completed for the UBR Charpy V-notch (CVN) specimens [24] and the R-tank Tensile (T) specimens [12]. The fracture mode of the irradiated material is completely ductile tearing, the same as the unirradiated materials. A summary of the fractography analyses are provided in Section 5.6.

8.2 Additional As-Irradiated Testing: 12M & Surveillance Specimens

The 12M capsule contained 18 CT, 9 CVN, and 9 T specimens and was identical in design to the HFIR 1Q and 4M capsules. The as-irradiated testing of the 12M specimens [28] will provide additional as-irradiated data at highly exposed (7 dpa) levels to evaluate the trend of "saturation" in degradation and to evaluate the effects of the helium at present and future tank wall maximum helium levels on the mechanical response. The testing of the 12M specimens will be performed at ORNL in 1992 [28].

The K-Surveillance program provides a total of 60 CT, 60 CVN, 40 T, and 20 Wedge-Opening Loaded (WOL) specimens loaded in 12 separate specimen holders with 4 holders per specimen rod. The rods are located in the core of the K-reactor in the far side spargers. The K-Surveillance will provide: confirmatory data to the HFIR (high exposure level results) for specimens irradiated at neutron spectral, fluence rate, and moderator environment conditions more typical of the tank wall exposure history; expanded testing options; and compliance with the intent of ASTM-C185-82 for LWR Surveillance Programs [41]. The irradiation plan and testing plan for the specimens in the Surveillance Irradiation will be provided in a future RMP report [5].

8.3 Microstructural Analysis and Mechanical Property Correlation

Microstructural characterization of the as-irradiated stainless steel involves the identification and quantification of the size and number density of the lattice defect complexes and helium bubbles produced during irradiation. These microstructural features, produced as a result of irradiation, are responsible for the changes in mechanical properties of the material. The scope of the studies includes R-tank material (7×10^{20} n/cm², $E_n > 0.1$ MeV), specimens from the UBR Screening Irradiation (1.1×10^{20} n/cm², $E_n > 0.1$ MeV), and the HFIR Full-Term Irradiation (0.9×10^{21} n/cm² (1Q), and 3.8×10^{21} n/cm² (4M), $E_n > 0.1$ MeV) [28].

The microstructural characterization of material from the sidewall of the R-tank has been completed and the results have been reported [57]; the characterization of base material specimens from the Screening and Full-Term irradiations is in progress. The dominant microstructural feature is an interstitial defect cluster distribution of non-specific geometry with a most-probable size of approximately 2 nm and a total cluster density of 10^{17} cm⁻³. Figure 8-1 shows a micrograph of the R-tank material at high resolution imaging conditions illustrating the defect complexes produced during irradiation. Note that the specimen was considered Type 304L based on the available carbon assay at the time the figure was produced; subsequent chemical analysis of disk RA3 has shown this material to be Type 304 stainless steel (see Table 2-4). Figure 8-2 is a histogram of the size of the defect complexes in the RA3 material.

A comparison of the results from the specimens listed above will provide quantification of the defect complex microstructure and will show whether the size/number density of the clusters has reached saturation levels. The final results of the microstructural characterization of the as-irradiated materials will be applied to models of radiation hardening to calculate the increase in yield strengths due to the defect complexes [5]. The results will be compared to the mechanical testing results in this report.

8.4 Microchemical Analysis and Solute Segregation Estimation

Microchemical mapping of selected RMP corrosion specimens is being performed [28] to measure the extent of radiation-induced segregation, a necessary but not sufficient condition for Irradiated-Assisted Stress Corrosion Cracking (IASCC). This degradation mode has been postulated for the SRS reactor tanks [58, 59], although corrosion specimen testing previously completed [60] has shown that IASCC would not occur at the SRS reactor irradiation conditions (temperature and exposure level). The scope of the mapping studies includes a 4x4 specimen matrix of sensitized/unsensitized and irradiated/unirradiated materials from the HFIR 4C corrosion capsule and a specimen of R-tank sidewall material.

Although IASCC is not predicted to occur in the SRS reactor tanks [61, 62], susceptibility to IASCC for SRS tank wall irradiation conditions is investigated in the RMP [5] both directly, by corrosion testing of irradiated Type 304 stainless steel, and indirectly, by analytical predictions and measurements of solute segregation at the microstructural grain boundaries as discussed above. The irradiated corrosion testing [58] provides the strongest technique for evaluating the effects of irradiation on the corrosion response of the stainless steel to the moderator environment. Analytic predictions or measurements of solute distribution, should it occur, do not provide quantification of the corrosion response, but do provide information and improved understanding of the potential for degradation of corrosion resistance of the tank sidewalls due to irradiation exposure.

DEFECT CLUSTERS IN 304L STAINLESS STEEL

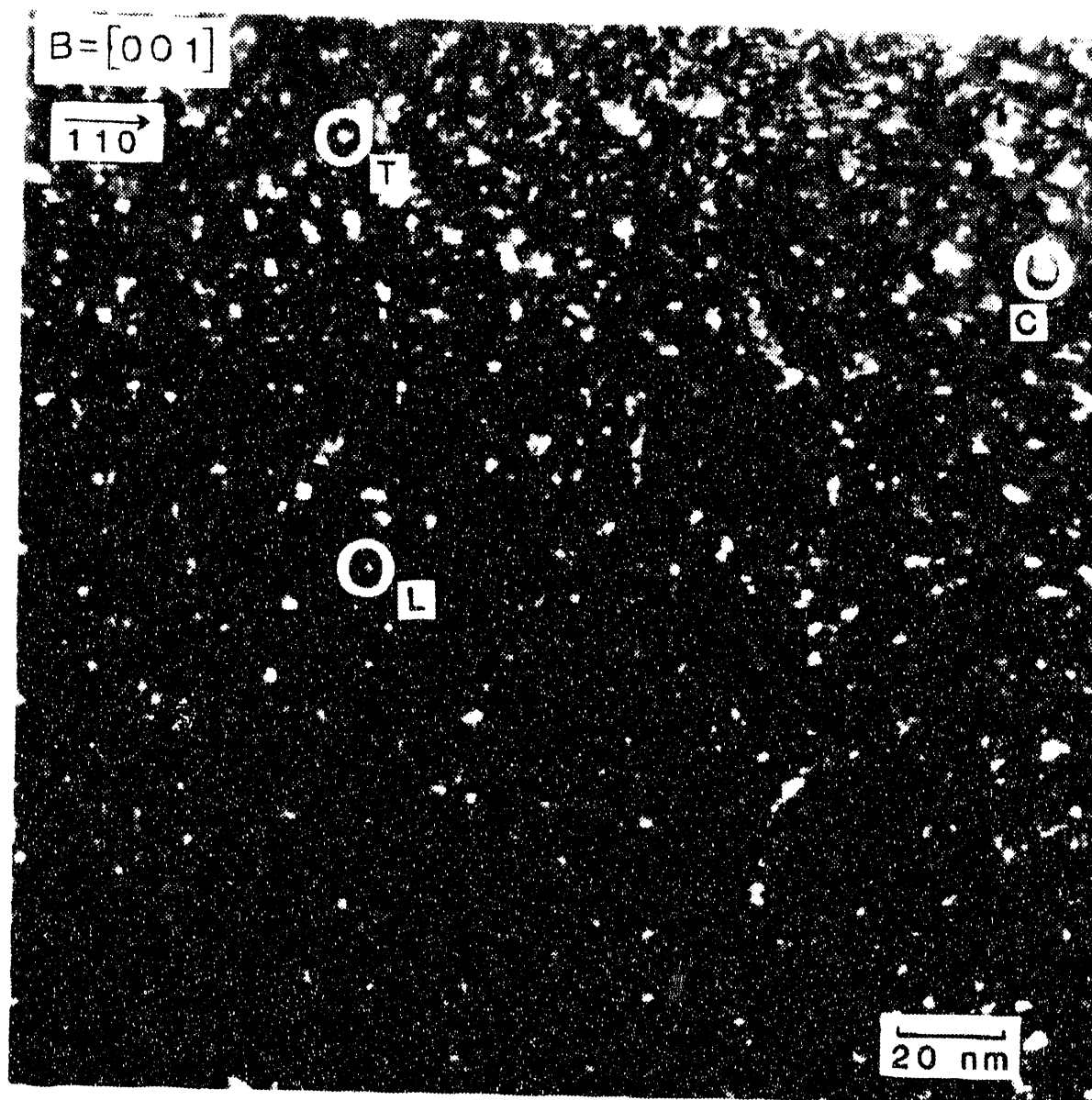


Figure 8-1: Weak-beam dark field Transmission Electron Micrograph of the irradiation-produced defect complex microstructure of R-tank sidewall (reproduced from reference [57]). The complexes are postulated to be predominantly interstitial clusters having a non-specific geometric configuration with most-probable size of 2 nm and total cluster volume density of 10^{17} cm^{-3} . A small percentage ($< 5\%$) of Stacking Fault Tetrahedra, triangular loops, and circular loops were produced and are identified by "T", "L", and "C", respectively, on the micrograph.

ORNL-DWG 87-15104

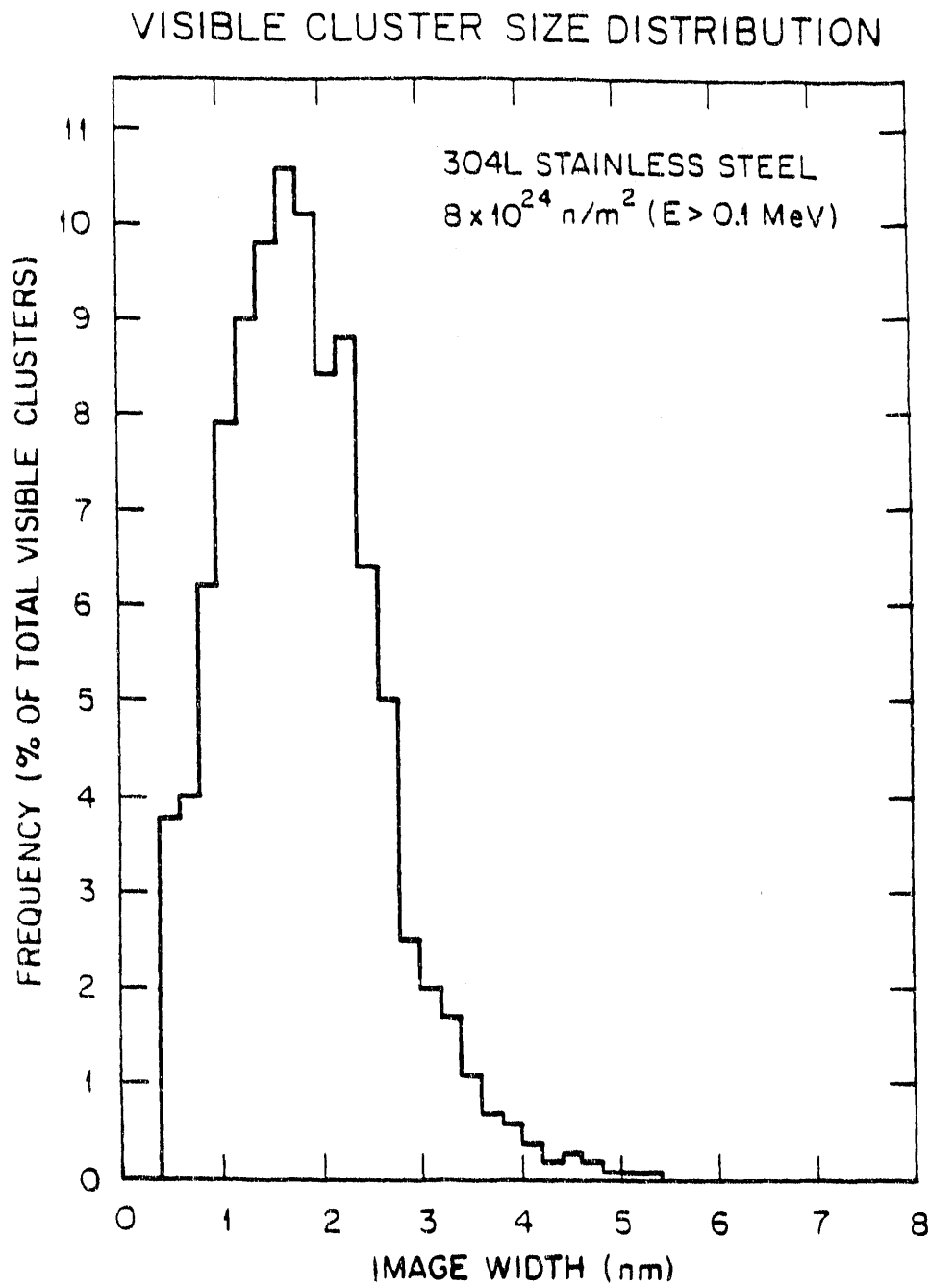


Figure 8-2: Histogram of the size/volume density of the defect complexes in R-tank specimen RA3.

9.0 ACKNOWLEDGMENTS

The development of as-irradiated mechanical properties as part of the Savannah River Laboratory Reactor Materials Program was achieved through the dedicated work of several past and present members of the RMP task group and the support of management from SRL and the Reactor Engineering Department. The authors of this report would like to acknowledge the following SRS personnel for their contributions to the RMP irradiation programs necessary to produce this report:

N.G. Awadalla
N.P. Baumann
D.S. Cramer
K.R. O'Kula
G.A. Abramczyk
K.J. Stoner
J.K. Thomas

The RMP was also supported by the technical excellence of Materials Engineering Associates and Oak Ridge National Laboratory in the irradiation (MEA-UBR; ORNL-HFIR) and testing (MEA) of the specimens contained in this report. Numerous individuals from the subcontractors provided expertise and were dedicated to supporting this project. The authors would like to acknowledge J.R. Hawthorne, F.J. Loss, B.H. Menke, A.L. Hiser, and W.E. Cullen of MEA for all their fine work in irradiating (UBR) and testing the irradiated materials. The success of the HFIR irradiation program was due in large part to the work of R.L. Senn, K.R. Thoms, C.A. Baldwin, D.W. Heatherly, L.F. Miller, and R. Taylor of ORNL.

10.0 REFERENCES

1. N.P. Baumann, "Neutron Fluence in SRP Reactor Tank Walls," **DPST-86-793**, Savannah River Laboratory, November 1986; N.P. Baumann, "Gamma Ray Irradiation Damage to SRP Reactor Tank Walls," **DPST-88-781**, Savannah River Laboratory, October 1988.
2. J.M. Morrison, "Reactor Tank Wall Temperatures," **DPSF 62-1517**, January 28, 1963.
3. R.L. Sindelar, N.G. Awadalla, N.P. Baumann, and H.S. Mehta, "Life Extension Approach to the Reactor Vessel of a Nuclear Production Reactor," in Life Assessment and Life Extension of Power Plant Components, PVP-Vol. 171, ASME 1989.
4. N.G. Awadalla, et. al., "Reactor Materials Program," **DPST-84-820**, December 1984.
5. Savannah River Laboratory, Nuclear Reactor Technology and Scientific Computations Department, "Reactor Materials Program Action Plan," **Task Technical Plan # 89-023-1**, December 1990.
6. E.M. Vessel to N.G. Awadalla, "Reactor Materials Program - Tank Weld Inspection," May 2, 1986, (in RMP Task Files 89-023-C-1).
7. K.J. Stoner, "Reactor Materials Program - Materials Source History for Type 304 Stainless Steel Testing Program," **DPST-88-1010**, December 1988; K.W. Murphy and K.J. Stoner, "Reactor Materials Program - Material Characterization of Archival Type 304 Stainless Steel Piping (U)," **WSRC-TR-91-496**, Savannah River Laboratory, September 1991.
8. Reactor Materials Program, "Specification for Sample Preparation, Irradiation and Testing," **SRP-SL-1101**, June 25, 1984 (in Task 89-023-1 Files).
9. Reactor Materials Program, "Revision to Specification for Sample Preparation, Irradiation and Testing," **SRP-SL-1108**, 1989 (in Task 89-023-1 Files).
10. J.W. Joseph Jr., "Mechanical Properties of Irradiated Welds in Stainless Steel," **DP-534**, Savannah River Laboratory, December 1960.
11. R.G. Lott and J.A. Begley, "SRP Reactor Operability Assurance Program: Fracture Toughness of Savannah River R-Tank Material," **WSRP-004**, April 1987.
12. J.W. Cunningham, R.P. Shogan, R.J. Jacko, and S. Wood, "SRP Reactor Operability Assurance Program: Tensile Properties of Savannah River Materials" **WSRP-005**, March 13, 1987.
13. Calculation Set #91-06 in RMP Task 89-023-B-1 Files, HFIR Irradiation Results: 1Q and 4M Specimen Temperatures and Neutron Exposures; J.K. Thomas to R. L. Senn, **SRL-ORNL-90-05**, "Reactor Materials Program, Specification SRP-SL-1107, ORNL-HFIR Capsule 1Q Measured Temperatures," Savannah River Laboratory, March 27, 1990.
14. W.L. Daugherty, Savannah River Laboratory - Nuclear Reactor Technology & Scientific Computations, Task number 88-001-01, Rev. 3, "Qualification of LOCA Definition Project," November 1990.

15. K.A. Crawford, W.L. Daugherty, and D.D. Sousa, "LOCA Definition Project Analysis of Controls Task Number:88-001-1," **WSRC-RP-90-1174**, November 1990.
16. W.L. Daugherty, "LOCA Definition Project Peer Review Report (U)," **WSRC-RP-89-341**, Rev. 1, November 1990.
17. W.L. Daugherty, "Evaluation Team Report on the Qualification of the LOCA Definition Project (U)," **WSRC-TR-90-567**, December 1990.
18. "Nuclear Reactor Technology and Scientific Computations Department Quality Assurance Manual (U)," **IQ-34**, Rev. 4, 9/1/91, Savannah River Laboratory.
19. DPSOX 2848, 6/10/59.
20. Marin, "SRP Reactor Operability Assurance Program: Executive Summary," **WSRP-001**, April 1987.
21. W.L. Daugherty, "Process Water System Temperatures and Pressures," **SRL-EDG-890119**, October 13, 1989.
22. ASTM Handbook A813/A813M-88a, Standard Specification for Single- or Double-Welded Austenitic Stainless Steel Pipe, A01.10, 1989.
23. E.F. Nipples, Metals Handbook, Ninth Edition, Volume 6 - Welding, Brazing, and Soldering, American Society for Metals, 1982.
24. J.R. Hawthorne, et. al., "Sample Preparation, Irradiation, and Testing of 304 Stainless Steel Specimens," Materials Engineering Associates, Report **MEA-2221**, August 1987.
25. R.L. Sindelar, G.E. Mertz, and K.J. Stoner, "Reactor Materials Program - Leak-Before-Break Analysis of the Reactor Process Water System Piping (U)," **WSRC-RP-90-91**, Savannah River Laboratory, March 1990.
26. R.P. Shogan, "SRP Reactor Operability Assurance Program: Characterization of Savannah River Materials," **WSRP-003**, April 1987..
27. R-Tank Construction Records: 1) M & E Activities at New York Ship, "Part VII, Section IV - R, P, & L Main Tank," May 28, 1954 (SRP File Box M-898, formerly box 394); 2) M & E Activities at New York Ship, "Part VII Section III - R, P, L Bottom Tube Sheet Assemblies," April 28, 1954 (SRP File Box M898, formerly box 394); 3) M & E Activities at New York Ship "Part VIII "K" Unit Plenum Chamber, Top Tube Sheet and Tank Assembly," June 3, 1954 (SRP File Box M898, formerly Box 394); 4) NYX Fabrication Manual, "L" Unit B.T.S. and Tank" (SRP File Box 6493 Formerly Box 393); 5) NYX Fabrication Manual, "C" Unit (SRP File Box 6493, Formerly Box 393); 6) NYX Fabrication Manual, "General Information," (SRP File Box 6818, Formerly Box 392).
28. Reactor Materials Program Specification No. **SRP-SL-1111**, "Specification for Shipping, Testing, and Analysis of Irradiated Stainless Steel Mechanical and Corrosion Specimens," Rev. 2 October 31, 1991 (in Task 89-023-1 Files).

29. D.S. Cramer, "SRP Irradiation Program in Support of the SRP Reactor Materials Program," **DPST-84-811**, Savannah River Laboratory, December 1984.
30. G.A. Abramczyk, "Selection of SRP Surveillance Specimens for Reactor Materials Program," **DPST-85-902**, Savannah River Laboratory, December 1985.
31. Reactor Materials Program, "Specification for Irradiation and Shipping of 304SS Utilizing the HFIR at ORNL," **SRP-SL-1107**, October 1985 (in Task 89-023-1 Files).
32. R.L. Senn, Experiment Number SRL-1Q, -4M, -12M, -4C, Experiment Information and Safety Analysis Form for Experiments in the ORNL Research Reactors, ORNL HFIR, April 24, 1986.
33. C.A. Baldwin and L.F. Miller to R.L. Senn, "Damage Exposure Parameters for the SRL 1Q and 4M Irradiation Capsules and Removable Dosimeter Tubes," ORNL Martin Marietta Energy Systems, Inc., Internal Correspondence, April 25, 1988.
34. R.L. Sindelar, G.A. Abramczyk, and K.R. O'Kula "Selection of HFIR Specimens for SRP Reactor Materials Program," **DPST-86-418**, Savannah River Laboratory, April 1987.
35. K.J. Stoner, R.L. Sindelar, and G.R. Caskey Jr., "Reactor Materials Program - Baseline Material Property Handbook-Mechanical Properties of 1950's Vintage Stainless Steel Weldment Components (U)," **WSRC-TR-91-10**, Savannah River Laboratory, April 1991.
36. D.G. Doran, "Neutron Displacement Cross Sections for Stainless Steel and Tantalum Based on a Lindhard Model," *Nuclear Science and Engineering* **49** (1972) p. 130.
37. L.R. Greenwood, in Alloy Development for Irradiation Performance, Semiannual Progress Report, DOE/ER-0045/11, pp.30-37, September 1983.
38. J.W. Joseph, "Reactor Tank Corrosion," in **DPSP 60-1-2**, Progress Report, Works Technical Department, February 1960, p.73.
39. J.W. Joseph, "Stress Relaxation in Stainless Steel During Irradiation," **DP-369**, Savannah River Laboratory, June 1959.
40. J.K. Thomas, "Reactor Materials Program - K-Reactor Surveillance Capsule Specimens," **SRL-EDG-90-0225**, Savannah River Laboratory, April 1990.
41. J.K. Thomas, R.L. Sindelar, and N.P. Baumann, "Overview of the Savannah River Reactor Surveillance Program (U)," **WSRC-MS-91-270**, ASME PVP Conference Nuclear Plant Systems/Components Aging Management and Life Extension, New Orleans, LA, June 1992.
42. J.R. Hawthorne, "Parametric Study of Fracture Resistance and Welding Variables of Irradiated Type 304 Stainless Steel," **Materials Engineering Associates, MEA-2465**, October 1991.
43. L.E. Steele, J.R. Hawthorne, and C.Z. Serpan Jr., in "Irradiation Effects on Reactor Structural Materials," **NRL Memorandum Report 1676**, U.S. Naval Research Laboratory, February 1966.

44. A.L. Hiser and J.R. Hawthorne, "Baseline Tests (125°C) of Type 304 Stainless Steel Piping Materials From Project 1101," Materials Engineering Associates, MEA-2345, May 1989.
45. A.L. Hiser, B.H. Menke, and J.R. Hawthorne, "Fracture Toughness Characterization of Type 304 Stainless Steel Plate F50 Irradiated in HFIR Assembly 1Q," MEA-2214, 1987.
46. A.L. Hiser, B.H. Menke, and J.R. Hawthorne, "Fracture Toughness Characterization of Type 304 Stainless Steel Piping Materials Irradiated in HFIR Assembly 4M," MEA-2241, 1987.
47. E.E. Bloom W.R. Martin, J.O. Stiegler, and J.R. Weir, "The Effect of Irradiation Temperature on Strength and Microstructure of Stainless Steel," Journal of Nuclear Materials, 22 (1967) pp. 68-76.
48. H.R. Higgy and F.H. Hammad, "Effect of Fast-Neutron Irradiation on Mechanical Properties of Stainless Steels: AISI Types 304, 316, and 347," Journal of Nuclear Materials, 55 (1975) pp.177-186.
49. T.C. Gorrell, "Neutron Fluence in P, K Reactor Tank Walls," DPST-80-445, Savannah River Laboratory, October 1980.
50. H.S. Mehta, "Fracture Mechanics Evaluation of Potential Flaw Indications in the Savannah River L, P and K Tanks," SASR#86-64, prepared by GE Nuclear Energy, San Jose, for Westinghouse Savannah River Company, October 1989.
51. W.L. Daugherty, "Reactor Tank UT Acceptance Criteria (U)," WSRC-RP-89-208-Rev.2, Savannah River Laboratory, January 1990.
52. G.E. Mertz and J.K. Thomas, "Structural Response of the Reactor Tank to the Gamma Heating Accident (U)," WSRC-TR-91-554, Savannah River Laboratory, November 1991.
53. C.F. Shih and J.W. Hutchinson, Transactions, American Society of Mechanical Engineers, Journal of Engineering Materials and Technology, Series H, Vol. 98, 1976, pp. 289-295.
54. J.W. Hutchinson and P.C. Paris, "Stability Analysis of J-Controlled Crack Growth," ASTM STP 668, 1979, pp. 37-64.
55. C.F. Shih, R.H. Dean, and M.D. German, "On J-Controlled Crack Growth: Evidence, Requirements, and Applications," General Electric Company, TIS Report 1981.
56. D.P. Rooke and D.J. Cartwright, "Compendium of Stress Intensity Factors," Her Majesty's Stationary Office, London, September 1974.
57. S.J. Zinkle and R.L. Sindelar, "Defect Microstructures in Neutron-Irradiated Copper and Stainless Steel," Journal of Nuclear Materials 155-157 (1988) p. 1196.
58. W.L. Daugherty, et.al., "K-Reacto Tank Integrity Status (U)," WSRC-RP-89-152 Rev.2, Savannah River Laboratory, August 1991.

59. W.L. Daugherty, et.al., "L-Reactor Tank Integrity Status (U)," **WSRC-TR-91-558**, Savannah River Laboratory, December 1991.
60. G.R. Caskey Jr., R.S. Ondrejcin, R.L. Sindelar, and E.W. Baumann, "Effect of Neutron Irradiation on Stress Corrosion Cracking of Type 304 Stainless Steel in Simulated Savannah River Reactor Environments (U)," **WSRC-TR-91-12**, Savannah River Laboratory, January 1991.
61. G.R. Caskey Jr. and R.L. Sindelar, "IASCC in SRS Reactor Tanks," **SRL-EDG-900158**, Savannah River Laboratory, May 1990.
62. R.L. Sindelar, "Irradiation-Assisted Stress Corrosion Cracking," **SRL-EDG-900425**, Savannah River Laboratory, December 1990.

APPENDIX 1

AS-IRRADIATED MECHANICAL PROPERTY TEST RESULTS

DISCUSSION

Appendix 1 contains tables of the as-irradiated mechanical property data from the Reactor Materials Program irradiated properties testing program, the Reactor Operability Assurance Program (R-Tank Testing), and the results from Walt Joseph (Thermal Shield Materials irradiation). The tables have been reproduced from the original reports that are listed below.

Tensile (T) Data

As-irradiated tensile specimen test data was produced from specimens irradiated in the UBR, HFIR 1Q & 4M, R-Tank, and Thermal Shield materials programs. The original source of the UBR data is MEA 2221 [24]. The final MEA data for the 1Q and 4M specimens is reported in MEA 2465 [44]. The R-Tank data is reported in WSRP-005 [12]. The Thermal Shield data is reported in DP-534 [10].

Charpy V-notch (CVN) Data

As-irradiated CVN specimen test data was produced from specimens irradiated in the UBR, and HFIR 1Q & 4M irradiation programs. The original source of the UBR data is MEA 2221 [24]. The final MEA data for the 1Q and 4M specimens is reported in MEA 2465 [44].

Compact Tension (CT) Data

As-irradiated CT specimen test data was produced from specimens irradiated in the HFIR 1Q & 4M and from the R-Tank sidewall. The final MEA data for the 1Q and 4M specimens is reported in MEA 2465 [44]. The R-Tank data is reported in WSRP-004 [11].

THERMAL SHIELD TENSILE DATA (25°C TEST)

APPENDIX

MECHANICAL PROPERTIES OF IRRADIATED WELDS IN STAINLESS STEEL

Specimen Location	Exposure, fast nvt	Ultimate Strength, psi	Yield Strength at 0.2% Offset, psi	Total Elongation to Fracture, %	Elastic Modulus, psi	Hardness, Rockwell "A"	
						Preirradiation	Postirradiation
Weld, longitudinal	0	83,700	57,700	31	24.1x10 ⁶	--	--
	0	88,500	--	42	23.0x10 ⁶	--	--
	2.5x10 ²⁰	103,200	97,500	28	25.7x10 ⁶	58	63
	1.0x10 ²¹	103,100	97,700	28	24.4x10 ⁶	57	66
	1.2x10 ²¹	106,100	101,300	15	24.7x10 ⁶	56	56
0	102,300	96,600	13	27.6x10 ⁶	59	66	
Weld, transverse	0	82,500	45,000	50	26.9x10 ⁶	--	--
	0	86,400	44,100	50	26.4x10 ⁶	--	--
	0	83,400	46,000	32	26.4x10 ⁶	--	--
	0	86,300	42,400	53	27.0x10 ⁶	--	--
	0	85,800	44,300	54	27.7x10 ⁶	--	--
	0	86,200	47,000	50	25.5x10 ⁶	--	--
	0	86,100	49,100	44	26.0x10 ⁶	--	--
	0	86,300	42,400	65	26.2x10 ⁶	--	--
	2.7x10 ²⁰	101,900	87,300	39	23.9x10 ⁶	51	59
	3.0x10 ²⁰	102,300	92,500	25	26.9x10 ⁶	52	60
	1.1x10 ²¹	105,300	94,800	31	27.9x10 ⁶	47	51
1.2x10 ²¹	107,200	96,600	33	28.8x10 ⁶	51	62	
Heat-affected zone, longitudinal	0	82,700	38,000	62	29.2x10 ⁶	--	--
	0	84,100	39,200	65	27.6x10 ⁶	--	--
	0	84,000	39,800	62	27.5x10 ⁶	--	--
	0	84,500	39,200	65	26.4x10 ⁶	--	--
	2.8x10 ²⁰	100,700	85,100	42	28.8x10 ⁶	52	61
1.1x10 ²¹	105,500	93,800	39	25.5x10 ⁶	51	63	
Heat-affected zone, transverse	0	83,800	36,200	54	30.2x10 ⁶	--	--
	0	84,000	37,200	54	27.0x10 ⁶	--	--
	0	84,700	39,300	51	27.9x10 ⁶	--	--
	0	84,000	41,400	51	30.2x10 ⁶	--	--
	0	84,100	41,600	51	28.3x10 ⁶	--	--
	2.9x10 ²⁰	100,400	82,900	31	23.6x10 ⁶	52	60
1.1x10 ²¹	104,600	93,800	33	25.4x10 ⁶	51	61	
Plate, longitudinal	0	83,500	32,800	55	27.3x10 ⁶	--	--
	0	83,400	34,100	55	26.4x10 ⁶	--	--
	0	83,600	35,300	65	28.5x10 ⁶	--	--
	2.9x10 ²⁰	98,900	79,800	36	28.2x10 ⁶	48	60
	3.0x10 ²⁰	99,400	80,600	42	28.1x10 ⁶	48	61
	1.2x10 ²¹	104,200	92,700	6	28.1x10 ⁶	52	65
1.2x10 ²¹	104,400	91,500	-2	26.1x10 ⁶	-7	62	
Plate, transverse	0	82,700	33,000	62	26.4x10 ⁶	--	--
	0	83,100	33,900	62	26.3x10 ⁶	--	--
	0	83,100	--	52	--	--	--
	0	83,600	34,700	68	27.1x10 ⁶	--	--
	0	83,700	34,800	65	28.8x10 ⁶	--	--
	2.9x10 ²⁰	99,800	83,900	42	25.5x10 ⁶	50	61
	3.0x10 ²⁰	99,300	83,700	39	29.9x10 ⁶	50	63
	1.2x10 ²¹	104,900	90,900	-2	27.5x10 ⁶	50	62
	1.2x10 ²¹	104,600	91,200	15	30.4x10 ⁶	50	63

UBR TENSILE DATA (STRENGTHS) (25 AND 125°C TEST)

Table 6.3 Postirradiation Tensile Properties Determinations (Weld Metal Specimens)

Ring No.	Orientation	Test Temp. °C	Specimen No.	Yield Strength ^a			Tensile Strength		
				(MPa)	(ksi)	(Incr., %) ^b	(MPa)	(ksi)	(Incr., %)
5	Axial	25	5W23	586	85.0		722	104.7	
			5W25	598	86.7		717	104.0	
		125	(Avg)	(592)	(85.8)	53.7	(720)	(104.4)	16.7
			5W24 ^d	390	56.6		450	65.2	
6	Axial	25	6W50	579	84.0		718	104.1	
			6W51	576	83.6		719	104.3	
		125	(Avg)	(578)	(83.8)	52.9	(718)	(104.2)	14.8
			6W52 ^d	380	55.1		441	63.9	
7	CMFL	25	7W7	646	93.7		739	107.2	
			7W8	638	92.6		731	106.2	
		125	(Avg)	(642)	(93.1)	53.3 ^c	(736)	(106.7)	17.9
			7W9	401	58.2		430	62.4	
	CMPL	25	8W8	641	93.0		732	106.2	
			8W9	651	95.0		751	109.0	
125	(Avg)	(646)	(94.0)	77.3	(742)	(107.6)	19.4		
	8W7	428	62.1		468	67.9			

¹ 0.2% Offset, static tests
² Increase over unirradiated condition average
³ Referenced to unirradiated ring no. 5 weld properties (CMFL)
⁴ Specimen broke outside of extensometer gage length of 13.4 mm

UBR TENSILE DATA (DUCTILITIES) (25 AND 125°C TEST)

Table 6.4 Post Test Measurements of Tensile Ductility (UBR-60 Irradiated Specimens)

Ring No.	Orientation	Specimen No.	Temp. (°C)	Reduction in Area (%)	Elongation (% in 0.80 inch)	Fracture Appearance
5	Axial	5W23	25	73.5	46.0 ^b	Cup Cone Slant Fracture
		5W25	25	66.8	37.0 ^c	
		(Avg)	(25)	(70.2)	(41.5)	Cup Cone
		5W24	125	69.7	29.3 ^b	
6	Axial	6W50	25	62.2	45.0 ^b	Slant Fracture 2-Prong
		6W51	25	40.7	36.0 ^c	
		(Avg)	(25)	(51.5)	(40.5) ^a	Cup Cone
		6W52	125	75.5	42.6	
7	CMPL	7W7	25	29.4	12.0 ^b	Slant Fracture Slant Fracture
		7W8	25	62.2	38.5 ^c	
		(Avg)	(25)	(45.8)	(25.3)	Slant Fracture
		7W9	125	60.9	36.4 ^c	
8	CMPL	8W8	25	61.6	42.3 ^c	Slant Fracture Slant Fracture
		8W9	25	57.7	35.8 ^c	
		(Avg)	(25)	(59.7)	(39.1)	Slant Fracture
		8W7	125	57.7	27.6 ^c	

^a Specimen fractured outside of 0.800 inch gage length (outside gage marks)

^b Specimen fractured at gage mark.

^c Specimen fractured at mid-gage length.

HFIR IQ TENSILE DATA (STRENGTHS) (125°C TEST)

Table 6 Tensile Strength Properties of Stainless Steel Plate F50 Before and After Irradiation

Specimen Number	Test Temp (°C)	Yield Strength		Tensile Strength		Applicable to CT Spec. No.
		(MPa)	(ksi)	(MPa)	(ksi)	
UNIRRADIATED CONDITION						
F50-115	24	288	41.74	619	-----	-----
F50-117	24	253	36.74	612	88.75	-----
F50-113	125	208	30.11	480	69.62	F50-76,77
F50-101	125	193	28.01	475	68.82	F50-76,77
F50-86	125	190	27.59	475	68.95	F50-76,77
F50-108	125	205	29.68	470	68.13	F50-76,77
IRRADIATED, HFIR ASSEMBLY IQ						
F50-1	125	462	67.05	563	81.70	F50-12
F50-6	125	445	64.46	527	76.44	F50-19
F50-8	125	435	63.14	513	74.34	F50-8,13
F50-9	125	471	68.26	570	82.68	F50-12,18
F50-12	125	448	64.94	559	81.01	F50-17

HFIR 4M TENSILE DATA (STRENGTHS) (125°C TEST)

Table 7 Strength Changes Observed for Pipe Ring Materials Irradiated in HFIR Assembly 4M

Determination		Pipe Ring Material Code			
		1BB (Axial) ^a	4BB (CMFL)	5BA (CMFL)	3HA (Axial)
Postirradiation Yield Strength	(Test 1)	71.2	76.7	72.2	81.2
	(Test 2)	74.6			
Preirradiation Yield Strength	(Range)	$\frac{30}{32}$	$\frac{28}{36}$	$\frac{28}{36}$	$\frac{43}{XX}$
Elevation due to Irradiation	(ksi)	42	45	40	37
	(%)	135	141	125	86
Postirradiation Tensile Strength	(Test 1)	84.4	88.8	83.9	88.6
	(Test 2)	85.6			
Preirradiation Tensile Strength	(Range)	$\frac{72}{74}$	$\frac{72}{74}$	$\frac{72}{74}$	$\frac{74}{XX}$
Elevation due to Irradiation	(ksi)	12	16	11	15
	(%)	14	18	13	17

HFIR 1Q & 4M TENSILE DATA (DUCTILITIES) (125°C TEST)

Table 8 Postirradiation Tensile Ductility
of HFIR Assembly 1Q and 4M Specimens^a

Assembly	Specimen No.	Reduction of Area (%)	Elongation in 20.3 mm (%)	Fracture Appearance
HFIR 1Q	F50-1	73.5	36.6	Cup/cone
	F50-6	66.2 ^b	33.0 ^b	Prongs/slant fracture
	F50-8	40.7	19.8 ^c	Cup/cone
	F50-9	72.4	41.0	Prongs
	F50-12	51.0	37.8 ^c	Slant fracture
HFIR 4M	1BBH1	64.6	62.2 ^c	Slant fracture
	1BBH4	72.4	43.0	Slant fracture
	4BBH2	71.4	42.4	Prongs
	5BAH5	75.5	32.0	Cup/cone
	3HAH8	- ^d	- ^d	-

^a 5.08-mm (0.200-in.) gage diameter specimens tested at 125°C

^b Measurements questioned (Specimen halves failed to mate readily)

^c Elongation in 13.4-mm referenced by extensometer knife edge marks (20.3-mm reference marks lost)

^d Specimen fractured at gage marks.

R-TANK TENSILE DATA (25 AND 125°C TEST)

Table 6-1

Sub-size Specimen Tensile Properties of As-Received Material

Spec. Location	Spec. No.	Test Temp. °F	Helium*	UTS-ksi	YS-ksi	Unif. %E	Tot. %E	%RA	Speed-in/min**
304 SS Plate Annealed, Unirradiated	A10	75	0	92.2	47.2	65.5	84.8	82.5	0.01
	A13	1000	0	59.3	28.9	39.5	49.7	76.7	0.002
	A11	1200	0	43.9	18.8	28.0	57.7	68.4	0.002
	A12	1500	0	17.2	12.2	8.5	95.7	75.3	0.002
	A4	1500	0	18.2	16.5	4.4	102.9		0.002
	A15	1800	0	6.0		6.0	72.5	62.1	0.002
R-Tank; RA3									
ID	3A1c	75	33.5	106.9	83.2	50.4	62.5	77.5	0.01
Midwall	3A2a	75	33.7	106.4	78.8	53.3	64.2	68.4	0.01
OD	3A3c	75	33.9	97.7	62.5	40.2	52.2	76.0	0.01
OD	3A3a	1200	33.9	31.4		19.9	28.9	17.9	0.002
OD	3A3b	1500	33.9	12.2	10.3	8.5	12.7	4.0	0.002
R-Tank; RD3									
ID	3G	1000	18.6	65.7	42.4	29.9	39.6	59.4	0.002
ID	3A	1100	18.6	43.0		20.7	22.3	32.8	0.002
ID	4G	1200	18.6	35.8	23.7	13.6	14.3	0	0.002
ID	4J	1500	18.6	17.1	9.6	4.9	5.3	0	0.002
ID	4A	1800	18.6	4.3		3.0	3.2	0	0.002
Midwall	4E	257	12.5	87.8	67.3	25.5	30.0	66.2	0.01
Midwall	4B	257	12.5	94.9	66.1	44.8	54.0	73.0	0.01
Midwall	3B	1500	12.5	19.5	15.2	4.9	6.4	0	0.002
OD	5I	75	5.9	107.9	76.2	35.5	45.2	57.0	0.01
OD	3P	257	5.9	88.3	59.6	31.9	42.4	55.8	0.002
OD	3I	1200	5.9	39.4	22.7	17.9	19.2	9.0	0.002
OD	3C	1500	5.9	18.7	15.9	4.2	5.0	0	0.002
R Tank; RB3									
ID	1F5	75	12.0	103.5	71.2	32.4	43.4	57.5	0.01
OD	1F3	75	3.25	106.8	76.8	32.9	46.0	75.6	0.01
OD	1F2	1500	3.25	18.9	16.4	5.7	7.1	17.6	0.002

UBR CVN DATA (25 AND 125°C TEST)

Temp (°C)	Ring No.	Test Orientation	Specimen No.	Energy Absorption (J)	Energy Absorption (ft-lb)	Lateral Expansion (mm)	Lateral Expansion (mils)
BASE METAL							
25	3	Axial	3BA43	114	84	1.854	73
			3BA44	111	82	1.829	72
			3BA45	114	84	1.397	55
		CMFL ^a	3BA19	90	66	1.270	50
			3BA20	83	61	1.194	47
			3BA21	84	62	1.21	52
125	3	Axial	3BA46	126	93	2.235	88
			3BA47	130	96	1.930	76
			3BA48	122	90	1.930	76
		CMFL	3BA16	100	74	1.778	70
			3BA17	99	73	1.803	71
			3BA18	100	74	1.702	67
WELD METAL							
25	1	Axial	1W2	87	64	1.422	56
			1W3	83	61	1.651	65
			1W4	84	62	1.499	59
			1W6*	92	68	1.549	61
	2	Axial	2W133	79	58	0.838	33
			2W135	73	54	0.914	36
	3	Axial	3W26	87	64	1.422	56
			3W27	84	62	1.473	58
			3W28	92	68	1.569	61
	4	Axial	4W13	79	58	0.914	36
			4W14	76	56	0.868	34
			4W15	79	58	0.991	39
	5	Axial	5W1	84	62	0.889	35
			5W2	79	58	1.067	42
			5W3	92	68	1.143	45
	6	Axial	6W1	100	74	1.829	72
			6W2	93	70	1.600	63
			6W3	90	66	1.397	55
	8	Axial	8W4	92	68	1.092	43
			8W5	92	68	1.194	47
			8W6	92	68	1.143	45

UBR CVN DATA (25 AND 125°C TEST) (CONT'D)

Temp (°C)	Ring No.	Test Orientation	Specimen No.	Energy Absorption		Lateral Expansion			
				(J)	(ft-lb)	(mm)	(mils)		
WELD METAL									
125	1	Axial	1W1	122	90	2.261	89		
			1W5	136	100	2.362	93		
	2	Axial	2W134	99	73	1.448	57		
	8	Axial CMFL	8W1	104	77	1.660	63		
			8W2	103	76	1.549	61		
			8W3	111	82	1.803	71		
	HAZ SPECIMENS								
	25	1	Axial	1HA21	121	89	1.448	57	
				1HA22	122	90	1.600	63	
1HA23				127	94	1.626	64		
1HB16				141	104	1.905	75		
1HB17				144	106	1.905	75		
1HB18				138	102	1.631	65		
2				Axial	2HA152	106	78	1.397	55
					2HA153	106	78	1.600	63
					2HA154	104	77	1.676	66
		2HB158	83		61	1.219	48		
		2HB159	79		58	1.219	48		
		2HB160	83		61	1.245	49		
3		Axial	3HA32	106	78	1.549	61		
			3HA34	100	74	1.448	57		
			3HA35	104	77	1.575	62		
		CMFL	3HA4	71	52	1.092	43		
			3HA5	75	55	1.092	43		
			3HA8	75	55	1.092	43		
4		Axial	4HA19	100	74	1.397	55		
			4HA20	100	74	1.499	59		
			4HA21	106	78	1.448	57		
	4HB31		119	88	1.499	59			
	4HB32		119	88	1.448	57			
	4HB33		114	84	1.572	62			

UBR CVN DATA (25 AND 125°C TEST) (CONT'D)

Temp (°C)	Ring No.	Test Orientation	Specimen No.	Energy Absorption		Lateral Expansion	
				(J)	(ft-lb)	(mm)	(mils)
HAZ SPECIMENS							
	5	Axial	5HA7	84	62	1.245	49
			5HA8	85	63	1.270	50
			5HA9	90	66	1.219	48
			5HB13	103	76	1.473	58
			5HB14	102	75	1.346	53
			5HB15	98	72	1.524	60
	6	Axial	6HA7	113	83	1.524	60
			6HA8	121	89	1.575	62
			6HA9	125	92	1.676	66
			6HB13	119	88	1.524	60
			6HB14	115	85	1.626	64
			6HB15	114	84	1.422	56
125	3	Axial	3HA33	117	86	1.803	71
			3HA36	121	89	1.905	75
			3HA37	119	88	1.626	64
		CMFL	3HA6	84	62	1.448	57
			3HA7	87	64	1.397	55
			3HA9	87	64	1.473	58

UBR ΔCVN DATA (25 AND 125°C TEST)

Table 6.2 Radiation-Induced Changes in Average C_v Energy Absorption of Materials

Ring No.	Base Metal (Side)	Preirradiation		Postirradiation		Decrease		
		(J) ^a	(ft-lb)	(J) ^a	(ft-lb)	(Δ J)	(Δ ft-lb)	(%)
WELD METAL (25°C)								
1	-	154	113.3	87	63.8	67	49.5	43.7
2	-	130	95.7	76	56.0	54	39.7	41.5
3	-	152	112.3	88	64.7	64	47.6	42.4
4	-	137	100.7	78	57.3	59	43.4	43.1
5	-	159	117.3	85	62.7	74	54.6	46.6
6	-	185	136.7	95	70.0	90	66.7	48.8
WELD METAL (125°C)								
1	-	241	177.7	129	95.0	112	82.7	46.5
2	-	158	116.7	99	73.0	59	43.7	37.5
BASE METAL (25°C)								
3	A	207	153.0	113	83.3	94	69.7	45.6
3 ^b	A	160	118.0	85	63.0	75	55.0	46.6
BASE METAL (125°C)								
3	A	300	221.3	126	93.0	174	128.3	58.0
3 ^b	A	154	113.5	100	73.7	54	39.8	35.1

UBR ΔCVN DATA (25 AND 125°C TEST) (CONT'D)

Table 6.2 Radiation-Induced Changes in Average C_v Energy Absorption of Materials (cont'd)

Ring No.	Base Metal (Side)	Preirradiation		Postirradiation		Decrease		
		(J) ^a	(ft-lb)	(J) ^a	(ft-lb)	(Δ J)	(Δ ft-lb)	(%)
MAX (25°C)								
1	A	225	166.0	123	91.0	102	75.0	45.2
1	B	246	181.5	141	104.0	105	77.5	42.7
2	A	183	135.0	105	77.7	78	57.3	42.4
2	B	145	107.3	81	60.0	64	47.3	44.1
3	A	192	142.0	103	76.3	89	65.7	46.3
3 ^b	A	136	100.0	73	54.0	62	46.0	46.0
4	A	165	122.0	102	75.3	63	46.7	38.3
4	B	206	151.7	118	86.7	88	65.0	42.9
5	A	149	109.7	86	63.7	62	46.0	41.9
5	B	159	117.0	101	74.3	58	42.7	36.5
6	A	188	138.7	119	88.0	69	50.7	36.6
6	B	201	148.0	116	85.7	85	62.3	42.1
MAX (125°C)								
3	A	226	167.0	119	87.7	107	79.3	47.5
3 ^b	A	139	102.5	86	63.3	53	39.2	38.2

^a Axial orientation unless noted

^b CMFL orientation

HFIR 1Q CVN DATA (125°C TEST)

Table 2 Charpy V-Notch Test Results for Plate Code F50
(HFIR Assembly 1Q; 125°C Tests)

Specimen No.	Orientation ^a	Energy Absorption ^b		Lateral Expansion	
		(J)	(ft-lb)	(mm)	(mils)
13	LT	117	85	2.261	89
14	LT	107	79	1.702	67
19	LT	118	87	2.032	80
23	LT	108	80	2.057	81

^a ASTM orientation LT (longitudinal).

^b Preirradiation range: 220-247 J (162-182 ft-lb)

Table 4 Charpy V-Notch Test Results for Plate Code F50
(Unirradiated Condition Plate Section No. 2; 125°C Tests)

Specimen No.	Energy Absorption		Lateral Expansion	
	(J)	(ft-lb)	(mm)	(mils)
88	220	162	2.210	87
90	247	182	2.108	83
93	244	180	2.210	87
92*	199	147	2.032	80

* 24°C test temperature

HFIR 4M CVN DATA (125°C TEST)

Table 3 Charpy V-Notch Test Results for Piping Materials (HFIR Assembly 4M, 125°C Tests)

Specimen No	Orientation	Energy Absorption		Lateral Expansion		Estimated Preirradiation Energy Absorption Range	
		(J)	(ft-lb)	(mm)	(mils)	(J)	(ft-lb)
4BBH9	CMFL ^a	87	64	1.397	55	225	166
1BBH5	Axial	134	99	2.007	79	340	251
3BBH1	Axial	102	75	1.397	55	<u>187</u> min <u>233</u> max	<u>138</u> <u>172</u>
6HAH6	Axial	110	81	1.600	63	331	245
6WH1	Axial	114	84	1.727	68	298	220

^a Circumferential, ASTM C-L orientation.

HFIR IQ CT DATA (125°C TEST)

Table 11A Stainless Steel Plate F50 Deformation J Analysis (0.394T-CT, 20X 9G, 125°C)

Specimen Number	ASTM E 319 ^a Orientation	(a/w) _i	Δa ₀ (mm)	Δa _p -Δa ₀ (mm)	J _{1c}		K _{1c}		T _{avg}		Flow Stress (MPa)	J = 8.8T (kJ/m ²)	E 813 ^b Validity	Exponent N	Coefficient C (kJ/m ²)
					Power Law	ASTM	Power Law	ASTM	Power Law	ASTM					
					(kJ/m ²)	(kJ/m ²)	(MPa√m)	(MPa√m)							
IRRADIATED CONDITION															
F50-76	L-T	0.539	3.66	-0.43	428.0	435.5	292.6	295.2	244	227	336.9	(> 722.9)	IV	0.3890	469.5
F50-77	L-T	0.529	3.31	-0.68	437.8	435.2	296.0	295.1	240	245	336.9	(> 714.9)	IV	0.3804	476.0
IRRADIATED, HWIR ASSEMBLY IQ															
F50-8	L-T	0.554	5.08	-0.59	243.3	250.9	220.6	224.0	100	99	473.9	463.9	IV	0.3572	334.8
F50-12	L-T	0.546	5.94	-0.93	266.2	266.7	230.8	231.0	85	83	516.6	466.2	IV	0.3342	358.5
F50-13	L-T	0.547	5.59	-0.92	274.6	276.6	234.4	235.2	114	119	473.9	476.0	IV	0.3747	373.8
F50-17	L-T	0.527	5.57	-1.53	294.2	302.7	242.6	246.1	109	105	503.1	504.6	IV	0.3783	399.7
F50-18	L-T	0.546	5.53	-1.08	260.0	266.0	228.1	230.7	109	109	520.3	530.2	IV	0.4167	379.3
F50-19	L-T	0.531	6.00	-0.95	251.2	261.9	224.2	228.9	129	124	485.7	506.1	IV	0.4390	371.1

^a Specimen designation: Circumferential = LC; Axial = CL
^b IV = ASTM invalid (specimen thickness insufficient)

HFIR 4M CT DATA (125°C TEST)

Table 11A Type 304 Stainless Steel Deformation J Analysis (0 394T-CT 201 SG 125°C)

Specimen Designation	ASTM E 192 ^a Orientation	a (mm)	b ₀ (mm)	b _p (mm)	J _{0.2}		K _{Jc}		T _{avg}		Flow stress (MPa)	J - 8 BT (kJ/cm ²)	E 813 ^b Validity	Exponent N	Coefficient C (kJ/m ²)
					Power Law (kJ/m ²)	ASTM (kJ/m ²)	Power Law (MPa/√m)	ASTM (MPa/√m)	Power Law	ASTM					
Irradiated, HFIR Assembly 4M															
<u>Case Data</u>															
3BH-8	CL	3.538	6.06	-0.88	327.6	327.5	256.0	256.0	122	125	544.1	689.6	IV	0.4310	460.6
3BH-9	CL	3.519	6.47	-1.06	248.2	247.0	222.9	222.3	138	141	544.1	587.2	IV	0.5255	412.3
3BH-16	CL	3.517	6.07	-0.79	334.4	341.1	258.7	261.2	120	115	544.1	660.3	IV	0.4725	464.2
3BH-10	CL	3.519	6.33	-1.01	194.0	192.8	197.0	196.4	53	55	570.6	332.9	IV	0.3059	274.2
3BH-7	CL	3.524	5.89	-0.90	135.7	113.2	164.8	150.5	86	106	534.3	352.3	IV	0.4647	252.2
<u>Weld Metal</u>															
4H-2	CL	3.512	5.42	-0.48	140.7	135.8	167.8	164.9	77	80	599.8	385.8	V	0.4979	270.1
<u>HAZ</u>															
3HAZ-5	CL	3.516	5.84	-0.74	186.6	175.2	193.2	187.2	76	87	585.1	403.8	V	0.4229	305.4
3HAZ-4	CL	3.527	5.62	-0.71	156.6	150.1	177.0	173.3	75	88	585.1	338.6	V	0.4550	276.6
3HAZ-5	CL	3.538	6.40	-0.99	77.8	88.3	124.7	132.9	11	7	585.1	96.0	IV	0.1600	99.1
3HAZ-7	CL	3.514	5.80	-0.53	72.8	77.2	120.7	124.3	25	24	585.1	137.8	V	0.3162	118.4

^a Specimen designation: Circumferential = LC; Axial = CL
^b IV = ASTM invalid (specimen thickness insufficient)

R-TANK CT DATA (25 AND 125°C TEST)

Table A-1. J_Q Values for Crack Initiation

	Side	Test	E813 R-Curve Limits				Relaxed R-Curve Limits		
			J_{Def}	J_{Def}	J_{Mod}	J_{Mod}	J_{Mod}	J_{Mod}	
	Size	Groove	Temp.	Linear Fit	Power Law	Linear Fit	Power Law	Linear	Power Law
RA37	.8T	No	25°C	1578*	2094	1589*	2153	1778	2165
RA38	.8T	No	25°C	1591*	2090	1658	2151	1834	2104
RD37	.8T	No	125°C	-	-	-	-	1730	1946
RD39	.8T	No	125°C	1371	1730	1011	1767	1562	1801
RD314	.4T	Yes	125°C	628	1153	481	1197	1109	1282
RD313	.4T	Yes	125°C	695	1091	664	1126	858	1129
RD315*	.4T	Yes	125°C	-	-	-	-	-	-
8BB51**	.4T	Yes	125°C	-	-	-	-	-	-

*Meets ASTM Validity Requirements

R-TANK CT DATA (25 AND 125°C TEST) (CONT'D)

<u>Sample</u>	<u>Size</u>	<u>Test Temperature</u>	<u>J_Q (in.-lb./in.²)</u>	<u>Tearing Modulus</u>
RA37	.8T	25°C	1780	120
RA38	.8T	25°C	1830	130
RD37	.8T	125°C	1730	120
RD39	.8T	125°C	1560	130
RD314	.4T	125°C	1110	80
RD313	.4T	125°C	860	110
RD315*	.4T	125°C	~2500	120
RD320	.4T	816°C	Nil	Nil
8EB51	.4T	125°C	~3000	-

* Annealed 15 mins. at 816°C

** Unirradiated sample from R-Reactor moderator piping

.4T samples are sidegrooved 20%

RA samples - 7×10^{20} n/cm² fast neutron fluence, 34 appm He

RD samples - 1×10^{20} n/cm² fast neutron fluence, 12 appm He

J_Q - Crack initiation fracture toughness with relaxed R-curve limits

APPENDIX 2

MECHANICAL TEST DATA - DIGITIZED PLOTS

DISCUSSION

The full mechanical test response from the RMP irradiated specimen testing and the R-Tank Tensile and Compact Tension specimen testing are retained in the RMP Task Files (SRL-NRTSC Task 89-023-1). Several of these mechanical response sets have been reproduced as discussed below:

Tensile Data

The full digitized true stress-strain curves from the HFIR 4M capsule specimens are fit to a Ramberg-Osgood format to provide the Ramberg-Osgood parameters for calculations of J-applied (see Section 6). The Ramberg-Osgood format of the True stress-strain curve is given by:

$$\frac{\sigma}{\sigma_y} = \frac{\sigma}{\sigma_y} + \alpha \left(\frac{\sigma}{\sigma_y} \right)^n$$

where σ_y is the yield strength and $\epsilon_y = \sigma_y/E$ where $E = 28 \times 10^6$ psi.

Compact Tension Data

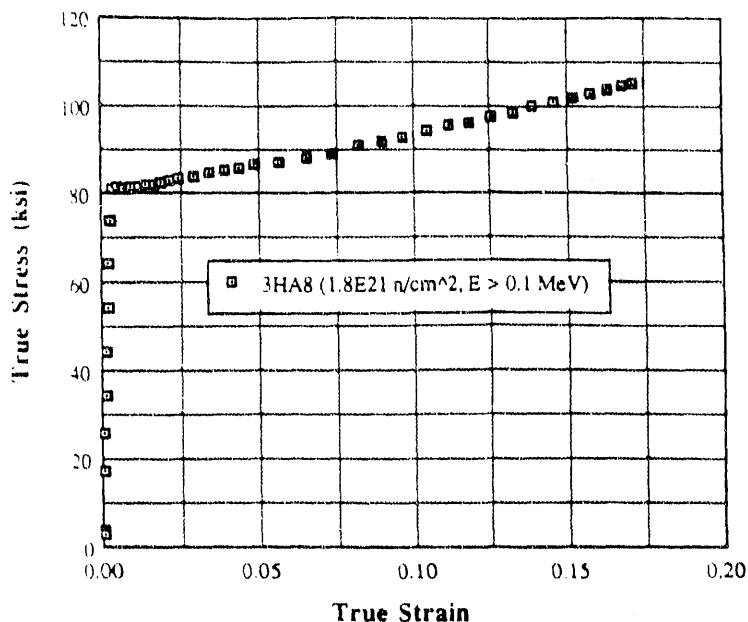
The $J_{\text{deformation}}$ -R curves from the R-Tank (0.4T planform specimens) and HFIR 4M CT are plotted. The J-R curve power law parameters and J-T curve equations are also provided on the respective figures for the 4M specimens. The J-R curves from the corresponding unirradiated specimens (ref. 35) are also shown together with the 4M curves.

Note that the calculation of J_{IC} (J_Q) from the J-R curves for the R-tank specimens did not use the data between the 0.15 and 1.5 mm exclusion lines that did not fit the criteria specified for in-plane dimensions for J-integral analysis [11].

The J-T curve from specimen 7HA5 (HAZ component, C-L orientation, and 125°C test temperature) is the "Lower Bound" fracture toughness from the as-irradiated database. The J-T curve from the specimen 2W2 is ascribed as the "Nominal" fracture toughness from the as-irradiated database (see Figure 6-1).

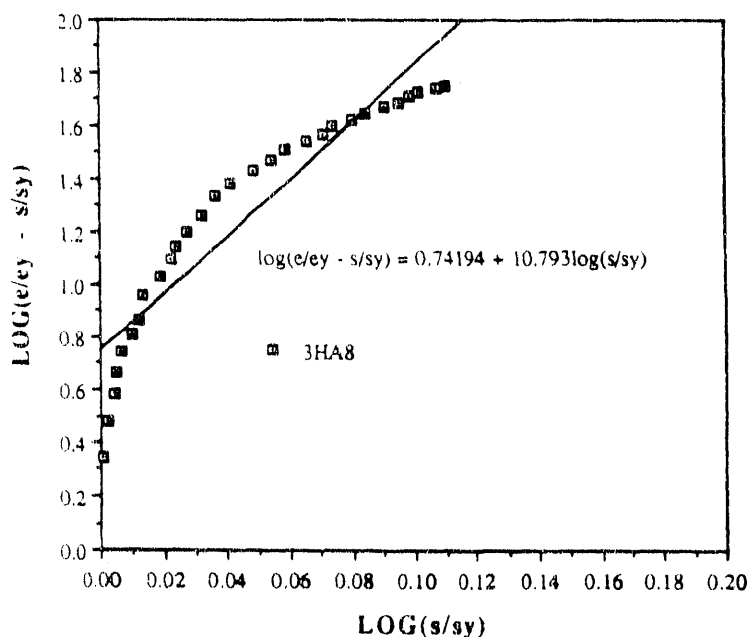
TRUE STRESS-STRAIN WITH RAMBERG-OSGOOD FORMAT FOR
 CATEGORY: HAZ; L-C; 125°C TEST

IRRADIATED HAZ, L-C, 125°C TEST



True stress/strain results from specimen 3HA8. The yield strength is 81.2 ksi.

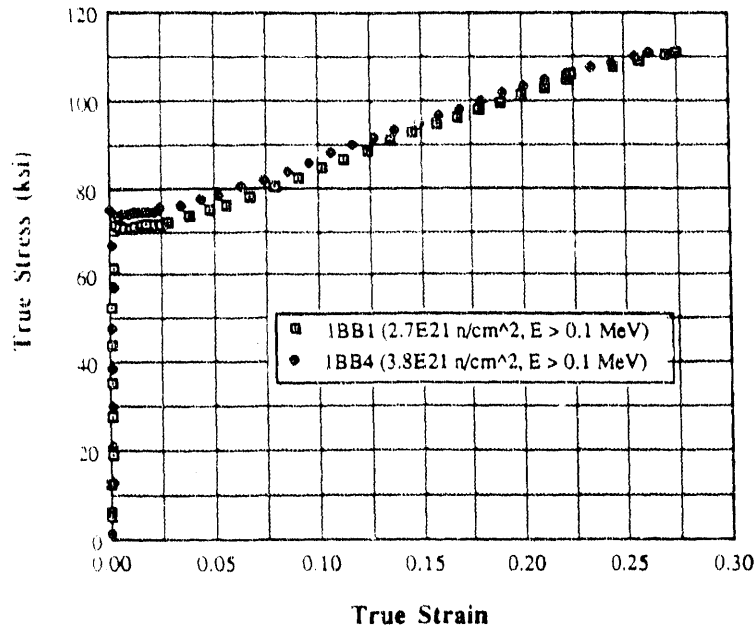
IRRADIATED HAZ, L-C, 125°C TEST



Ramberg Osgood format of True Stress-Strain curve. The results of a linear least square fit to the data give the Ramberg Osgood parameters $\alpha = 5.52$ and $n = 10.8$.

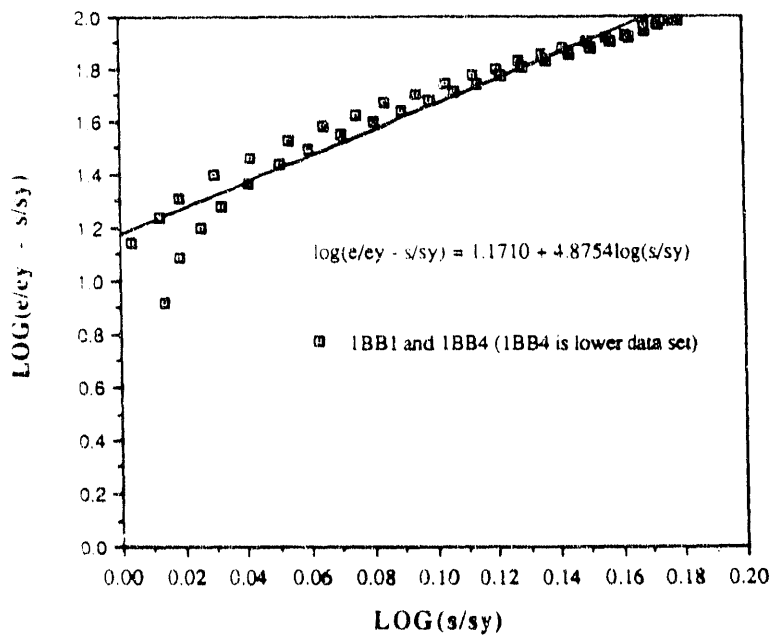
TRUE STRESS-STRAIN WITH RAMBERG-OSGOOD FORMAT FOR
 CATEGORY: BASE; L-C; 125°C TEST

IRRADIATED BASE, L-C, 125°C TEST



True stress/strain results from specimens 1BB1 and 1BB4. The yield strength for this set is taken as the average of the yield strengths from 1BB1 and 1BB4 and is 72.9 ksi.

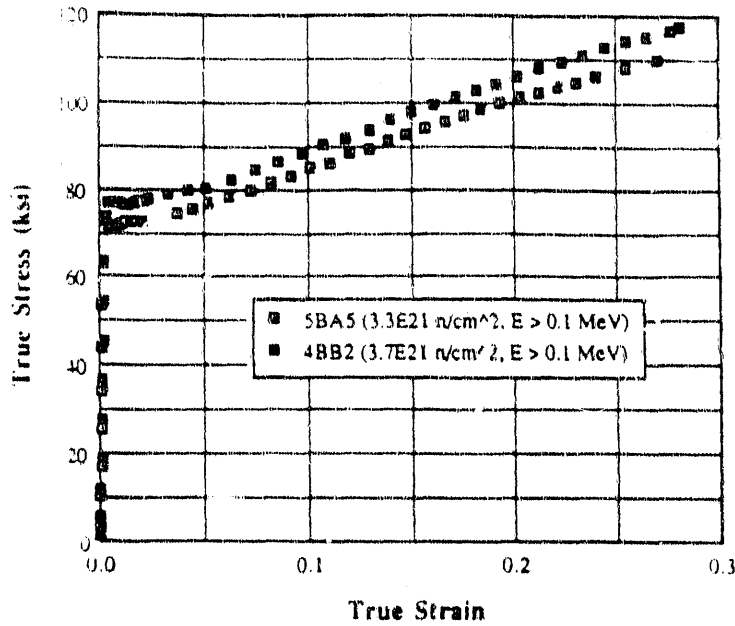
IRRADIATED BASE, L-C, 125°C TEST



Ramberg Osgood format of True Stress-Strain curve. The results of a linear least square fit to the data give the Ramberg Osgood parameters $\alpha = 14.8$ and $n = 4.88$.

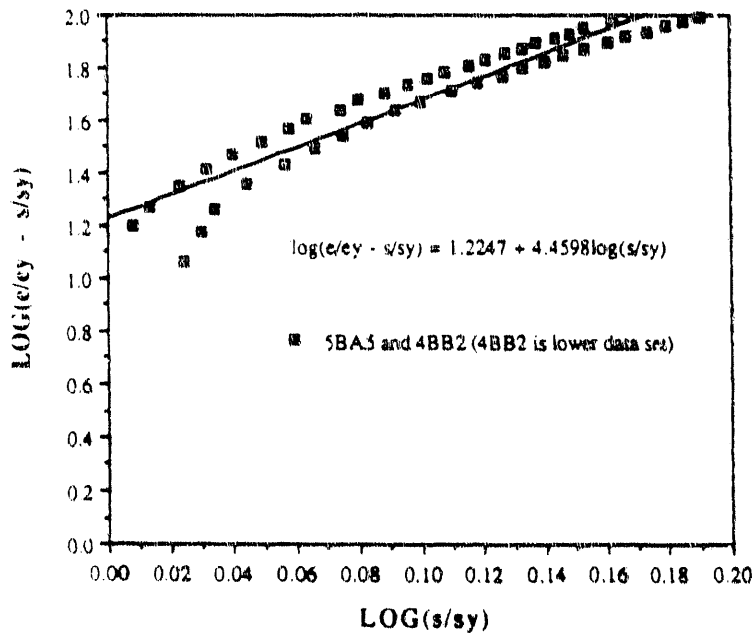
**TRUE STRESS-STRAIN WITH RAMBERG-OSGOOD FORMAT FOR
 CATEGORY: BASE; C-L; 125°C TEST**

IRRADIATED BASE, C-L, 125°C TEST



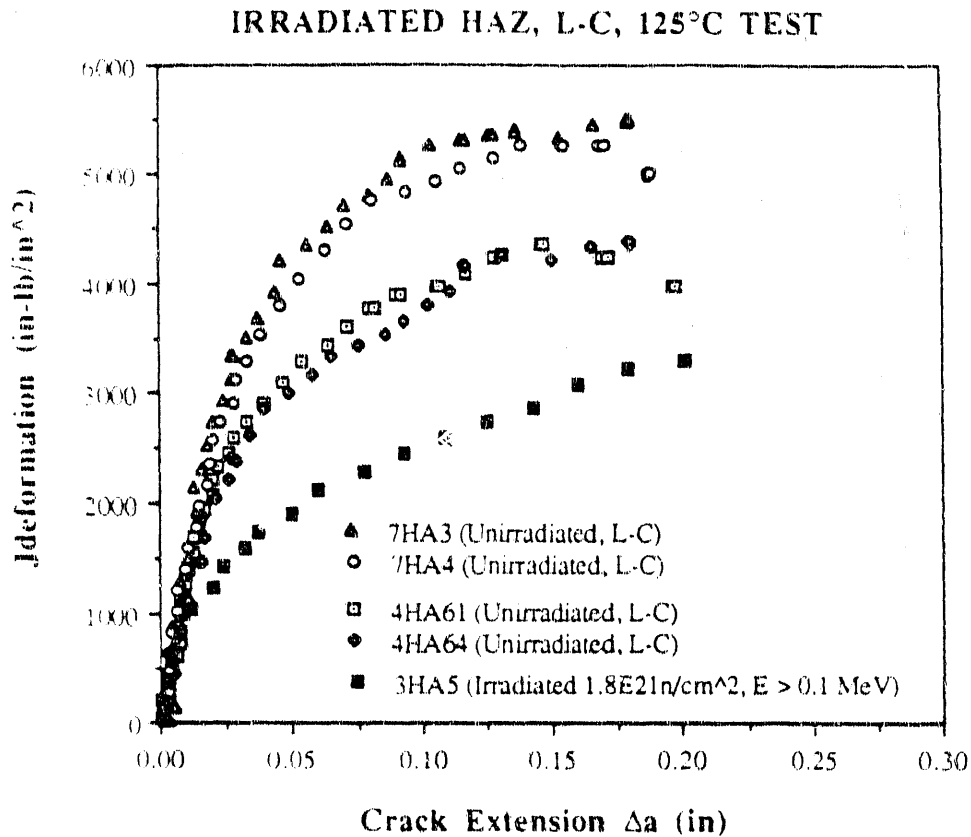
True stress/strain results from specimens 5BA5 and 4BB2. The yield strength for this set is taken as the average of the yield strengths from 5BA5 and 4BB2 and is 74.5 ksi.

IRRADIATED BASE, C-L, 125°C TEST



Ramberg Osgood format of True Stress-Strain curve. The results of a linear least square fit to the data give the Ramberg Osgood parameters $\alpha = 16.8$ and $n = 4.46$.

Jdeformation-R CURVE: HFIR 4M SPECIMEN 3HA5 (HAZ, L-C, 125°C)



The J-T curve (3HA5) equations are:

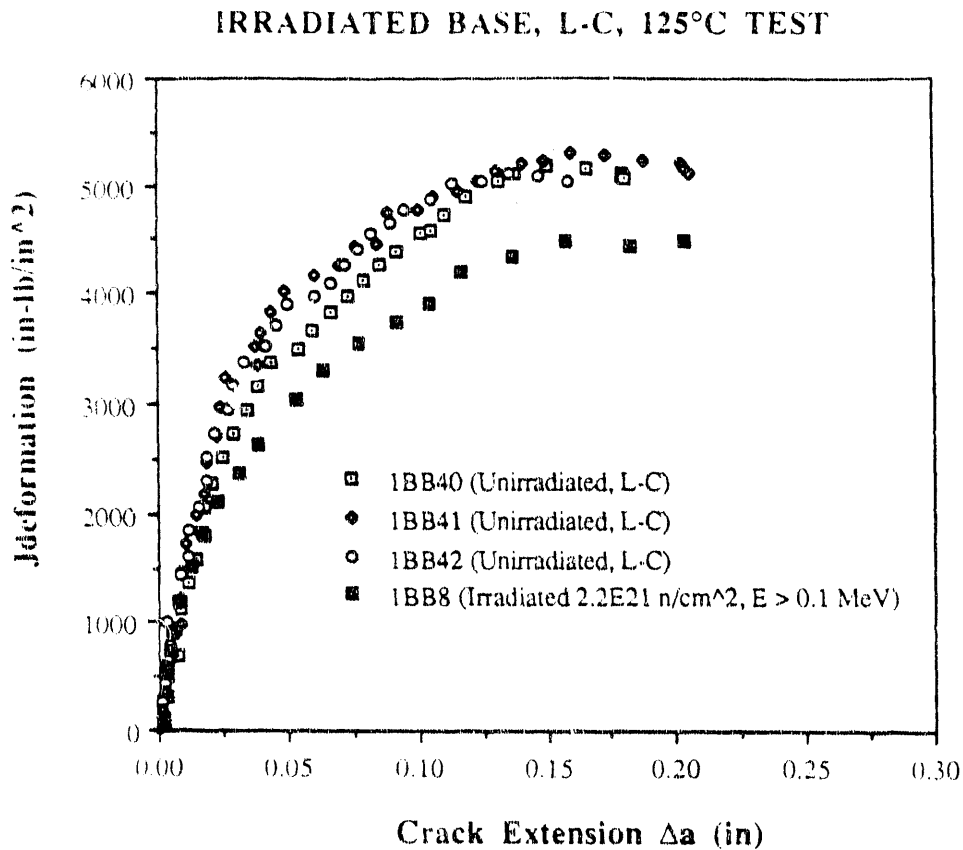
$$J_D \left[\frac{\text{in-lb}}{\text{in}^2} \right] = 6849 \Delta a^{0.4229}, \text{ with } \Delta a \text{ in inches}$$

and,

$$T = \frac{11.25}{\Delta a^{0.5771}}$$

for $s_f = 84.9$ ksi, with the limit on Δa of 0.1181 inches corresponding to $J = 2780$ in-lb/in².

Jdeformation-R CURVE: HFIR 4M SPECIMEN 1BB8 (BASE, L-C, 125°C)



The J-T curve (1BB8) equations are:

$$J_D \left[\frac{\text{in}\cdot\text{lb}}{\text{in}^2} \right] = 10590 \Delta a^{0.4310}, \text{ with } \Delta a \text{ in inches}$$

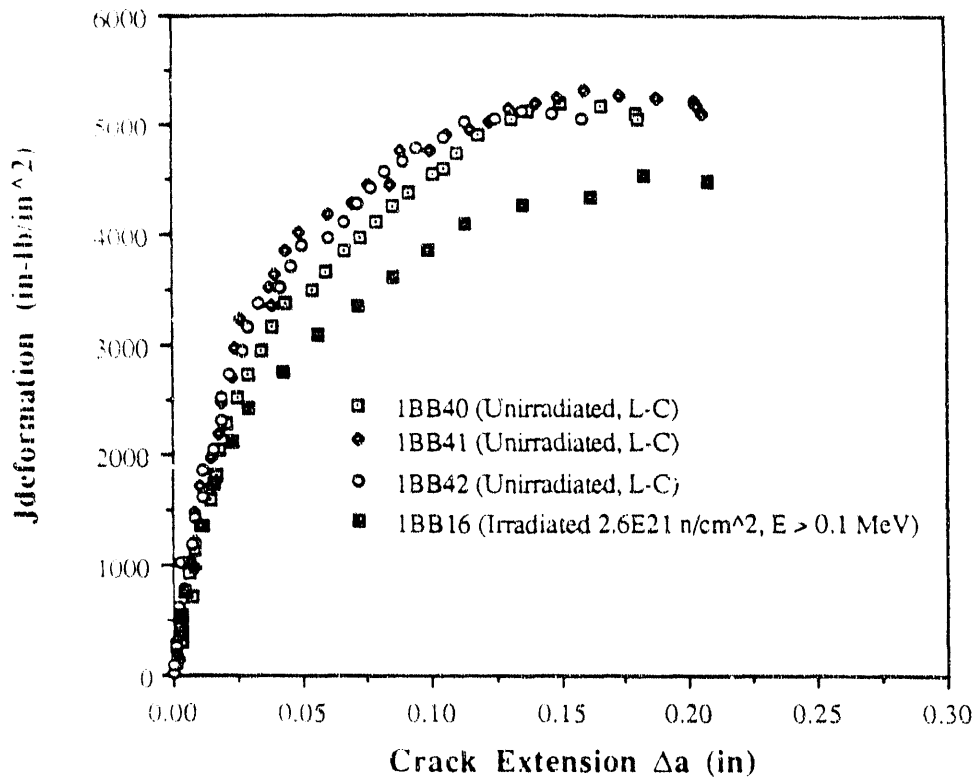
and,

$$T = \frac{20.48}{\Delta a^{0.5690}}$$

for $s_f = 79.0$ ksi, with the limit on Δa of 0.1181 inches corresponding to $J = 4220$ in-lb/in².

Jdeformation-R CURVE: HFIR 4M SPECIMEN 1BB16 (BASE, L-C, 125°C)

IRRADIATED BASE, L-C, 125°C TEST



The J-T curve (1BB16) equations are:

$$J_D \left[\frac{\text{in-lb}}{\text{in}^2} \right] = 10390 \Delta a^{0.4223}, \text{ with } \Delta a \text{ in inches}$$

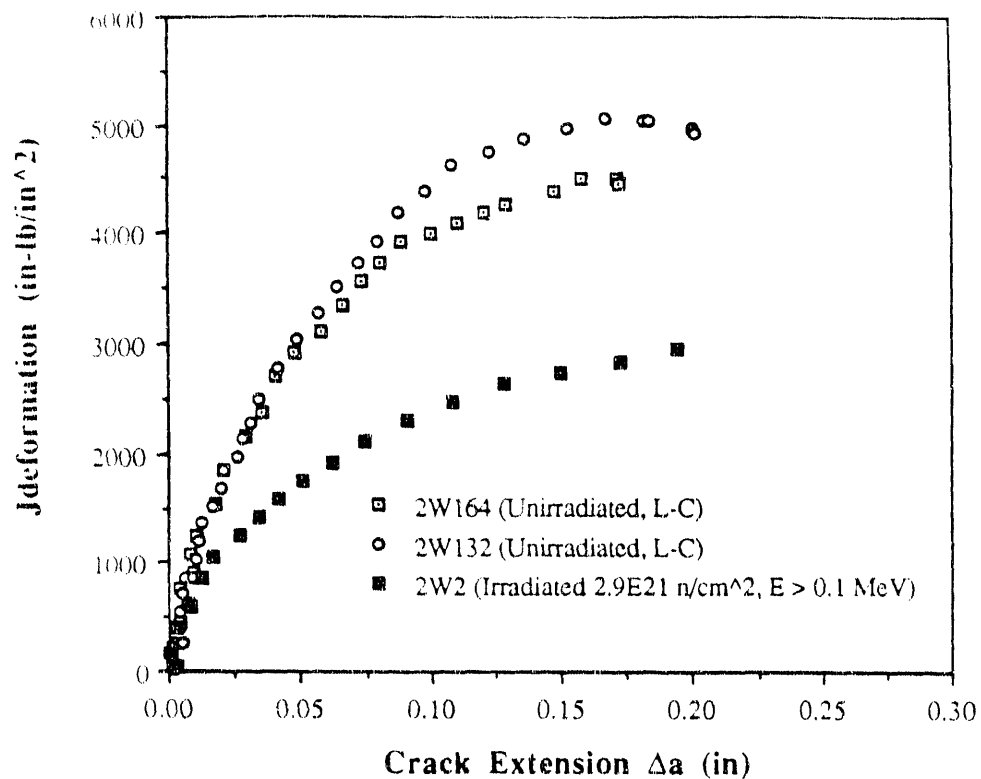
and,

$$T = \frac{19.69}{\Delta a^{0.5777}}$$

for $s_f = 79.0$ ksi, with the limit on Δa of 0.1181 inches corresponding to $J = 4220$ in-lb/in².

Jdeformation-R CURVE: HFIR 4M SPECIMEN 2W2 (WELD, L-C, 125°C)

IRRADIATED WELD, L-C, 125°C TEST



The J-T curve (2W2) equations are:

$$J_D \left[\frac{\text{in}\cdot\text{lb}}{\text{in}^2} \right] = 7720 \Delta a^{0.4979}, \text{ with } \Delta a \text{ in inches}$$

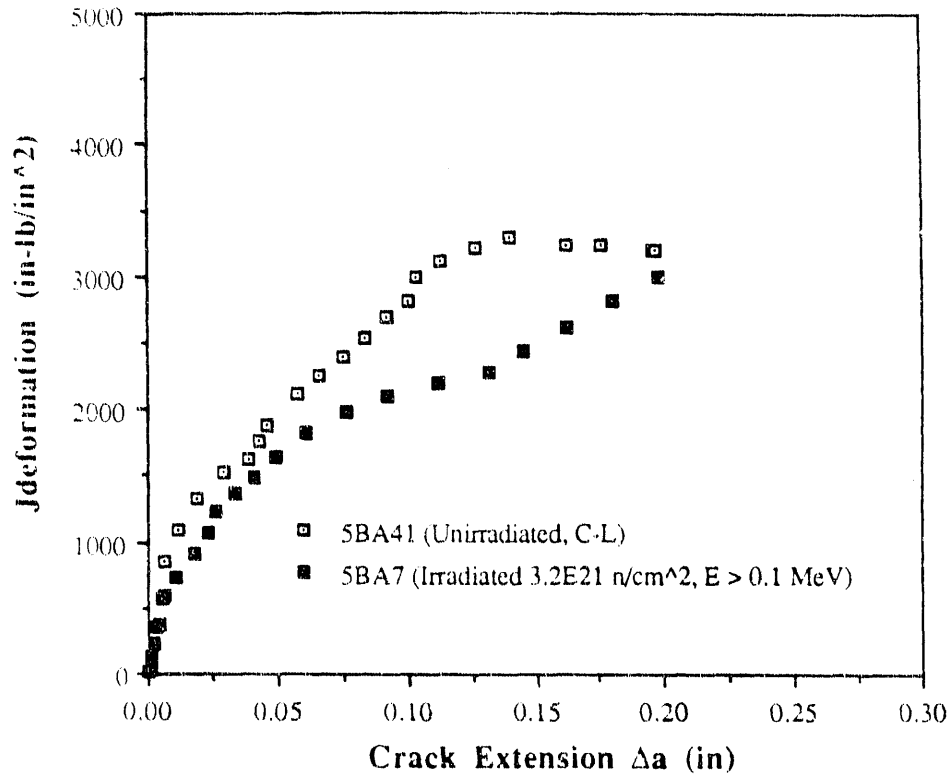
and,

$$T = \frac{14.93}{\Delta a^{0.5021}}$$

for $s_f = 84.9$ ksi, with the limit on Δa of 0.1181 inches corresponding to $J = 2660$ in-lb/in².

Jdeformation-R CURVE: HFIR 4M SPECIMEN 5BA7 (BASE, C-L, 125°C)

IRRADIATED BASE, C-L, 125°C TEST



The J-T curve (5BA7) equations are:

$$J_D \left[\frac{\text{in-lb}}{\text{in}^2} \right] = 6907 \Delta a^{0.4847}, \text{ with } \Delta a \text{ in inches}$$

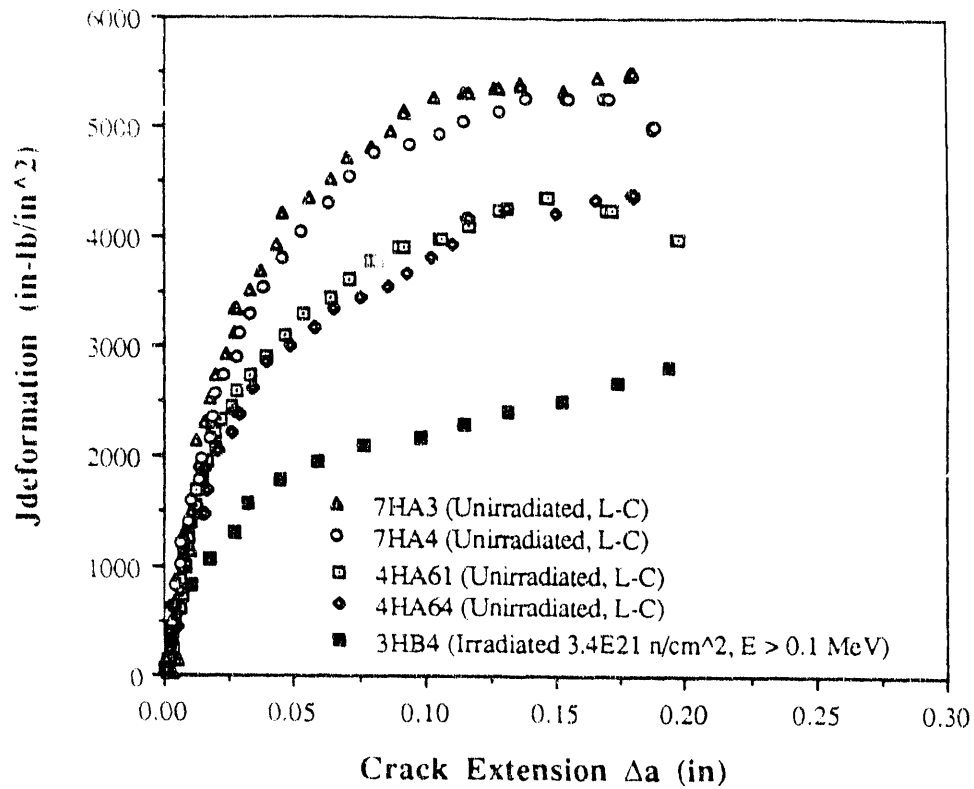
and,

$$T = \frac{15.39}{\Delta a^{0.5153}}$$

for $s_f = 78.05$ ksi, with the limit on Δa of 0.1181 inches corresponding to $J = 2450$ in-lb/in².

Jdeformation-R CURVE: HFIR 4M SPECIMEN 3HB4 (HAZ, L-C, 125°C)

IRRADIATED HAZ, L-C, 125°C TEST



The J-T curve (3HB4) equations are:

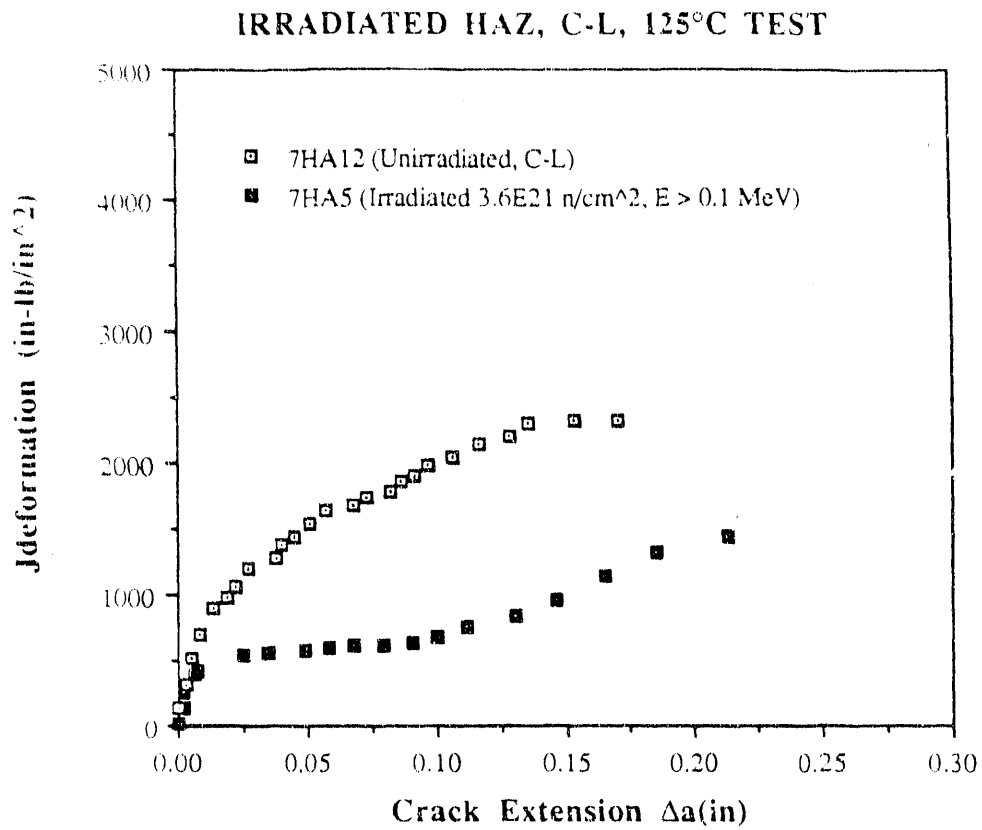
$$J_D \left[\frac{\text{in-lb}}{\text{in}^2} \right] = 6882 \Delta a^{0.4550}, \text{ with } \Delta a \text{ in inches}$$

and,

$$T = \frac{12.16}{\Delta a^{0.5450}}$$

for $s_f = 84.9$ ksi, with the limit on Δa of 0.1181 inches corresponding to $J = 2600$ in-lb/in².

Jdeformation-R CURVE: HFIR 4M SPECIMEN 7HA5 (HAZ, C-L, 125°C)



The J-T curve (7HA5) equations are:

$$J_D \left[\frac{\text{in-lb}}{\text{in}^2} \right] = 949 \Delta a^{0.1600}, \text{ with } \Delta a \text{ in inches}$$

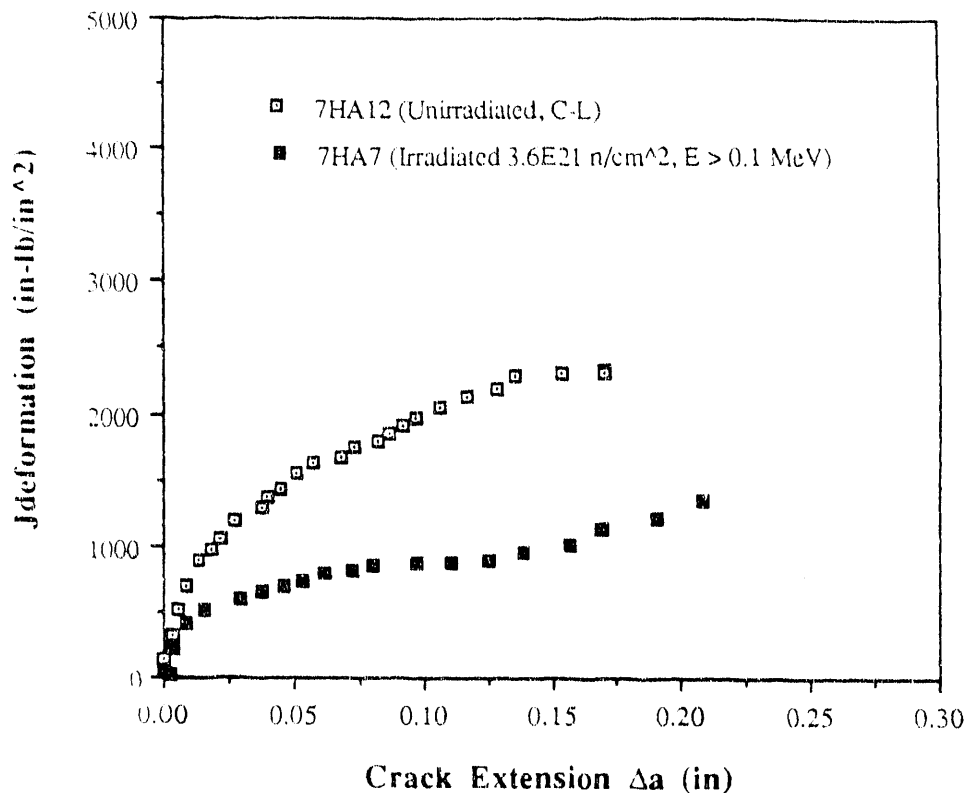
and,

$$T = \frac{0.5901}{\Delta a^{0.8400}}$$

for $s_f = 84.9$ ksi, with the limit on Δa of 0.1181 inches corresponding to $J = 674$ in-lb/in².

Jdeformation-R CURVE: HFIR 4M SPECIMEN 7HA7 (HAZ, C-L, 125°C)

IRRADIATED HAZ, C-L, 125°C TEST



The J-T curve (7HA7) equations are:

$$J_D \left[\frac{\text{in-lb}}{\text{in}^2} \right] = 1880 \Delta a^{0.3162}, \text{ with } \Delta a \text{ in inches}$$

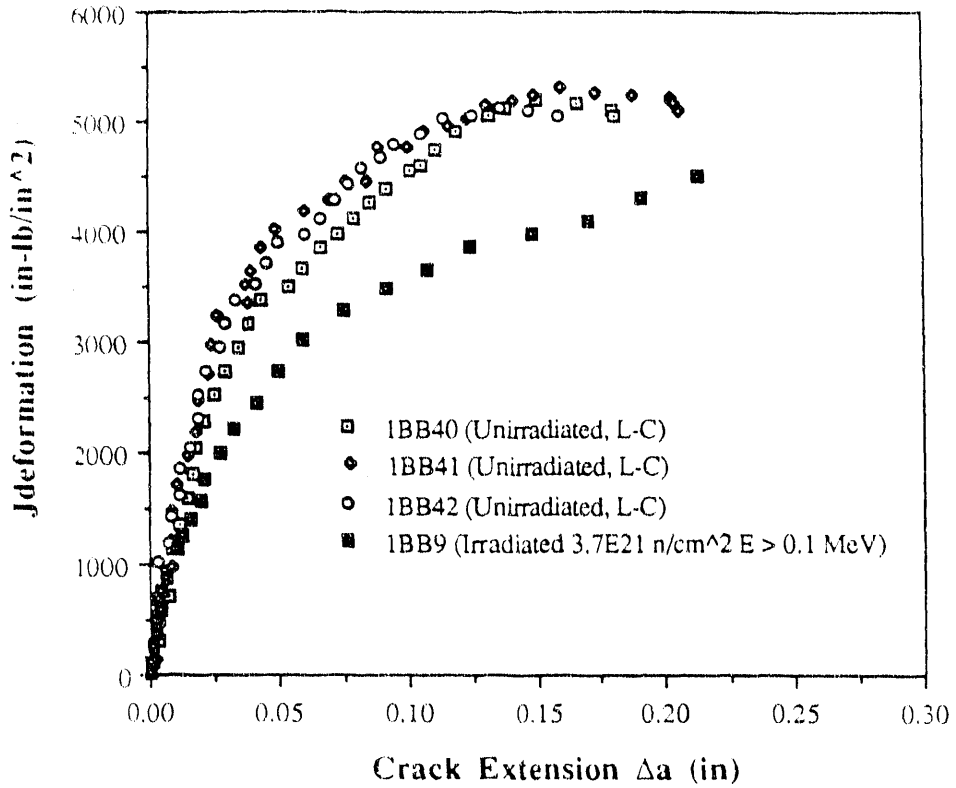
and,

$$T = \frac{2.309}{\Delta a^{0.6838}}$$

for $s_f = 84.9$ ksi, with the limit on Δa of 0.1181 inches corresponding to $J = 957$ in-lb/in².

Jdeformation-R CURVE: HFIR 4M SPECIMEN 1BB9 (BASE, L-C, 125°C)

IRRADIATED BASE, L-C, 125°C TEST



The J-T curve (1BB9) equations are:

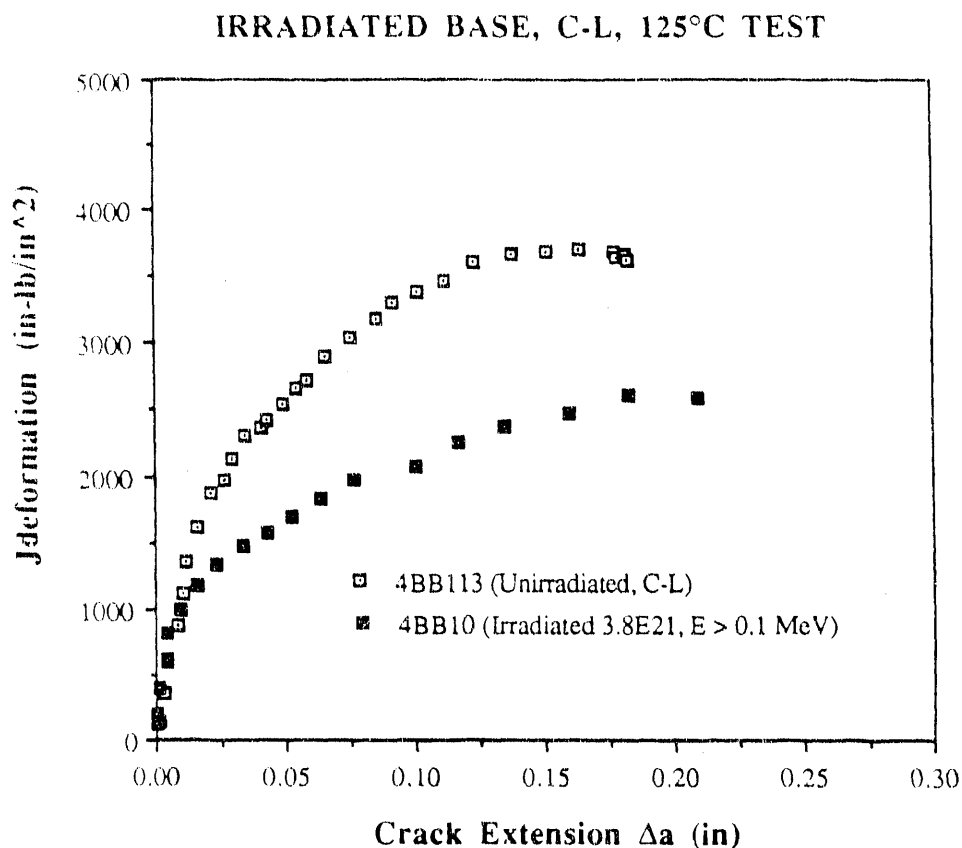
$$J_D \left[\frac{\text{in-lb}}{\text{in}^2} \right] = 12880 \Delta a^{0.5255}, \text{ with } \Delta a \text{ in inches}$$

and,

$$T = \frac{30.37}{\Delta a^{0.4745}}$$

for $s_f = 79.0$ ksi, with the limit on Δa of 0.1181 inches corresponding to $J = 4190$ in-lb/in².

Jdeformation-R CURVE: HFIR 4M SPECIMEN 4BB10 (BASE, C-L, 125°C)



The J-T curve (4BB10) equations are:

$$J_D \left[\frac{\text{in-lb}}{\text{in}^2} \right] = 4212 \Delta a^{0.3059}, \text{ with } \Delta a \text{ in inches}$$

and,

$$T = \frac{5.27}{\Delta a^{0.6941}}$$

for $s_f = 82.75$ ksi, with the limit on Δa of 0.1181 inches corresponding to $J = 2190$ in-lb/in².

J_d deformation-R CURVE: R-TANK SPECIMEN RD314 (0.4T, BASE, 125°C)

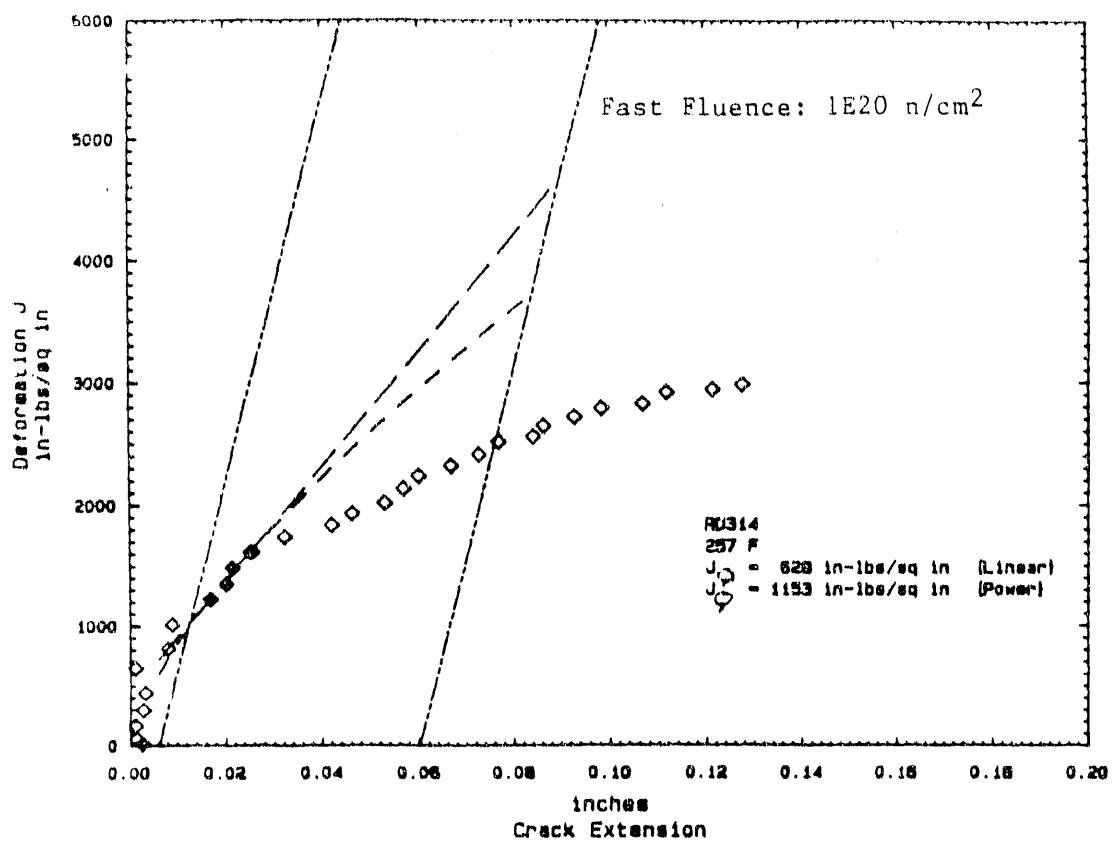


Figure A5 - Deformation J versus crack extension for specimen RD314, 0.304T GTS, sidgrooved, 257 F, ASTM E813 analysis procedures.

Jdeformation-R CURVE: R-TANK SPECIMEN RD313 (0.4T, BASE, 125°C)

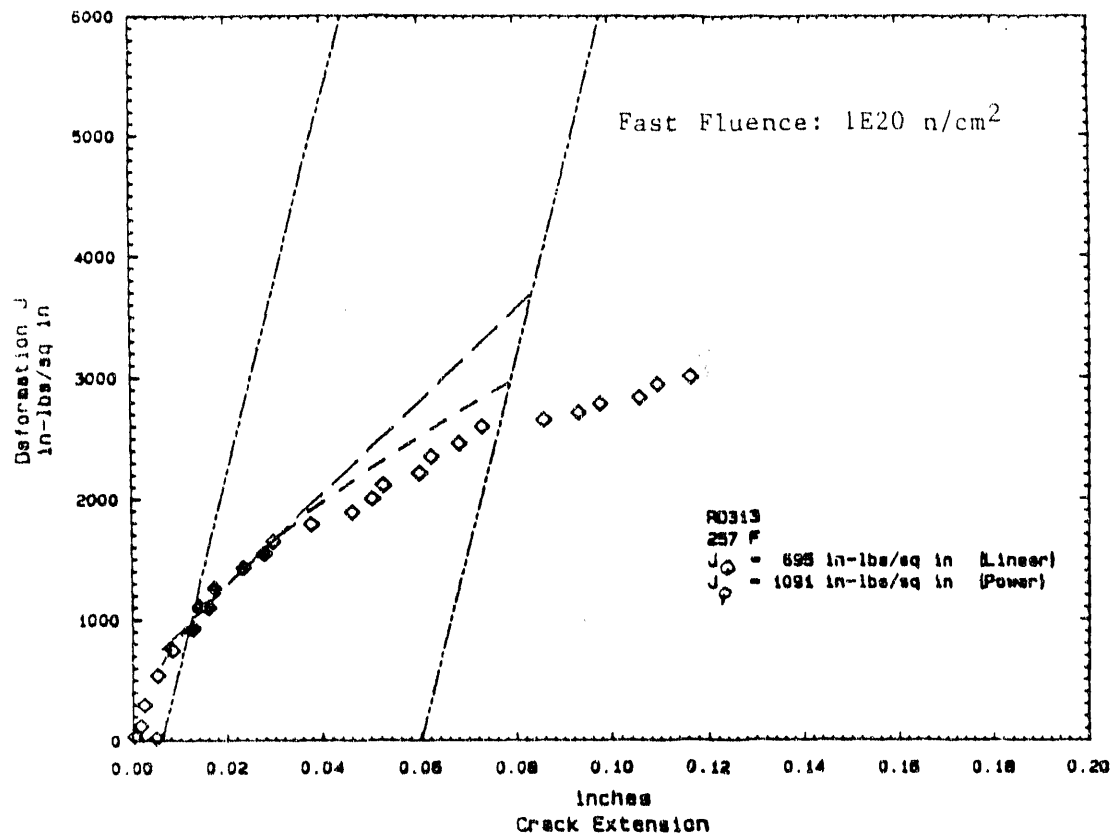


Figure A4 - Deformation J versus crack extension for specimen RD313, 0.394T CTS, sidgrooved, 257 F, ASTM E813 analysis procedures.

END

**DATE
FILMED**

9 / 2 / 92